Graz University of Technology

Diploma Thesis

(Diplomarbeit zur Erlangung des akademischen Grades eines Diplom-Ingenieurs der Studienrichtung Technische Chemie an der Technischen Universität Graz)

Immobilization and Patterning of Organometallic Pd-Catalysts on Si(111) Surfaces via UV-Lithography

Georg Johannes Lichtenegger

Univ. Prof. DI Dr. Johannes Khinast

DI Dr. Heidrun Gruber-Wölfler

process & particle engineering

Institute for Process and Particle Engineering

Graz 2011

DECLARATION

The work presented in this diploma thesis is to the best of my knowledge and belief, original, except acknowledged in the text. This material has not been submitted, either in the whole or in part, for a degree at this or any other university.

_____ _____

Place, Date Signature

EIDESSTATTLICHE ERKLÄRUNG

Ich erkläre an Eides Statt, dass ich die vorliegende Arbeit selbstständig und ohne fremde Hilfe verfasst, andere als die angegebenen Quellen nicht benutzt und die den benutzten Quellen wörtlich und inhaltlich entnommenen Stellen als solche kenntlich gemacht habe. Ich versichere, dass ich dieses Diplomarbeitsthema bisher weder im In- noch im Ausland in irgendeiner Form als Prüfungsarbeit vorgelegt habe.

_____ _____

Ort, Datum Unterschrift

DANKSAGUNG

An dieser Stelle möchte ich die Gelegenheit wahrnehmen, mich bei einigen Menschen, die mich während meines Studiums und während des Verfassens meiner Diplomarbeit in vielfältiger Weise unterstützt haben, zu bedanken.

Zuallererst möchte ich mich natürlich bei meinen Betreuern, Herrn Univ.-Prof. DI Dr. Johannes Khinast und Frau DI Dr. Heidrun Gruber-Wölfler, bedanken. Herrn Professor Khinast danke ich dafür, dass er es mir ermöglicht hat, meine Diplomarbeit am Institut für Prozess- und Partikeltechnik zu schreiben.

Allerherzlichster Dank gebührt selbstverständlich auch Frau Dr. Gruber-Wölfler, die aufgrund ihrer außerordentlichen fachlichen und menschlichen Kompetenzen, letztlich aber auch durch das Aufbringen einer erklecklichen Portion Geduld erheblichen Anteil am Gelingen meiner Abschlussarbeit hatte.

Ich möchte es auch nicht versäumen, mich bei Herrn Ao.Univ.-Prof. Mag. Dr.rer.nat. Robert Schennach zu bedanken, der mir bei der Aufnahme und Interpretation der Infrarotspektren stets hilfsbereit mit Rat und Tat zur Seite stand.

Dank gilt auch meinen Kolleginnen und Kollegen vom Institut für Prozess- und Partikeltechnik. Die gehaltvollen Gespräche und Diskussionen fachlicher und persönlicher Natur, die ich oftmals mit ihnen führen durfte, haben mich, wie ich meine, meinem Ziel, nicht nur Titelträger, sondern irgendwann tatsächlich ein Akademiker im besten Sinne des Wortes zu werden, sicherlich einen kleinen Schritt näher gebracht.

Auch all meinen Freunden, Studien- und Musikkollegen in Graz und in meiner Kärntner Heimat, die mich in meiner Studienzeit durch dick und dünn begleitet haben, sei hier mein Dank versichert.

Schlussendlich möchte ich mich aus tiefstem Herzen bei meiner Familie bedanken. Meinen drei Schwestern danke ich vor allem dafür, dass sie mich in langen Wohngemeinschaftsjahren meist mit bewundernswerter Ruhe als Mitbewohner ertragen haben. Ich danke auch meinem Großvater, der mir von frühester Kindheit an ein lebensfroher und bodenständiger Wegbegleiter war.

Mein allergrößter Dank gilt jedoch meinen Eltern, die mich nicht nur während meines Studiums, sondern schon mein ganzes Leben lang in jeder erdenklichen Art und Weise unterstützt haben. Sie gaben mir stets jenen menschlichen Halt, der zur erfolgreichen Bewältigung einer so langwierigen und fordernden Aufgabe, wie sie ein Hochschulstudium darstellt, unabdingbar ist.

KURZFASSUNG

Die Reaktion von endständig ungesättigten Kohlenwasserstoffen mit wasserstoffterminierten monokristallinen Silizium(111)-Oberflächen unter Bestrahlung mit ultraviolettem Licht, die sogenannte UV- oder photoinduzierte Hydrosilylierung, ist eine gut erforschte und vielfältig angewandte Methode, um organische Moleküle kovalent an ein Siliziumsubstrat zu binden. Da die Reaktion ausschließlich auf bestrahlten Oberflächen stattfindet, können durch den Einsatz geeigneter Photomasken örtlich definierte, organisch funktionalisierte Strukturen auf der Siliziumoberfläche geschaffen werden. Abgedunkelte Teile des Substrats bleiben hingegen wasserstoffterminiert.

Das Ziel der vorliegenden Arbeit war die kovalente und örtlich definierte Immobilisierung eines katalytisch aktiven, organometallischen Palladium-Komplexes auf H-terminierten Si(111)-Oberflächen. Pd-Komplexe katalysieren eine Vielzahl von Reaktionen, unter anderem die industriell häufig eingesetzte Suzuki-Miyaura Kreuzkupplungsreaktion. Um eine strukturierte Funktionalisierung der Oberfläche zu erreichen, wurde eine zweistufige Synthesestrategie verfolgt. Im ersten Schritt wurde mithilfe von Photomasken ein organischer Bis(oxazolin)-Ligand kovalent und strukturiert durch UV-induzierte Hydrosilylierung an das Siliziumsubstrat gebunden. Im zweiten Schritt wurde der katalytisch aktive Komplex durch Metallierung des immobilisierten Liganden mit Palladium(II)acetat gebildet.
Die Charakterisierung der funktionalisierten Oberflächen erfolgte durch Messung der Oberflächenbenetzbarkeit sowie mittels Infrarot- und Röntgen-Photoelektronenspektroskopie. Die Form und Größe der modifizierten Bereiche konnte aufgrund unterschiedlicher physikalischer Eigenschaften von funktionalisierten und nicht funktionalisierten Oberflächenteilen direkt durch optische Mikroskopie bestimmt werden. Außerdem wurde die katalytische Aktivität des immobilisierten Komplexes in einer Suzuki-Miyaura-Kreuzkupplungsreaktion überprüft.

Die Ergebnisse der Charakterisierung legen die Schlussfolgerung nahe, dass der organometallische Palladium-Komplex tatsächlich örtlich definiert an das Siliciumsubstrat gebunden werden konnte. Die funktionalisierten Oberflächen zeigten auch nach mehrfacher Verwendung in Suzuki-Reaktionen deutliche katalytische Aktivität.

Gleichbleibende physikalische Eigenschaften der modifizierten Oberflächen beweisen die hohe Stabilität der Funktionalisierung. Mittels optischer Mikroskopie konnte außerdem gezeigt werden, dass linienförmige, funktionalisierte Muster mit deutlich weniger als 50 µm Streifenbreite mithilfe der verwendeten lithographischen Einheit hergestellt werden können.

ABSTRACT

The UV-light induced hydrosilylation reaction of terminally unsaturated hydrocarbons with hydrogen terminated monocrystalline Si(111) is a well established method for the covalent attachment of organic molecules on flat silicon surfaces. Simple masking procedures allow the creation of two-dimensional organic patterns on the surface since hydrosilylation occurs exclusively on irradiated surface parts. The non irradiated areas remain hydrogen terminated.

The aim of the present work was the covalent and spatially defined immobilization of a catalytically active organometallic palladium complex on H-terminated Si(111). Organometallic Pd-complexes are known to catalyze a range of reactions including the industrially important Suzuki-Miyaura cross coupling reaction. Immobilization and patterning was achieved pursuing a two-step strategy. The first step was the attachment of a bis(oxazoline) ligand in a spatially controlled fashion using an UV-lithographic approach. In the second step, the immobilized ligand was metallated with palladium(II) acetate to form the catalytically active complex.
The created surfaces were characterized using water contact angle measurements, infrared and X-ray photoelectron spectroscopy. Due to different physical properties of functionalized and non-functionalized surface parts, direct determination of shape and size of the created organic patterns via optical microscopy was possible. Finally, the catalytic activity of the modified surfaces was tested employing the Pd-catalyzed cross-coupling reaction of *p*-bromotoluene with phenylboronic acid.

The obtained results of the characterization strongly indicate successful and laterally controlled immobilization of the organometallic Pd-complex. The functionalized surfaces show significant catalytic activity, even after repeated use, and good stability under both, storage and reaction conditions. Furthermore, optical microscopy revealed that organic patterns with linewidths below 50 µm can easily be created with the developed lithographic unit.

TABLE OF CONTENTS

LIST OF FIGURES

LIST OF TABLES

LIST OF ABBREVIATIONS

ABCN	1,1'-azobis(cyclohexanecarbonitrile)
AFM	atomic force microscope
AIBN	azo-bis-(isobutyronitrile)
ATR	attenuated total reflectance
BOX	2,2'-(1-methyl-11-dodecenylidene)bis(4,5-dihydrooxazole)
CCD	charge-coupled device
DMF	dimethylformamide
DNA	deoxyribonucleic acid
e^-	electron
E_a	activation energy
EBI	ethylenbis(indenyl)
FTIR	Fourier transform infrared spectroscopy
FZ	float-zone
GC	gas chromatography
h^+	exciton
IR	infrared
LO	longitudinal optical
MCT	mercury cadmium telluride
NMR	nuclear magnetic resonance
PTFE	polytetrafluoroethylene
RCA	Radio Corporation of America
SAM	self-assembled monolayer
SC-1	standard cleaning solution 1
SC-2	standard cleaning solution 2
Si-BOX	silicon surface, functionalized with the BOX-ligand
Si-BOX-$Pd(OAc)_2$	silicon surface, functionalized with the organometallic BOX-Pd-complex
Si-H	hydrogen terminated silicon
STM	scanning tunneling microscope
TEMPO	(2,2,6,6-Tetramethylpiperidin-1-yl)oxyl

TO	transverse optical
TS	transition state
UHV	ultra-high vacuum
USAF	United States Air Force
UV	ultraviolet
WCA	water contact angle
XPS	X-ray photoelectron spectroscopy
λ	wavelength
θ	water contact angle
σ	conductivity

1 MOTIVATION AND OBJECTIVES

Organic modification of non-oxidized silicon surfaces has gained much attention over the last two decades. Especially the reaction of 1-alkenes and 1-alkynes with hydride-terminated single-crystalline Si(100) and Si(111) surfaces is an area of intense research activity. This so-called hydrosilylation reaction results in the formation of covalent Si-C bonds which show excellent chemical stability even under rather harsh conditions.

Surface hydrosilylation on H-terminated flat Si(111) can be induced by irradiation with ultraviolet light. In recent years the successful attachment of a wide variety of organic molecules using this technique has been reported[1-6]. Furthermore, UV-induced hydrosilylation allows the creation of two-dimensional organic patterns on the silicon surface[7]. Since the reaction occurs solely at the irradiated parts of a surface, the use of suitable photomasks results in the organic functionalization of UV-exposed areas, whereas non-irradiated parts remain H-terminated. These parts are prone to further reactions with unsaturated organic compounds. Hence, UV-induced hydrosilylation is potentially a suitable technique for step-by-step immobilization of different functional molecules on a silicon substrate. The laterally controlled way of functionalization is, thus, not merely a desirable side effect, but rather a fundamental prerequisite for the creation of multifunctional silicon surfaces via UV-lithography.

Monocrystalline Si(111) as solid support provides not only the possibility for straightforward, spatially controlled functionalization but offers numerous further advantages. Due to their ubiquitous use in microelectronic applications, high quality single-crystal silicon substrates of different crystal orientations are commercially available at comparatively low costs. The chemical and physical properties of both, the bulk silicon and the silicon surface have extensively been investigated and are well understood. Furthermore, several methods for the analysis and characterization of organically modified silicon surfaces are available.

An interesting application for multiple functionalized surfaces could be the use as multifunctional heterogeneous catalysts. Successful immobilization of organometallic catalysts on Si(111) via hydrosilylation reactions has already been reported[4, 5]. Therefore, multicatalytic and continuous processes employing different transition

metal complexes seem to be accessible. Surfaces with laterally defined and intelligently arranged areas of different catalytic functionalities could, for example, be the catalytically active component in microreactor approaches. A possible bifunctional catalytic process would be the synthesis of chiral compounds: a palladium-complex catalyzes a cross coupling reaction whereas a titanocene-compound subsequently catalyzes a stereoselective reduction.

Multicatalytic surfaces could principally also be created by immobilizing active complexes or their precursors from mixed solutions of the respective compounds. However, this approach would lead to a random distribution of the different catalytically active molecules on the surface. Dense packing of different organometallic complexes can cause undesired interactions between various functional molecules and, thus, lead to a loss of catalytic activity of each compound. The prevention of such kind of deactivation by spatial division of areas with different catalytic functionalities is another motivation for the development of techniques to laterally define functionalization of the surface even at the micrometer scale.

The creation of multifunctional heterogeneous catalysts via UV-lithography is the overall objective which stands behind the idea of this thesis. The present work concentrates on the first and indispensable step of this development: the covalent and spatially defined immobilization of a catalytically active compound on H-terminated Si(111). An organometallic bis(oxazoline)-palladium-complex was chosen as model molecule in our approach. This complex, which is known to catalyze a range of cross-coupling reactions as well as the oxidation of benzylic alcohols, can be immobilized employing a two-step strategy. The first step is the covalent attachment of the organic Bis(oxazoline)-ligand via UV-induced hydrosilylation. In the second step, the immobilized ligand is metalated with palladium(II)acetate to form the catalytically active complex.

A number of tasks had to be accomplished to reach the overall objective:

- Development of a suitable lithographic arrangement for the spatially defined functionalization of the silicon surface
- Successful covalent attachment of the catalytically active complex

- Characterization of the functionalized surfaces with appropriate analytical techniques
- Determination of shape and size of the functionalized patterns on the surface
- Examination of the catalytic acitivity of the functionalized surfaces

2 INTRODUCTION

The present work aims at the covalent immobilization of organometallic catalysts on Si(111)-surfaces in a laterally controlled fashion. In our approach, this should be achieved by a UV-induced hydrosilylation reaction. A bis(oxazoline)-palladium-complex was used as a catalytically active model molecule in our experiments.

2.1 Catalysis

A catalyst is defined as a substance that increases the rate of attainment of chemical equilibrium by decreasing the activation energy E_a without, itself, being permanently chemically changed[8]. Catalysts generally interact with one or more reactants forming a reactive intermediate which subsequently reacts to the final product(s). The substrate:catalyst interaction provides an alternative reaction mechanism involving a different, stabilized transition state (TS) with a lower activation energy than would be needed in a non-catalyzed reaction (see Figure 2-1). By offering this energetically more favored pathway, catalysts can accelerate chemical reactions, make them more specific or enable them to occur at lower temperatures.

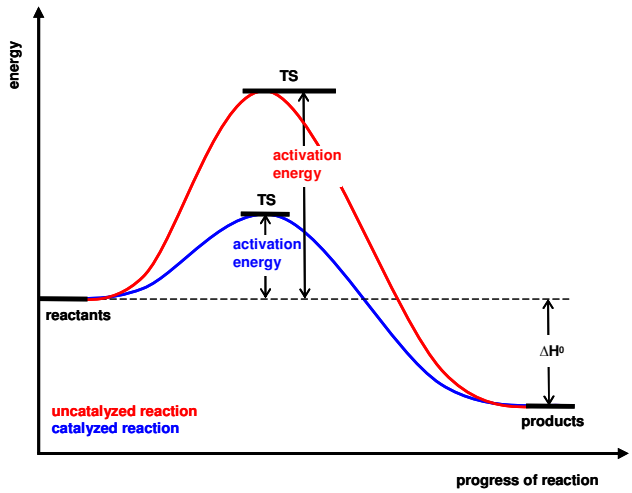

Figure 2-1: Scheme of the effect of a catalyst on the activation energy in a hypothetical exothermic chemical reaction

However, since the catalyst does not undergo any chemical change, it accelerates both the forward and the reverse reaction. The chemical equilibrium of the catalyzed reaction equals that of the uncatalyzed reaction. Thus, catalysis is a kinetic but not a thermodynamic phenomenon. It can not initiate energetically unfavorable reactions.
In general, catalysts can be roughly divided into five groups:

1. Heterogeneous catalysts
2. Homogeneous catalysts
3. Biocatalysts
4. Electro- and photocatalysts
5. Organocatalysts

Homogeneous catalysts are available in the same phase as the substrate whereas heterogeneous catalysis occurs at the interface between two phases, usually using a solid catalyst with liquid or gaseous reactants. Biological catalysis is often seen as an intermediate, because the enzyme is in solution but the reaction occurs on the surface of the large biomolecules. Electro- and photocatalysts accelerate electrochemical and photoreactions, respectively. The use of small organic molecules, which predominantly consist of C, H, O, N, S and P, to catalyze chemical reactions is called organocatalysis. Compared to (transition) metal catalysis, the use of organocatalysts provides a number of benefits, particularly regarding availability, costs and toxicity of the catalysts.

Although especially biocatalysis and organocatalysis are doubtlessly areas of great interest and intense research, the present work will focus on the immobilization and patterning of organometallic catalysts.

2.2 Heterogeneous Catalysis

Approximately 90 % of all chemical manufacturing processes use catalysts in one form or another[9, 10]. The major problem of homogeneous catalysis is the recovery of the catalysts from the reaction solution. Whereas heterogeneous catalysts can be removed by simple methods such as filtration or centrifugation, more complex processes like distillation or liquid-liquid extraction must be used in the case of homogeneous catalysis. Thus, the market share of homogeneous catalysts amounts only to 10 – 15 %[11].

2.2.1 The Catalytic Cycle

In contrast to homogeneously catalyzed reactions, where reaction rates can be expressed straightforwardly as a function of the concentrations of substrates and catalyst, heterogeneously catalyzed processes are more complex concerning kinetic as-

pects. Considering a two phase system with the catalyst in the solid phase, five steps are needed to complete the catalytic reaction [8]:

1. Transport of the reactants to the catalyst.
2. Interaction of the reactants with the catalyst (adsorption).
3. Reaction of adsorbed species to give the product(s).
4. Desorption of the product(s) from the catalyst.
5. Transport of the product(s) away from the catalyst.

Although chemical changes occur only in step two, three and four, with the desired reaction taking place in step three, even the merely physical transport processes in step one and five can be the rate limiting factors for the overall process. Hence, the performance of a heterogeneous catalyst is not only determined by the efficiency of its active sites, but also by hysical and morphological properties of the catalyst, such as hardness, density, surface area, pore volume, pore size or pore distribution.

2.2.2 Immobilization of Catalytically Active Compounds

Heterogeneous catalysts can be either used as unsupported bulk catalysts or as supported catalysts, where a catalytically active species is deposited on an inert solid support material.

The immobilization of homogeneous catalysts on solid supports can be considered as the attempt to combine the potential advantages of heterogeneous catalysts, such as easy separation, efficient recycling or minimization of metal traces in the product with those of homogeneous catalysts (e.g. high activity, good reproducibility, possible enantioselectivity)[12]. Generally, homogeneous catalysts can be immobilized by the covalent or noncovalent attachment of (a) a ligand, (b) the metal or (c) the preassembled complex via the following techniques[13]:

1. Covalent linkage
2. Adsorption
3. Electrostatic interactions
4. Encapsulation (Entrapment)

Since product contamination by metal leaching is problematic especially for the production of fine chemicals and pharmaceuticals, covalent bonding is by far the most

frequently used technique for immobilization due to the strong linkage between catalyst and solid support. Strategies for covalent tethering include:

- Covalent immobilization on polymeric resins
- Covalent immobilization by copolymerization
- Covalent immobilization on inorganic supports

Various types of inorganic solids have been used as supports for catalysts such as silica, alumina, zeolite, zirconia, ZnO or clay[14]. This work will focus on the covalent tethering of transition metal complexes on flat silicon (111) surfaces.

2.3 Palladium Catalyzed Cross Coupling Reactions

In this work, palladium acetate, covalently linked to the solid support via a bis(oxazoline) ligand, was chosen as the catalyst which should be patterned on the silicon surface. Palladium catalyzes a range of cross coupling reaction and is widely used in organic chemistry.

Cross coupling is a general term for metal catalyzed reactions, in which two different organic compounds are coupled. The importance of these reactions was strongly emphasized in 2010, when Richard F. Heck, Ei-ichi Negishi and Akira Suzuki won the Nobel Prize in chemistry “for palladium-catalyzed cross couplings in organic synthesis”[15].

Palladium catalyzes the cross coupling of an electrophilic organohalide RX with a nucleophilic partner, either an olefin (e.g. the Heck reaction, Figure 2-2(1)) or an organometallic compound (e.g. the Suzuki-Miyaura cross-coupling, Figure 2-2(2)).

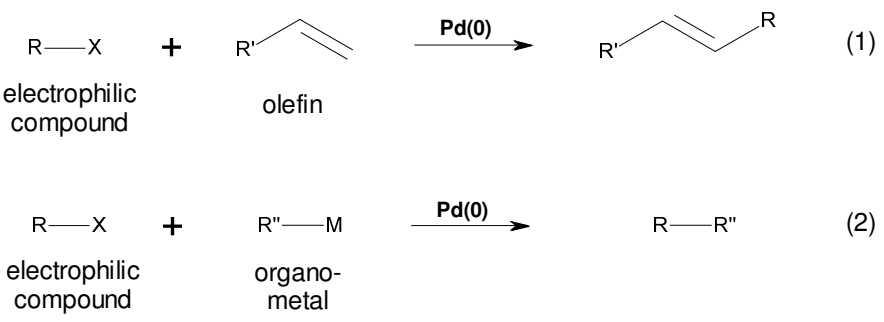

Figure 2-2: Pd-catalyzed cross coupling reactions

It's generally assumed, that most coupling reactions with organometallic nucleophiles follow a similar reaction mechanism, shown as a catalytic cycle in Figure 2-3[16].

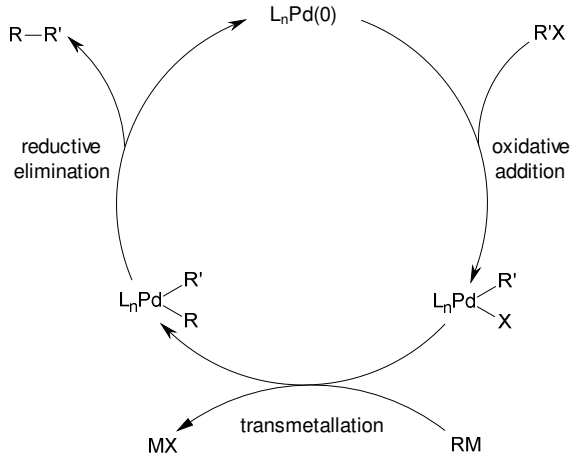

Figure 2-3: Catalytic cycle for C-C cross coupling

Commonly used coupling reactions which employ organometallic nucleophiles are the Suzuki-Miyaura coupling[17], the Stille reaction[18] and the Negishi reaction[19] (Figure 2-4).

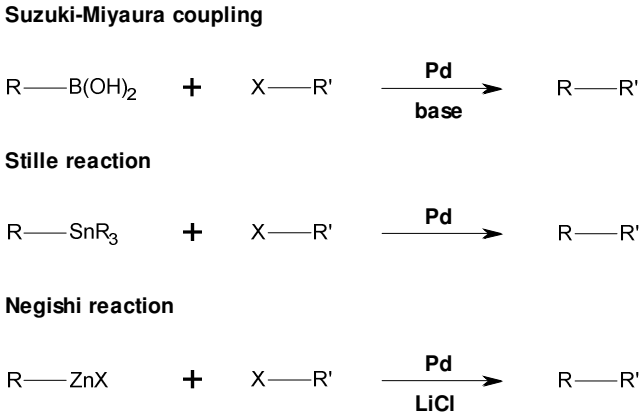

Figure 2-4: Cross coupling reactions employing organometals

Reactions for the coupling of olefins with organohalides are the Heck reaction[20] and the Sonogashira reaction[21] (Figure 2-5). Both reactions can formally be considered as the substitution of a hydrogen atom at an unsaturated bond of an olefin.

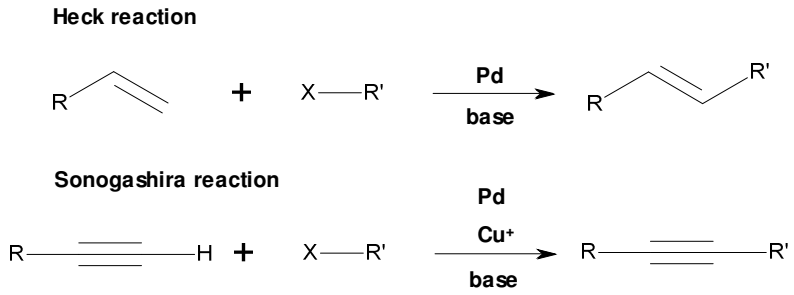

Figure 2-5: Cross coupling reactions employing olefins

Not only carbon-carbon but also carbon-nitrogen bonds can be created using Pd-catalyzed cross-couplings. Examples for such reactions are the Buchwald-Hartwig amination[22] and the Tsuji-Trost reaction[23] (Figure 2-6).

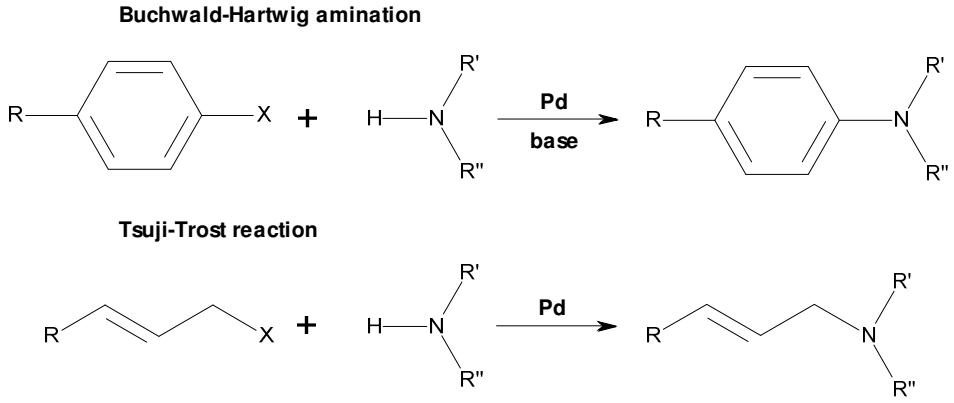

Figure 2-6: Cross coupling reactions for C-N bond forming

In our approach, the Suzuki-Miyaura coupling was employed for testing the catalytic activity of the immobilized Pd-catalyst. This reaction was chosen due to the wide use of this coupling in pharmaceutical and chemical syntheses and because our group has gained much know-how in heterogeneous catalysis of Suzuki coupling reactions[24].

2.3.1 The Suzuki-Miyaura Cross Coupling

The Suzuki-Miyaura coupling is a versatile and widely used reaction for the coupling of organic moieties via formation of a carbon-carbon bond. In contrast to other Pd-catalyzed cross couplings, this reaction allows sp^2-sp^2 couplings (i.e., the production of biphenyl systems), shows no air sensitivity and does not involve toxic compounds[24].

The Suzuki-Miyaura reaction employs a vinyl- or arylboronic acid, which reacts with a vinyl- or arylhalide, and is catalyzed by a palladium(0)-complex[25]. Since organic groups on boron are only weakly nucleophilic, a suitable negatively charged base (e.g. OH^-, CO_3^{2-}, $OtBu^-$) has to be coordinated to the boron atom to increase its nucleophilicity. Although Grignard-like intermolecular transfer reactions are relatively rare, the reactivity of the organoborate is sufficient for the transmetallation to other metals.

The reaction mechanism is generally believed to be divided into three main steps: (a) oxidative addition, (b) transmetalation and (c) reductive elimination (Figure 2-3). It's widely assumed that transmetalation takes place in the *trans*-isomer[25]. This requires the introduction of two isomerization steps (see Figure 2-7), since both oxidative addition and reductive elimination involve the *cis*-isomer[26, 27].

Although several theoretical studies concerning the reaction mechanism of the Suzuki coupling have been published in the last decade[27-30], an entirely evidenced mechanism has not been reported so far. Points of contention are the role of the base, the number of ligands attached to Pd during the process and the *cis/trans* nature of the intermediates. Figure 2-7[27, 29] illustrates a possible associative (i.e. without the release of a ligand during the reaction) *trans* transmetalation mechanism with sodium hydroxide as basic compound. Computational studies by Braga et al.[27] indicate that the exact reaction mechanism depends on the involved ractants.

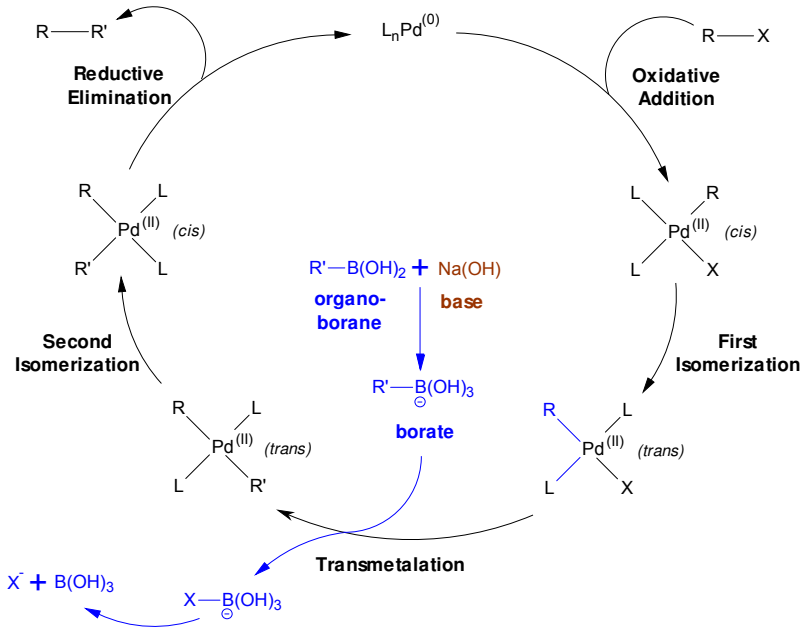

Figure 2-7: Possible associative *trans* transmetalation mechanism for the Suzuki-Miyaura coupling

2.3.2 Heterogeneous Palladium Catalysis

Homogeneous palladium catalysis is widely used in a number of coupling reactions but suffers from a serious problem: to avoid the loss of expensive metal and to exclude contamination of the products, great effort has to be made to recycle the catalyst from the reaction solution.

To address this problem, a vast number of heterogeneous palladium catalysts has been developed over the last years. Various organic and inorganic support materials have been employed to immobilize either metallic palladium or palladium complexes. Examples for solid supports are[16]:

- Activated carbon (charcoal)
- Zeolites and molecular sieves
- Metal oxides (silica, alumina, MgO, ZnO, TiO_2, ZrO_2)
- Clays
- Alkali and alkaline earth salts ($CaCO_3$, $BaSO_4$, $BaCO_3$, $SrCO_3$)
- Porous glass
- Organic polymers
- Polymers embedded in porous glass

This work is mainly inspired by a paper published in 2007 by Kenji Hara et al.[4] who reported the immobilization of a bis(oxazoline)-Pd complex on hydrogen terminated silicon via thermally induced hydrosilylation. This complex, shown in Figure 2-8, will be used as a model molecule to demonstrate the creation of catalytically active patterns on silicon.

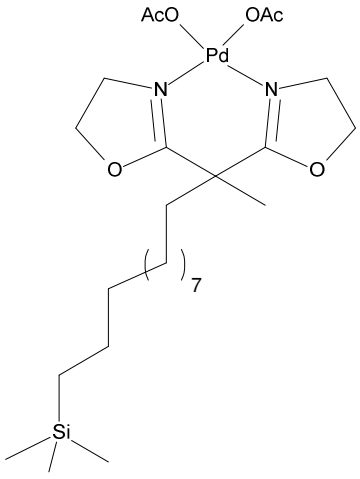

Figure 2-8: Bis(oxazoline)-Pd complex, immobilized on silicon

2.4 Organic Modification of H-Terminated Silicon Surfaces

Since the early 90's, when Linford and Chidsey described first the wet chemical preparation of densely packed, self-assembled alkyl monolayers directly bonded to Si(111) and Si(100) surfaces[31], the attachment of organic groups to hydrogen-terminated Si(111) and Si(100) has been an area of intense research.

There is a number of reasons for the attention paid to this specific system: Firstly, due to their ubiquitous use in microelectronic applications, high quality single-crystal silicon wafers are commercially available and comparatively cheap[32]. Secondly, the preparation of hydrogen-terminated surfaces from native oxidized silicon wafers is relatively easy and can be done under ambient conditions without the need for complex and expensive equipment. The resulting surfaces show excellent chemical homogeneity (>99 % H-termination[5]) and good stability in air for short periods of time[33] and during short water rinse procedures[6, 34]. Finally, Si-H surfaces are reactive towards various organic groups (including 1-alkenes[2, 5, 6, 34], primary alcohols[35], aldehydes[7, 36], 1-alkynes[1] and diacyl peroxides[31]). On the other hand, they are chemically stable in a range of common solvents (e.g., acetonitrile[35], chlorobenzene[2, 5, 6], mesitylene[4] or toluene[36]). This features offer manifold wet chemical strategies for the covalent attachment of organic monolayers to silicon surfaces. Due to the abundant literature on this topic, reviews have been written by Wayner et al.[37], Buriak[32] and, more recent, Ciampi et al.[38] to bring together common functionalization routes and promising applications.

2.4.1 The Silicon Surface

Silicon, like other group IV elements such as carbon and germanium, crystallizes in a diamond cubic crystal structure. This structure can be described as "two interpenetrating face-centered cubic lattices displaced from each other along the body diagonal by a distance equal to one-fourth of its length."[39] The silicon atoms are sp^3-hybridized and bonded in tetrahedral coordination to the four nearest neighbors.

The arrangement of the atoms on the surface of a single crystal silicon wafer depends on its crystal orientation. Si(111) and Si(100) are the most common surface orientations, although other Si(hkl) orientations are known. Figure 2-9 shows silicon unit cells with the (100) plane (a) and the (111) plane (b) and the arrangement of the surface silicon atoms for each orientation (surface atoms are marked red).

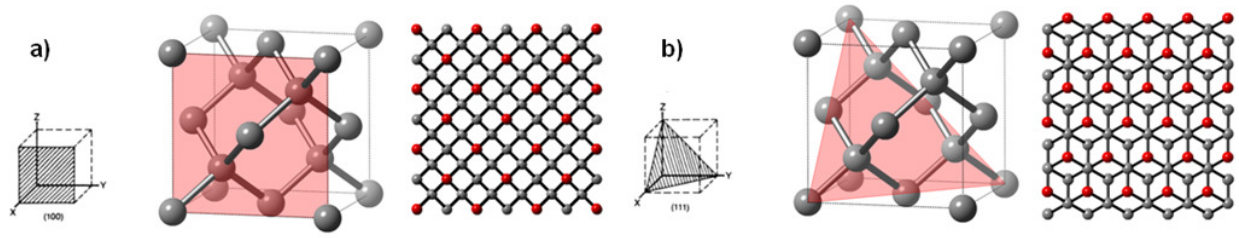

Figure 2-9: Si(100) and Si(111) lattice planes and the arrangement of the surface atoms

The chemistry on silicon crystals is intensely determined by the geometrical and electronic structure of the surface atoms. Each silicon atom on a bulk (100) plane is bonded to two atoms in the plane above and to two atoms in the plane below. Hence, each surface silicon atom on an ideally hydrogen-terminated Si(100) surface is bonded to two bulk-Si and to two hydrogen atoms. In the (111) direction, silicon bulk atoms are arranged in "double layers"[40]. Every atom is bonded to three atoms in the other layer of the double layer and to one atom of the next double layer. Therefore, two configurations of the surface silicon atoms are possible: either every surface atom is bonded to three bulk atoms and to one hydrogen atom or to only one bulk atom and to three hydrogen atoms. Infrared studies showed that wet chemical etching procedures with fluorine containing aqueous solutions (aqueous HF and NH_4F) are able to produce ideally H-terminated Si(111) surfaces with silicon monohydride oriented normal to the surface[41] as well as Si(100) surfaces with silicon dihydride being the most dominant surface species[42]. Figure 2-10 shows models of a Si(100) (a) and a Si(111) (b) surface ideally terminated by monohydride and dihydride, respectively.

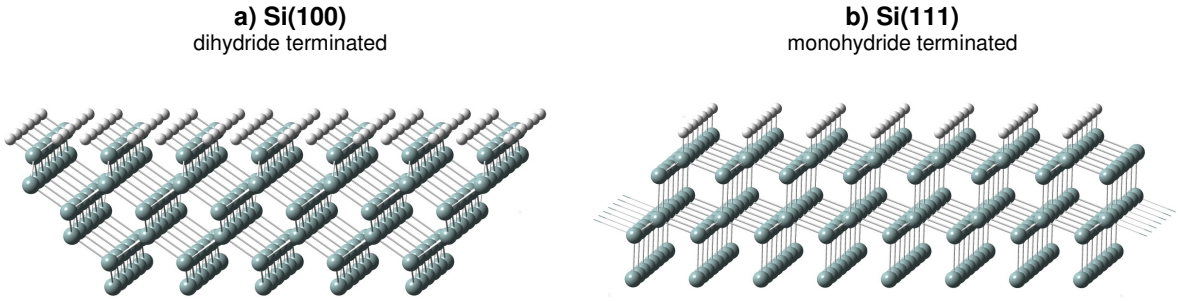

Figure 2-10: Ideally H-terminated Si(100) and Si(111) surfaces

2.4.2 Preparation of H-terminated Silicon (111) Surfaces

As mentioned before H-terminated silicon is the starting material for a range of strategies to bind organic molecules directly to silicon. For these techniques, the preparation of a clean, well defined and homogeneously hydrogen-terminated silicon surface is an essential precondition for successful organic functionalization of silicon wafers.

When silicon is exposed to air, it forms a thin oxide film on the surface, the so called "native oxide layer". The removal of this layer and the simultaneous hydrogen termination of the surface are typically achieved by etching with aqueous, fluorine containing solutions[41]. Over the last years, several critical parameters have been identified which influence morphology, chemical homogeneity and reproducibility of the resulting surface[43, 44]: the cleanliness of the initial wafer[45], the choice of the etchant (HF or NH_4F), the pH value and temperature of the etching solution[46-48], the doping level of the substrate[4950], the angle and orientation of the miscut[47, 48] and dissolved oxygen in the etching solution[51, 52]. The influences of those parameters are discussed in the following chapters.

2.4.2.1 The Cleaning of Silicon Wafers

The aim of wafer cleaning is "the removal of particles and chemical impurities from the semiconductor surface without damaging or deleteriously altering the substrate surface."[53] Contaminations are conventionally classified into: organic contamination, metallic contamination, particle contamination, surface defectivity, atmospheric molecular contamination and moisture[54]. The reduction of surface impurities is a crucial requirement for the creation of high quality H-terminated surfaces. Contaminants act as etching masks in the subsequent wet chemical etching and lead to chemically and morphologically inhomogeneous surfaces[45].

Commonly used techniques to achieve a clean surface are wet chemical, plasma, dry-physical, vapor phase and supercritical fluid methods. The majority of cleaning and conditioning processes are done in aqueous solutions using hydrogen peroxide mixtures. A frequently used technique is the cleaning in hot piranha solution, a mixture (by volume) of 4:1 to 1:1 sulfuric acid (96 wt%):hydrogen peroxide (30 wt%) for 10 minutes at temperatures above 100 °C[44, 45, 51, 55]. However, the most commonly used method is the RCA (Radio Corporation of America) cleaning process, designed

by Kern et. al and first published in 1970[53]. This method is based on the use of two "standard cleaning"-solutions, SC-1 and SC-2.

The SC-1 solution is a mixture of ultrapure water, hydrogen peroxide and ammonium hydroxide. The originally reported composition ranges from 5:1:1 to 7:2:1 parts by volume of H_2O:H_2O_2(30 wt%):NH_4OH(27 wt%). Cleaning is carried out at 70-75°C for 10-20 minutes followed by a careful rinse with water. The SC-1 solution was designed to remove organic impurities and particles from the surface. Both, the solvating action of NH_4OH as well as the oxidizing capability of the H_2O_2 attack organic contaminants: ammonium hydroxide dissolves the thin native oxide layer on Si at a very low rate, while the hydrogen peroxide oxidizes the surface, forming a new chemical oxide layer at nearly the same rate. The sequential etching and growth of the surface facilitates the removal of impurities and particles. Moreover, ammonium hydroxide acts as complexing agent for a number of metals.

The SC-2 solution is used to remove residual alkali, trace metals and metal hydroxides. This solution is a mixture by volume of between 6:1:1 and 8:2:1 of ultrapure water, hydrogen peroxide (30 wt%) and hydrochloric acid (37 wt%). The cleaning conditions are the same as for the SC-1 cleaning step (70-75°C, 10-20 minutes, subsequent water rinse). Reattachment of the dissolved metals is prevented by the formation of soluble metal complexes with the dissolved ions.

For both solutions, the exact composition is no critical parameter for efficient cleaning. Hence, the RCA cleaning process is a very simple and robust method to produce clean silicon surfaces for further processing.

2.4.2.2 Etching of Silicon Surfaces

The removal of the native oxide layer from silicon and the termination of the surface by atomic hydrogen are commonly achieved by treating the surface with aqueous, fluorine containing solutions.[38] Whereas etching of Si(100) with dilute hydrofluoric acid (1 %, pH = 2) leads to predominately dihydride terminated surfaces[42], the preferred etchants for the preparation of ideally monohydride terminated Si(111) surfaces are aqueous ammonium fluoride solutions (40 wt%, pH = 7,8)[43].

The morphology and the chemical properties of H-terminated Si(111) surfaces depend drastically on the pH-value of the etching solution. Etching of Si(111) with concentrated or diluted hydrofluoric acid (pH ≤ 2) results in the formation of completely H-terminated surfaces. However, these surfaces are microscopically rough and

chemically not uniform. IR-spectra taken from HF-etched Si(111) indicated that the surface is terminated by mono-, coupled mono-, di- and trihydrides[41]. The microroughness of the surface was evidenced by scanning tunneling microscopy[48].

Figure 2-11 shows possible surface structures on Si(111) at steps toward the $\langle \bar{1}\bar{1}2 \rangle$ and the $\langle 11\bar{2} \rangle$ direction.

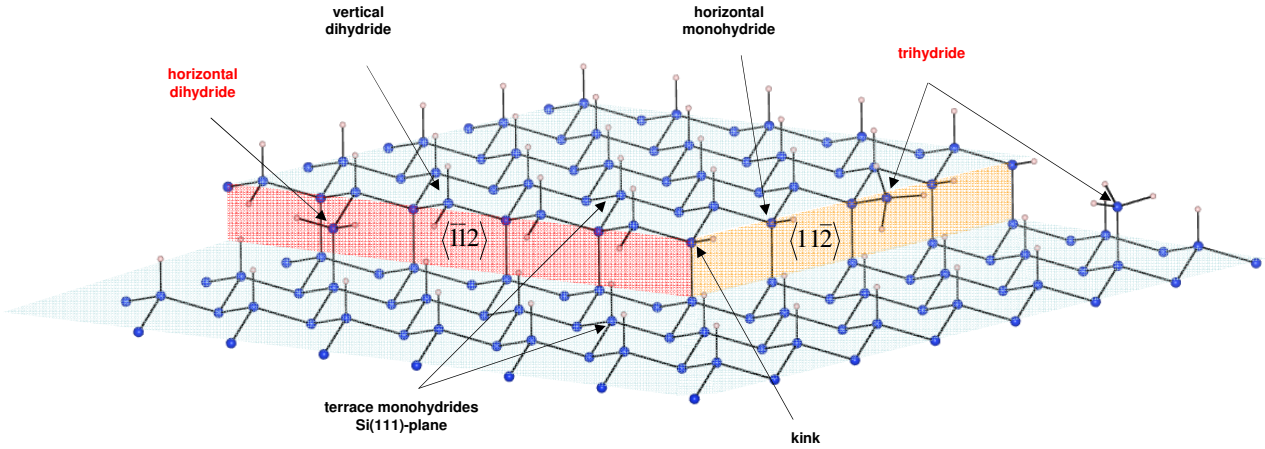

Figure 2-11: Possible surface structures on H-terminated Si(111) after removal of the native oxide layer

In contrast, the use of highly basic NH_4F solutions leads to perfectly monohydride terminated surfaces. Moreover, the surface is significantly flattened during NH_4F-etching.

This smoothening is based on the mechanism of bulk silicon etching. Etching in concentrated HF solutions leads to a fast and efficient removal of the native oxide layer and H-termination of the initial oxide/substrate interface. However, the etching process stops when H-termination is achieved. On the other hand, usage of diluted HF or basic NH_4F solution induces a slow etching reaction and Si dissolution from the H-terminated surface.

Wet chemical etching occurs through sequential oxidation and etching steps, which are assumed to be the following[56]:

Oxidation: $(\equiv Si)_3Si\text{-}H + OH^- + H_2O \rightarrow (\equiv Si)_3Si\text{-}OH + H_2 + OH^-$ **Eq. 1**

Etching: $(\equiv Si)_3Si\text{-}OH + 3\ HF \rightarrow 3\ (\equiv Si\text{-}H) + SiF_3OH$ **Eq. 2**

Although slightly different mechanisms have been published (particularly regarding the chemical structure of the leaving silicon-compound[43, 57]), it is widely accepted that the initial oxidation step is rate determining. This assumption is confirmed by the full H-termination and the absence of oxides, which would be formed by condensation of vicinal silanol groups. Additionally, it was shown that the reaction rate of the oxidation reaction is linearly dependent on the concentration of OH^- ions and independent of the fluoride concentration[56].

NH_4F-etching is a highly anisotropic process. This means that defect sites on the surface (steps, kinks) are rapidly attacked while the flat (111)-surface is left essentially unetched. Different explanations for this site specificity have been proposed. While Allongue et al.[55] suggested that steric reasons are responsible for different site reactivities, Hines et al.[56] assumed that the different ability of various surface species to form a pentavalent transition state plays the key role. Anyway, kinetic Monte Carlo simulations have shown that etching on the most reactive site, the kink site, is 10^7 times faster than terrace etching[56]. Also step edges are etched at least 1000 times more rapid than terraces. This eventually leads to the formation of large surface domains, which are atomically flat and ideally monohyride terminated.

The above mentioned surface roughening, which occurs if etchants with relatively low pH-values (e.g. diluted or concentrated HF) are used, can be explained by the influence of a common impurity in the etching solution: dissolved oxygen. Dissolved oxygen reacts slowly with H-terminated silicon surfaces, introducing a second, competing oxidation reaction which corresponds to[52]:

O_2-Oxidation: $(\equiv Si)_3Si\text{-}H + \frac{1}{2}O_2(aq) \rightarrow (\equiv Si)_2(=SiO)Si\text{-}H$ **Eq. 3**

The following etching reaction is the same as for NH_4F-etching. O_2-oxidation is much less site specific than the OH^--attack. Consequently, O_2-induced oxidation also occurs at flat terrace sites and leads to the formation of surface defects and ultimately to generation of etch pits and microscopic surface roughening.

Thus, the surface morphology is determined by kinetic competition between the above mentioned oxidation mechanisms. This competition is schematically illustrated in Figure 2-12. At high pH values, highly anisotropic etching by OH^- will be the dominant reaction, whereas oxidation by dissolved oxygen will gain importance at low pH

values (i.e. low OH^- concentration) or in O_2-saturated solutions (i.e. high O_2 concentration).

This also means that removal of oxygen from the etching solution will improve significantly the quality of the resulting surface, which has been confirmed by STM-imaging[51] and atomic force microscopy (AFM)[58]. Elimination of dissolved oxygen is generally achieved by two techniques: purging the etchant with inert gas, commonly argon[51, 52], or adding of ammonium sulfite as deoxygenator to the solution[44, 58].

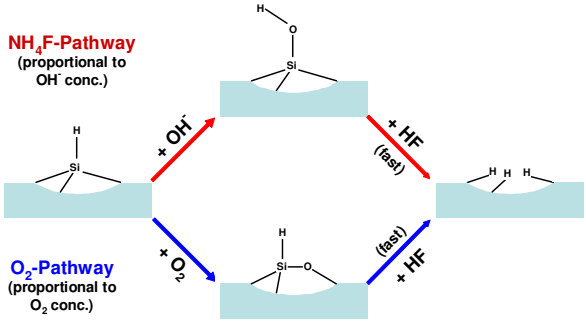

Figure 2-12: Competition between OH^- and O_2 attack on hydrogen terminated silicon (modified from [52])

Furthermore, it has been shown, that atomically flat surfaces can exclusively be prepared with low doped silicon whereas the use of highly doped wafers leads to surface roughening[49]. This roughening can be explained by the relevance of another, so-called electrochemical etching pathway, which involves proton release from the surface and electron injection into the silicon conduction band. The electrochemical etching mechanism is much less site specific than the above mentioned, purely chemical mechanism and becomes enhanced with increasing doping level of the substrate. The dominance of this more isotropic reaction pathway is assumed to be the reason for surface roughening on highly doped silicon.

2.4.3 Creation of Si-C bonded Monolayers on H-Si(111)

As mentioned before, hydrogen terminated silicon surfaces are reactive towards a range of unsaturated organic groups via so-called hydrosilylation reactions. Especially the covalent attachment of Si-C linked monolayers has gained much attention due to the high stability of the silicon carbon bond towards various organic solvents, acidic and basic aqueous solutions and ambient air[31, 59, 60]. Surface hydrosilylation on H-terminated silicon can be performed by wet chemical approaches, chemomechanical methods (wetting and scribing with AFM or STM tips)[61-63] or ultra high vacuum (UHV) reactions[64]. Wet chemical strategies require, at least compared to UHV and

AFM/STM methods, a relatively low expenditure on equipment but yield good and reproducible results. Thus, wet chemical procedures are most commonly used to prepare monolayers on silicon.

Linford and Chidsey were the first to create Si-C bonded monolayers on hydrogen terminated Si(111) via hydrosilylation of unsaturated alkyl chains (1-alkenes) using diacylic peroxides or heat as initiator of the reaction[31, 34]. Ellipsometric results, Infrared spectroscopy, X-ray photoelectron spectroscopy (XPS) and stability tests showed that the resulting organic layer was of monomolecular thickness, covalently bonded via Si-C linkage, densely packed, highly ordered and stable in hot organic solvents as well as in aqueous basic and acidic solutions. Such monomolecular, highly organized layers are often reffered to as “self-assembled monolayers” (SAMs). The attachment of monolayers on silicon can be understood either as a passivation or as an activation of the surface. On the one hand, organic monolayers protect the substrate from oxidation and help to control the physical surface properties. On the other hand, surface hydrosilylation provides a range of routes to bind functional molecules directly and covalently to the silicon substrate. Over the last years, a wide variety of molecules, for example cyclodextrines for the creation of molecular recognition devices[3], catalytically active organometallic complexes[5] or their organic precursors[4] and biomolecules (proteins[6], DNA[65], carbohydrates[66]) could be attached successfully to silicon.

Wet chemical attachment of organic monolayers to H-Si surfaces can be achieved by one of the following methods[32].

- Hydrosilylation involving a radical initiator
- Thermally induced hydrosilylation
- Photochemical hydrosilylation using UV-light or white light
- Hydrosilylation mediated by metal complexes
- Reactions with alkyl/aryl carbanions
- Electrochemical grafting

2.4.3.1 Hydrosilylation involving a Radical Initiator

Hydrosilylation reactions occur through insertion of an unsaturated bond into a Si-H group. The usage of 1-alkenes and 1-alkynes as unsaturated compounds leads to alkyl and alkenyl termination, respectively (Figure 2-13)[32].

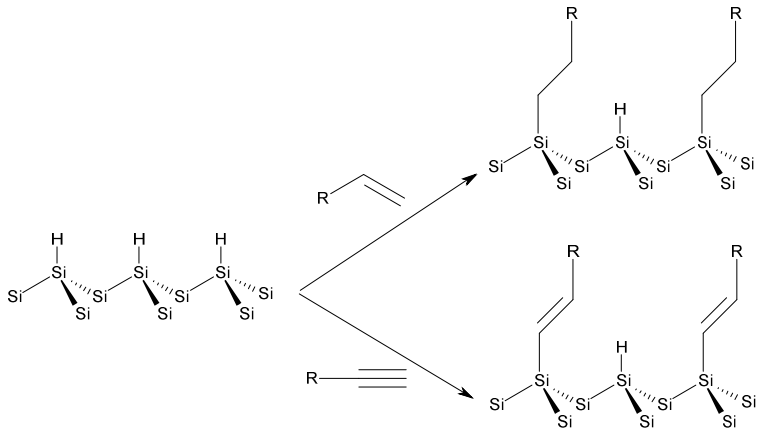

Figure 2-13: Reaction of 1-alkenes and 1-alkynes with the hydrogen terminated Si(111) surface

The initiation of this reaction by radical initiators was the first method developed to create monolayers on crystalline silicon surfaces[31]. The proposed surface propagated radical chain mechanism (suggested by Linford and Chidsey[31] and based on analogous gas-phase reactions in organosilane chemistry[67]) starts with the creation of a surface silyl radical (silicon dangling bond), initiated by radical precursors at elevated temperatures. This silicon radical reacts with the terminal double bond of the alkene, creating a β-carbon centered radical on the attached molecule. The secondary alkyl radical can abstract hydrogen at an adjacent Si-H group. This leads to the formation of a new dangling bond and, thus, to the initiation of the next hydrosilylation step.

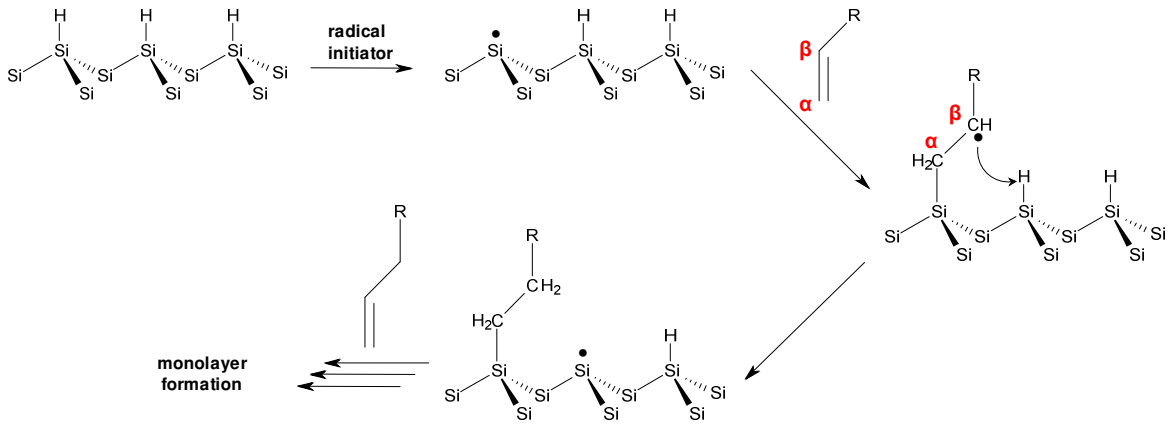

Figure 2-14: Radical chain mechanism of the surface hydrosilylation reaction

The radical chain mechanism was confirmed by UHV-STM analysis[68-70]. Whereas alkene reactions on 2x1 reconstructed, H-terminated Si(100) surfaces form one-

dimensional lines of chemisorbed molecules along one side of a silicon dimer row[70], hydrosilylation on H-Si(111) leads to the formation of compact islands of hydrocarbon adsorbates due to the hexagonal array of the silicon surface molecules[68, 69]. The dependence of the direction of monolayer growth on the geometrical arrangement of the surface silicon atoms indicates strongly the major role of interactions between the attached molecule and adjacent H-Si groups. Although these observations were made under UHV- and not under wet chemical conditions, the results are in good agreement with the suggested radical chain mechanism.

Examples for successfully used radical precursors are: diacylic peroxides[34], azo-bis-(isobutyronitrile) (AIBN), 1,1'-azobis(cyclohexanecarbonitrile) (ABCN) and (2,2,6,6-Tetramethylpiperidin-1-yl)oxyl (TEMPO)[4]. The chemical structures of these radical initiators are shown in Figure 2-15.

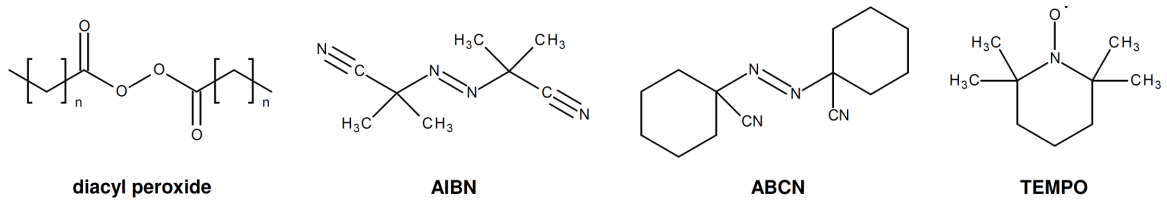

Figure 2-15: Radical initiators used for surface hydrosilylation

2.4.3.2 Thermally Induced Hydrosilylation

The formation of alkyl monolayers on H-Si(111) occurs also in the absence of radical starters at higher temperatures (150 – 200°C) [34]. From a mechanistic point of view, the reaction is analogous to that in the presence of a radical precursor with the first silyl radical being produced through thermal induced homolytic cleavage of the Si-H bond.

Thermal hydrosilylation is a simple and straightforward method but suffers from some major limitations. Creation of high quality monolayers requires the use of neat alkenes[32], which is acceptable for simple and relatively cheap alkenes but problematic for more complex molecules that are rather expensive or difficult to synthesize. The formation of well defined monolayers from diluted alkenes has only been reported for the Si(100) surface with mesitylene as solvent[71].

Furthermore, this technique is categorically inappropriate for the direct attachment of thermally sensible molecules.

2.4.3.3 Photochemical Hydrosilylation using UV-Light or White Light

Photochemical initiation of hydrosilylation reactions is well known in the organic and metallorganic chemistry. Terry et al.[72, 73] were the first, who carried out alkene hydrosilylation on flat H-Si(111) surfaces by irradiation with UV-light. Photochemical hydrosilylation occurs at room temperature and provides monolayer attachment strategies with minimal thermal input[74].

A wide range of terminal alkenes can be attached via UV-initiation from the neat olefins. Densely packed and well ordered monolayers occur within one hour of irradiation, which was evidenced by FTIR and ellipsometric measurements[1].

In contrast to thermally induced hydrosilylation several approaches have been reported in which organic layers were successfully attached from diluted solutions of 1-alkenes in various solvents including toluene[3, 75], cyclohexane[6] and chlorobenzene[5, 6]. The possibility to use diluted alkenes in combination with the thermally mild reaction conditions makes photoactivated hydrosilylation to the method of choice for the attachment of more complex organic molecules. Moreover, the formation of SAMs occurs only at light exposed areas whereas non irradiated parts remain completely reactive[7]. This invites photopatterning techniques in order to create laterally defined functional domains.

White light promoted hydrosilylation has first been observed by Stewart et al.[76, 77] on porous silicon but has also been reported more recently on crystalline Si(111) and Si(100)[78, 79]. The reaction on crystalline silicon occurs at room temperature but is significantly slower than UV-induced hydrosilylation. Irradiation times of five hours and more[79] are needed to create monolayers with physical properties comparable to those of SAMs created by UV-irradiation. However, due to the mild reaction conditions (room temperature, wavelengths up to 658 nm[79]), hydrosilylation driven by visible light is a promising strategy to directly attach sensible molecules, such as proteins or DNA, to the crystalline surface.

The mechanism of UV-induced hydrosilylation is assumed to be identical to the above mentioned radical chain mechanism[1]. The initial silyl radical is created by photolytic homolysis of a surface Si-H bond (Figure 2-16 a). However, homolytic dissociation can not be the introducing step of white light mediated hydrosilylation: based on the dissociation energy of the silicon-hydrogen bond (79[80] - 84[81] kcal mol^{-1}, determined from tris(trimethylsilyl)silane), Si-H homolysis requires wavelengths shorter than 360 nm. The occurrence of hydrosilylation at longer wavelengths and

the fact that optimal monolayer formation from octadecene takes place at 385 nm[7] indicate that the photohomolytically induced radical chain reaction is not the only mechanism which leads to photoinitiated SAM formation. The invalidity of the radical chain mechanism for white light hydrosilylation was confirmed by mechanistic studies using radical traps, which did not show the presence of surface radicals during the reaction[77].

Stewart et al.[77] proposed an exciton mediated mechanism for hydrosilylation on nanocrystalline silicon (Figure 2-16 b). The first step in this mechanism is the production of a hole-electron (h^+/e^-) pair, a so-called exciton by light absorption and the formation of a positive charge localized at a surface silicon atom. This silyl cation is prone to reactions with nucleophiles. Nucleophilic attack by terminal alkenes results in the formation of a Si-C bond and creates a β-carbokation, which can abstract a hydride, formally the product of a hydrogen atom and the electron from the exciton h^+/e^- pair, from an adjacent hydridic Si-H bond. This leads to the formation of a C-H bond at the β-carbon and completes the hydrosilylation reaction. Langner et al.[2] suggested that the exciton mechanism is also accountable for hydrosilylation under UV light since the photoinduced reaction could be observed on oxide free H-terminated Si(111) but not on a oxidized H/SiO_2/Si(100) surface. Simple photohomolysis of Si-H bonds should result in functionalization of both surfaces. The unreactivity of oxidized silicon was explained as follows: the oxide insulating barrier inhibits the diffusion of excitons from the substrate towards the surface and, thus, suppresses the first step of the reaction.

Plausible alternative reaction mechanisms are based on radical formation from impurities in the reaction solution[69], appearance of delocalized radical cations and subsequent Si-Si bond cleavage (Figure 2-16 c)[79] or photoemission of electrons from the surface[82]. All in all, one can say that, although light promoted hydrosilylation is a widely used technique, the exact reaction mechanism still remains a matter of controversy.

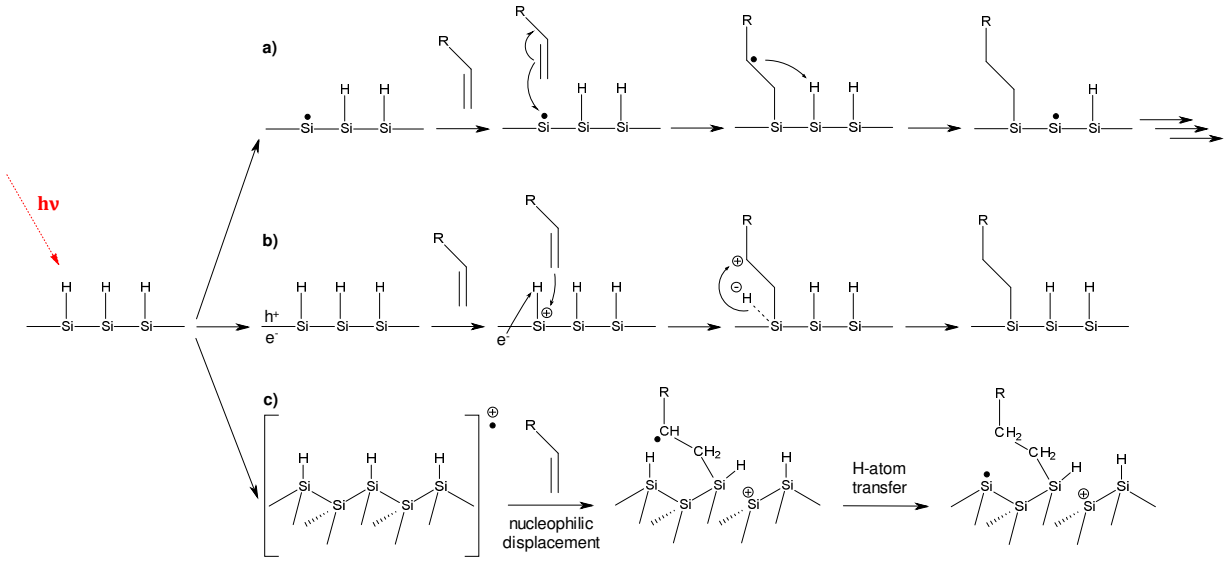

Figure 2-16: Proposed mechanisms of photoinduced hydrosilylation: (a) radical chain mechanism[1], (b) exciton mediated mechanism[77], (c) mechanism involving delocalized radial cations[79]

2.4.3.3.1 Side reactions competing with Si-C bond formation

Although H-terminated silicon is stable in air for short periods of time, extended storage under ambient conditions leads to continuous oxidation and finally results in a completely oxidized surface. The rate of this reaction is strongly dependent on the humidity of the ambient air, indicating that the surface is prone to water induced oxidation. A mechanism of this oxidation was suggested by Miura et al.[83]. The reaction starts with the creation of a Si-OH group via a pentavalent silicon species formed by electron donation from a water molecule to the silicon conduction band[37]. Subsequently, the oxygen atom is inserted into a Si-Si back bond and the terminal Si-H bond is regenerated. This process is repeated until all silicon back bonds are oxidized (Figure 2-17).

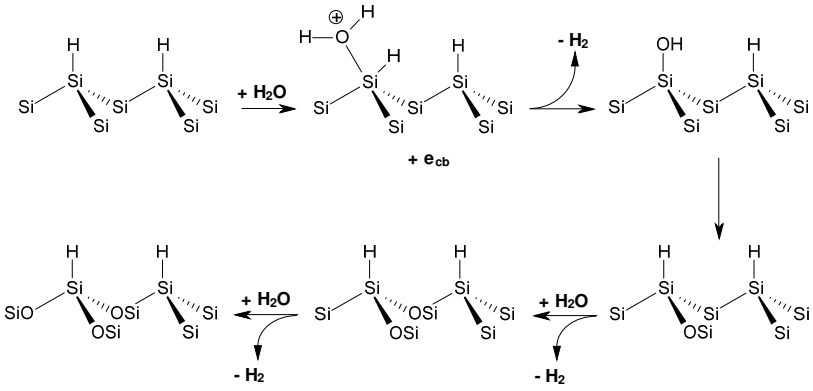

Figure 2-17: Water induced oxidation of H-Si(111)

The insertion of oxygen into the silicon back bonds was confirmed by infrared studies which showed that $(SiO)_3Si$-H groups are the predominant surface species after oxidation in humid air.

Especially under photochemical conditions not only water, but also molecular oxygen itself induces surface oxidation. Cicero et al.[1] performed photooxidation experiments in ambient air and found that this reaction is UV-activated and requires irradiation with wavelengths of about 350 nm or lower. In the same paper it was shown that not only gaseous oxygen but also dissolved oxygen in reaction solutions cause considerable surface oxidation. While photoinduced hydrosilylation reactions (λ = 254 nm) with deoxygenated 1-alkenes yielded high quality alkyl monolayers, the same experiment with oxygen saturated 1-octene resulted in the formation of a highly oxidized surfaces with almost no attachment of organic molecules. These findings indicate that dissolved oxygen is much more reactive with the H-Si surface than 1-alkenes.

Due to the strong wavelength dependence of photooxidation with a threshold near 350 nm, Cicero supposed a free radical mechanism similar to the radical chain mechanism proposed for alkene hydrosilylation. Although further oxidation reactions, including oxygen insertion into Si back bonds and radical chain termination were not described in detail in this work, it seems clear that the resulting surface is terminated mainly by silanol (Si-OH) groups, since photooxidized areas readily react with octadecyltrichlorosilane[84].

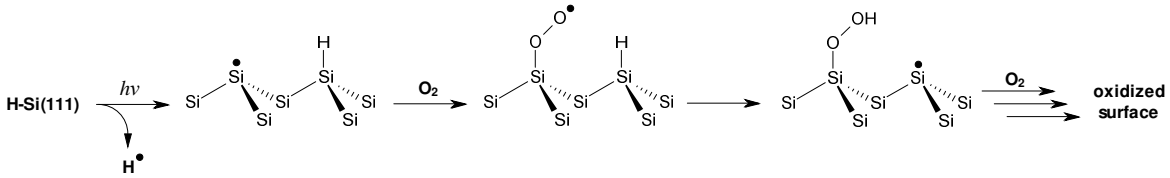

Figure 2-18: Photooxidation of H-Si(111)

The high affinity of the H-Si(111) surface towards oxidation under photochemical conditions makes it indispensible to thoroughly exclude both oxygen and water from the reaction solution.

Considering a radical chain mechanism for Si-C bond formation, one could assume that radical polymerization of the terminal alkenes could be a notable side reaction. However, even if styrene or phenylacetylene, two readily polymerizable substrates, are photolytically attached, no significant polymerization can be observed; the thick-

ness of the organic coverage never exceeds one monolayer, even after 5 hours of irradiation[1].

2.4.3.4 Hydrosilylation Mediated by Metal Complexes

The utility of late transition metal complexes as hydrosilylation catalysts was examined on flat H-terminated Si(100) and porous silicon[32]. Platinum-, rhodium- and palladium complexes have been used with moderate success. Although alkyl termination could be obtained, at least on porous silicon using rhodium catalysts[85], this technique suffers from some major limitations: even if considerable care is taken to reduce the amount of dissolved oxygen in the reaction solution, substantial oxidation of the surface occurs. Moreover, transition metal catalysts can cause side reactions with the solvent and post contamination of the surface with elemental metals is not inconceivable[2].

The use of Lewis acids (e.g., $EtAlCl_2$) to catalyze hydrosilylation on porous silicon is a well established approach[86]. On crystalline surfaces this synthesis could not gain as much attention as other strategies presumably due to the comparatively low surface coverage, the need of elevated temperatures (100 °C) and the relatively long reaction times (18 h).

2.4.3.5 Reactions with Alkyl/Aryl Carbanions

Creation of Si-C bonded organic monolayers on flat H-Si(111) with alkyl Grignard or alkyllithium carbanions can be done either directly, using alkylmagnesium bromide[87], or following a two step halogenation (chlorination[88], bromination[89])/alkylation strategy. Both routes yield stable monolayers but require moderate heating (60 – 85 °C) and, depending on the chain length of the alkyl group, partially very long reaction times (up to 8 days[90]).

2.4.3.6 Electrochemical Grafting

Electrochemical attachment is another technique to bind organic molecules covalently to the Si surface. Allongue and coworkers described a cathodic process, which yields phenyl monolayers by reduction of commercially available diazonium salts[91, 92]. The mechanism of this reaction is proposed to be as follows (with X = NO_2, Br, COOH, CN):

$$X\text{-}Ar\text{-}N^{+}\equiv N + e^{-} \rightarrow X\text{-}Ar^{\bullet} + N_2 \qquad \textbf{Eq. 4}$$

$$\equiv Si\text{-}H + X\text{-}Ar^{\bullet} \rightarrow \equiv Si^{\bullet} + X\text{-}Ar\text{-}H \qquad \textbf{Eq. 5}$$

$$\equiv Si^{\bullet} + X\text{-}Ar^{\bullet} \rightarrow \equiv Si\text{-}Ar\text{-}X \qquad \textbf{Eq. 6}$$

The resulting layers have proven to be of monomolecular thickness, linked via Si-C bonds and stable against 40% HF. In contrast to the above mentioned wet chemical approaches, cathodic electrografting can be done in aqueous solutions. Due to the electron rich surface, nucleophilic attack by water does not lead to oxidation but to abstraction of a hydrogen atom from a water molecule and to regeneration of the hydride termination.

$$\equiv Si\text{-}H + H_2O + e^{-} \rightarrow \equiv Si^{\bullet} + H_2 + OH^{-} \qquad \textbf{Eq. 7}$$

$$\equiv Si^{\bullet} + H_2O + e^{-} \rightarrow \equiv Si\text{-}H + OH^{-} \qquad \textbf{Eq. 8}$$

2.4.4 Lateral Patterning of SAMs on Silicon Surfaces

The fabrication of multifunctional heterogeneous catalysts requires not only routes for the reliable and reproducible immobilization of the active molecules but also techniques that make laterally defined deposition of the catalytic species possible.

On silicon substrates, several strategies for the creation of spatially defined functionalized areas have been developed. Patterned monolayers can generally be created either by locally controlled synthesis of the layer or by partial removal of the organic coating from an entirely covered surface. Reported structuring methods are based on various physical principles and pursue manifold objectives, for example the control of the wetting properties of the silicon substrate[84], the formation of organic resists for metal deposition[93] or the creation of biofunctional patterns for the use in biosensors and biosensor arrays[75]. Routes for silicon surface patterning include:

- Photolithographic techniques (UV and white light)
- Chemomechanical and electrochemical patterning
- Electron beam lithography
- Nanoshaving with AFM tips

2.4.4.1 Photolithographic Methods

Since UV and white light promoted hydrosilylation occurs only at illuminated areas while non-exposed parts remain H-terminated, this method invites surface patterning by simple masking procedures.

Effenberger et al.[7] were the first who generated patterned monolayers on Si(111) by partially illuminating the H-terminated surface with UV-light through a photomask in the presence of melted octadecanal. Taking advantage of the different hydrophilicity of coated and non coated wafer parts, the patterned structure could be observed directly under an optical microscope when the surface was wetted with a mixture of isopropanol and lubricating oil. The non polar oil aggregates at the highly hydrophobic octadecyl-coated wafer parts, coloring these areas dark (see Figure 2-19). Furthermore, it could be demonstrated, by means of FTIR-spectra, that the non irradiated areas remain hydrogen terminated.

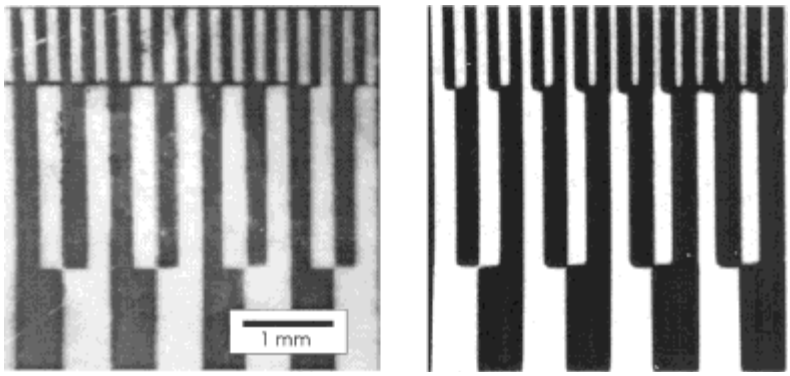

Figure 2-19: Optical microscopy picture of a patterned octadecyl monolayer (left) and the corresponding mask[7]

Wayner and coworkers[75, 84, 94] reported another patterning strategy: irradiation of the H-terminated surface in ambient air leads to oxidation of the exposed areas whereas non irradiated wafer parts can be reacted with unsaturated hydrocarbons in a subsequent thermal or photochemical hydrosilylation process. The resulting patterned monolayers can be the fundament for further reactions, for example the attachment of polythiophenes or single strand DNA. The successful patterning was visualized by optical microscopy after exposure to water vapor, scanning auger electron spectroscopy, atomic force microscopy and scanning electron microscopy.

On porous silicon, white light promoted photopatterning was successfully applied[76]. The identification of the exposed areas can be done very conveniently since the

monomolecular organic layer significantly alters the photoluminescence properties of the porous silicon surface.

2.4.4.2 Chemomechanical and Electrochemical Patterning

Nanoscale patterns of alkyl and alkenyl monolayers on H-Si(111) can be created employing AFM tips.

Wacaser et al.[63] described a chemomechanical method to generate functionalized lines with widths down to 30 nm. Scribing of a H-terminated Si(111) surface with a AFM tip leads to mechanical breakage of Si-H or Si-Si bonds, producing a localized chemically active surface. This surface can react with various molecules, for example 1-alkenes and primary alcohols, and bind them covalently to the surface. The dimension of scribed lines (30 – 400 nm) can be controlled varying the force applied by the AFM tip and the tip shape.

AFM tips can also be used to perform an electrochemical cathodic electrografting reaction on the H-Si surface[62]. This reaction occurs, when the surface is biased (-) and the AFM tip is biased (+) in the presence of excess terminal alkynes. As the anodic tip is moved along the surface, lines of the immobilized alkyne (40 – 300 nm in diameter, controlled by varying the shape of the AFM tip) are drawn. Since the cathodically biased silicon surface is well protected against water induced oxidation (see Eq. 7 and Eq. 8), the reaction can be carried out in ambient air with moderate humidity levels (< 27%).

2.4.4.3 Electron Beam Lithography

In contrast to the above mentioned patterning techniques, electron beam lithography aims not at a spatially controlled synthesis of organic layers but is based on the local removal of an already existing coating by the electron beam.

Patterned monolayers created in this way can be used as a kind of positive tone resist for further surface modification. Balaur et al.[93] showed that copper attachment by immersion plating or electrodeposition on Si(111) occurs only at monolayer free patterns, which were created from a fully monolayer covered surface. Harnett et al.[95] reported a strategy to produce bioactive templates on H-Si(111). An inert monolayer was partially removed from the surface by e-beam exposure. The monolayer free areas were backfilled with an amine terminated monolayer, which was the starting point for the subsequent attachment of bioactive molecules.

2.4.4.4 Nanoshaving and Nanoscratching

Not only electron beams can be used to remove organic monolayers locally from the underlying substrate. Also the nanoshaving technique, the mechanical detachment of SAMs by scanning a sharp AFM tip with a high load over defined surface regions, can be applied to create patterned monolayers on silicon[96].

Another patterning method which involves mechanical treatment of the surface is nanoscratching[97]: an AFM tip is used to scratch hydrogen terminated silicon creating Si-H and SiO_2 surfaces at different locations. Subsequent thermal hydrosilylation with 1-alkenes leads to monolayer formation on all surfaces except the scratched areas.

Table 2-1 summarizes the main characteristics of the different patterning techniques. Among the mentioned techniques, photolithography is the only method which can be carried out with comparatively simple equipment (i.e. without the use of atomic force or electron microscopes). Given that non-irradiated areas remain H-terminated and, thus, reactive during the lithographic process, step-by-step functionalization with various molecules in a laterally controlled fashion should be possible. Since this work does not focus explicitly on creating structures at the nanoscale, spatial resolution achievable by lithographic methods is absolutely sufficient for our purposes. Overall, one can say that lithographic patterning is the method of choice for our approach.

Table 2-1: Different methods for the formation of patterned monolayers on silicon

Method	Laterally defined SAM creation/displacement	Physical principle	Pattern sizes	References
UV- and White Light Lithography	Creation	Photoinduced hydrosilylation/ oxidation	Several micrometers to millimeters	7, 75, 76, 84, 94
Chemomechanical Patterning	Creation	Mechanical cleavage of surface bonds	30 nm to several micrometers	63
Electrochemical Patterning	Creation	Cathodic electrografting	40 – 300 nm	62
Electron beam Lithography	Displacement	Electronic sputtering	250 nm to several micrometers	93, 95
Nanoshaving	Displacement	Mechanical scraping	nanoscale	96
Nanoscratching	Displacement of the initial H-termination	Mechanical scraping	nanoscale	97

3 APPROACH

The aim of this work was the creation of spatially defined catalytically active areas on silicon (111) surfaces. This should be achieved by the covalent attachment of organic ligands to a hydrogen terminated Si(111) wafer employing a UV-induced hydrosilylation reaction. Since hydrosilylation occurs only at UV-light exposed parts, the formation of functionalized patterns can be achieved by irradiating the surface through lithographic masks.

The first task was the design of a lithographic unit which allows the creation of organic SAMs on H-Si(111) in a laterally controlled manner.

The second step was the immobilization of a bis(oxazoline) ligand which is capable of binding to palladium acetate in a subsequent metalation reaction (Figure 3-1). The resulting organometallic complex is known to catalyze cross coupling reactions[24] as well as the aerobic oxidation of benzylic alcohols[4].

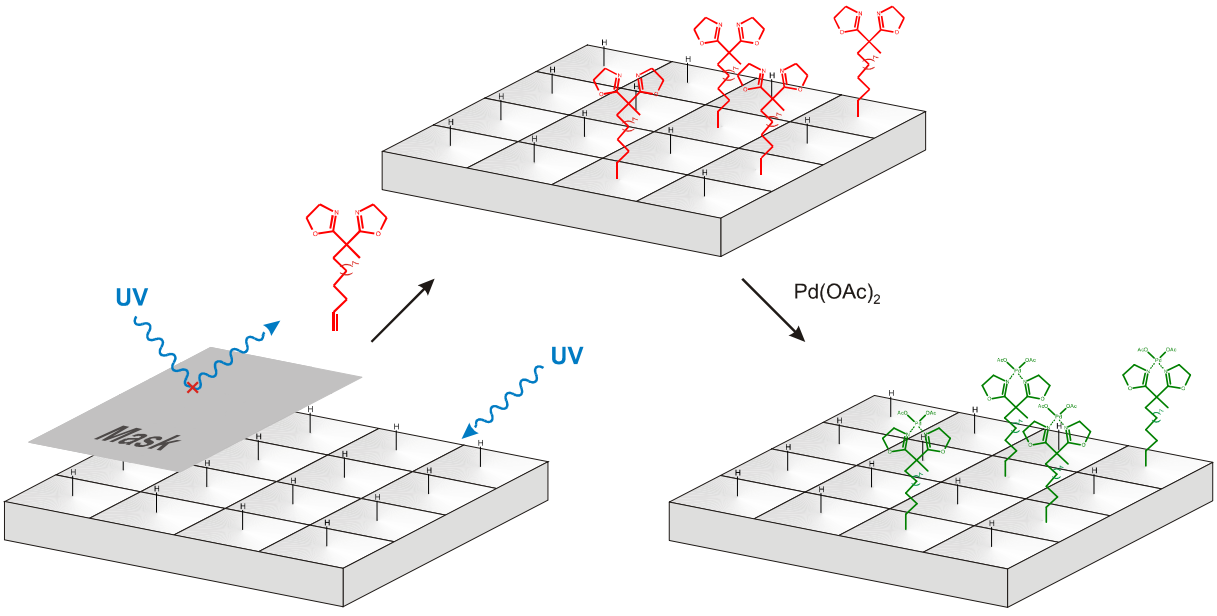

Figure 3-1: Immobilization of a Pd-BOX-complex on Si(111) via UV-lithography

The functionalized surfaces were characterized using optical microscopy, goniometric measurements, transition Fourier transform infrared spectroscopy (FTIR) and X-ray photoelectron spectroscopy (XPS).

Finally, the catalytic activity of the functionalized wafers was determined employing a Suzuki-Miyaura cross coupling reaction. This reaction, the coupling of 4- bromotolu-

ene and phenylboronic acid with potassium carbonate as base (Figure 3-2), was tested and optimized by our group in previous works[24, 98].

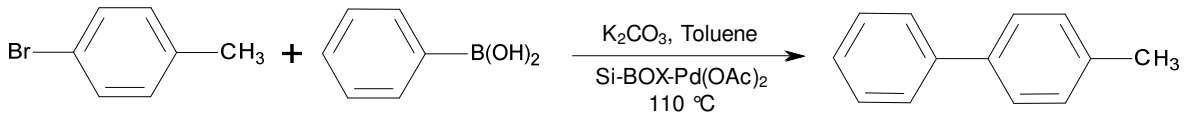

Figure 3-2: Coupling of 4-bromotoluene with phenylboronic acid

4 REALIZATION, RESULTS AND DISCUSSION

4.1 H-termination of Silicon Wafers

Silicon (111) samples were cut from n-type, two sides polished wafers (high resistivity, ≥10000 Ω cm) purchased from Topsil (DEN).

The samples were cleaned using a modified RCA-cleaning process and etched in fluoride containing aqueous solutions. The separate cleaning and etching steps are described in detail in the following list:

1. Cleaning of the needed equipment (beaker, tweezers, magnetic stir bars) with standard cleaning solution 1 (SC1: H_2O:H_2O_2:NH_4OH = 5:1:1 in volume) at 70 °C for 15 minutes.
2. Degreasing the wafer by rinsing with acetone.
3. Wafer cleaning in SC-1 solution for 15 minutes at 70 °C (removal of organic contamination and particles).
4. Careful rinse with copious amounts of ultrapure water.
5. Wafer cleaning in standard cleaning solution 2 (SC2: H_2O:H_2O_2:HCl = 5:1:1 in volume) at 70 °C for at least 10 minutes (removal of inorganic contaminants).
6. Careful rinse with copious amounts of ultrapure water.
7. Etching in diluted aqueous hydrofluoric acid (~2 Vol%) for 3 minutes at room temperature.
8. Etching in 40% aqueous NH_4F + 1 wt% ammonium sulfite (deoxygenator) for 2 minutes at room temperature.
9. Short water rinse
10. Drying in an inert N_2-gas stream.

Successful H-termination can be observed visually since the surface is strongly hydrophilic after cleaning and oxidation but distinctly hydrophobic after the etching steps. The chemical nature of the H-termination can be determined by FTIR spectroscopy. Figure 4-1 shows the spectral region for Si-H_x stretching vibrations (2050 – 2150 cm^{-1}). After etching in diluted (~2 Vol%) hydrofluoric acid, the surface is inhomogeneously covered with various silicon hydride species (Figure 4-1(a)). In contrast, etching with 40% NH_4F leads to a significant simplification of the spectrum. The single and sharp band at 2083 cm^{-1} (Figure 4-1(b)) indicates that the surface is cov-

ered homogeneously by monohydrides with Si-H on flat Si(111)-terraces (M`) being the most prominent species[99].

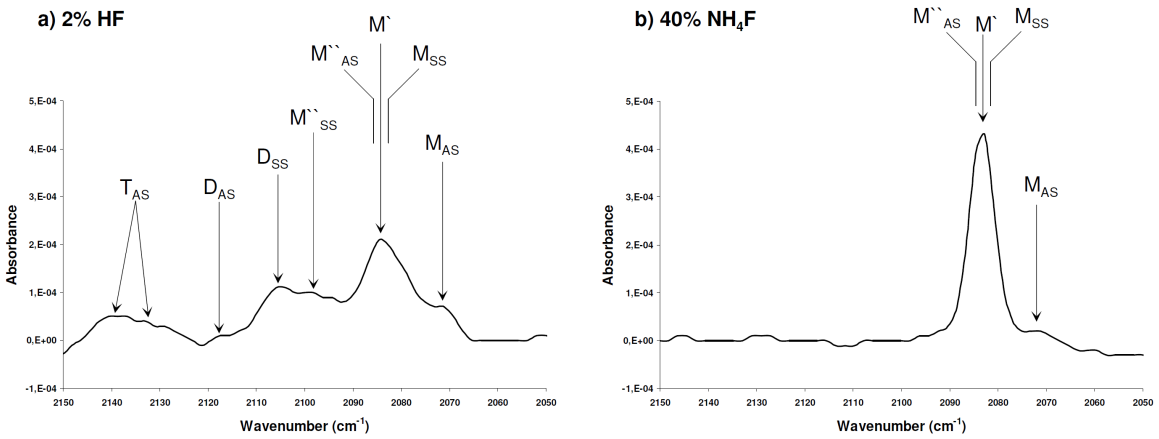

Figure 4-1: Transmission FTIR-spectra of HF- and NH_4F-etched Si(111) wafers

Table 4-1: Legend for Figure 4-1

Notation	Wavelength (cm^{-1})	Vibration*
M`	2083	Stretching vibration of monohydride on Si(111) terraces
M_{AS}	2071	Asymmetric stretching of coupled monohydrides on doublelayer steps
M_{SS}	slightly below 2083	Symmetric stretching of coupled monohydrides on doublelayer steps
$M``_{AS}$	slightly above 2083	Asymmetric stretching of coupled monohydrides on (100) steps
$M``_{SS}$	2098	Symmetric stretching of coupled monohydrides on (100) steps
D_{SS}	2105	Symmetric dihydride stretching
D_{AS}	2115	Asymmetric dihydride stretching
T_{AS}	2130 – 2143	Trihydride stretching modes

*Interpretation according to Watanabe et al.[99]

For monolayer attachment, the freshly etched wafers were transferred immediately into a nitrogen purged glovebox to prevent surface oxidation.

4.2 The Lithographic Unit

The design of the lithographic unit was intentionally kept as simple as possible. An acceptable angular resolution can be achieved without the need for complex and expensive optical equipment by minimizing the distance between the photomask and the silicon sample and by irradiation with a point source of light.

To allow sample placement as close as possible to the lithographic mask, a custom made PTFE-sample holder was constructed. This holder possesses a quasi quadratic deepening (21 x 21 x 1 mm^3) which provides space for the silicon wafer and the reaction solution and acts as reaction vessel during the UV-hydrosilylation. A fused silica window or a photolithographic mask (both 50 x 50 mm^2) can be fixed directly above the reaction chamber. Figure 4-2 shows schematic drawings (left side: top view, true to scale; middle: profile, not true to scale) and a photograph of the sample holder with the lithographic mask.

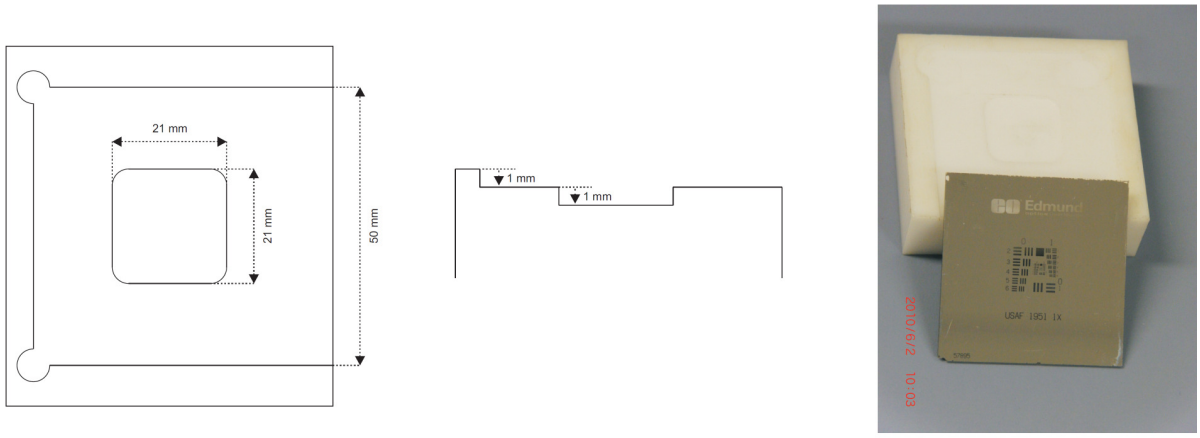

Figure 4-2: Schematic drawing and photograph of the sample holder

A point-shaped light source can be simulated by irradiation with a conventional UV-lamp (in this case a mercury vapor lamp) through a pinhole. This was achieved by placing a bottom side opened box (which will be referred to as “lithographic box in the following) with a 2 x 2 mm^2 pinhole on the topside between the light source and the sample holder. The entire arrangement is schematically shown in Figure 4-3. Since the wafer thickness is only 525 µm ± 10 µm, three microscope cover slips (glass, 0,13 – 0,15 mm thick) were used as spacer to further reduce the distance between the silicon wafer and the lithographic mask/fused silica window. Thus, the film of the reaction solution on the wafer is approximately of 55 µm thickness.

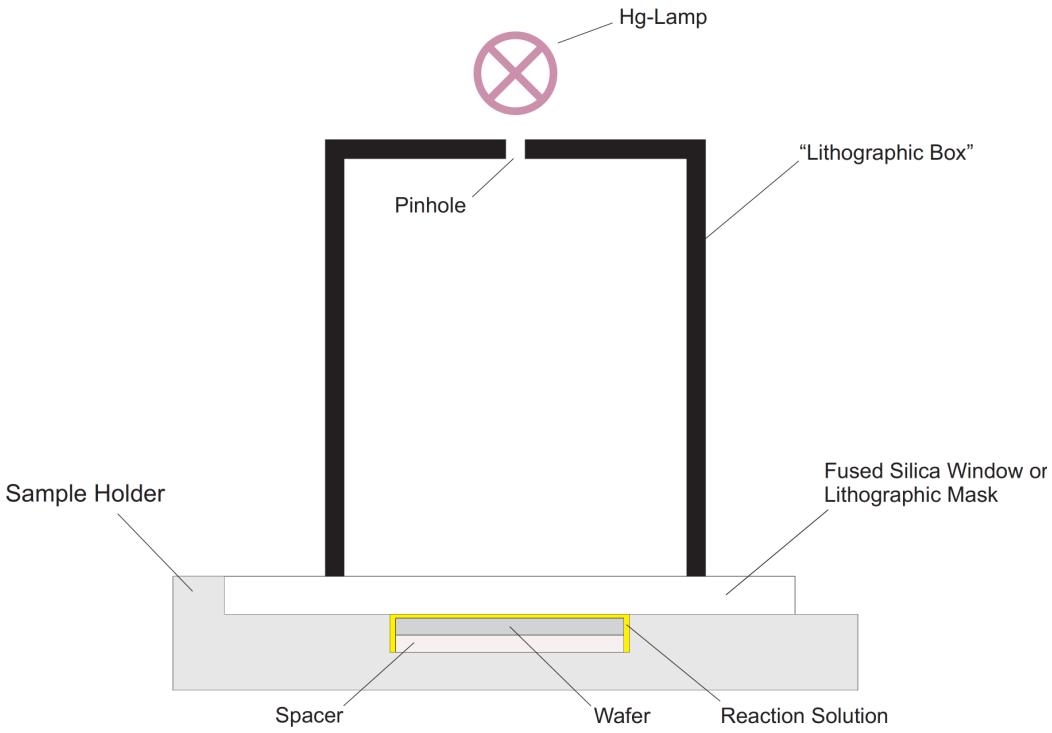

Figure 4-3: Lithographic arrangement (not true to scale)

4.3 Monolayer Formation

Two types of partially functionalized wafers were produced in our approach. For contact angle measurements and FTIR-analysis, comparatively large areas of functionalized surfaces had to be created. This was achieved by illuminating the front and the back side of one half of a silicon wafer (approximately 20 x 10 mm^2 in size). The back side was functionalized to maximize the obtainable signal in transmission FTIR-measurements.

To determine the quality of the optical system, quasi quadratic silicon shards were illuminated through a lithographic mask. Half side illuminated and masked samples will be referred to as "half/half" and "patterned" wafers, respectively. Both types of functionalization are schematically shown in Figure 4-4.

4.3.1 Experimental Details of Monolayer Formation

Since H-terminated silicon surfaces undergo considerable oxidation in ambient air all hydrosilylation reactions were carried out in an inert gas atmosphere. Hence, the silicon samples were transferred immediately after etching in a nitrogen purged glovebox.

Freshly etched wafers were placed in the sample holder as shown in Figure 4-3 and wetted with a solution of the box ligand in anhydrous chlorobenzene (c_{BOX} = 0.05 mol

L^{-1}). The reaction solution was degassed carefully prior to use by at least 3 freeze-pump-thaw cycles (for detailed information see experimental section) and dried over a molecular sieve.

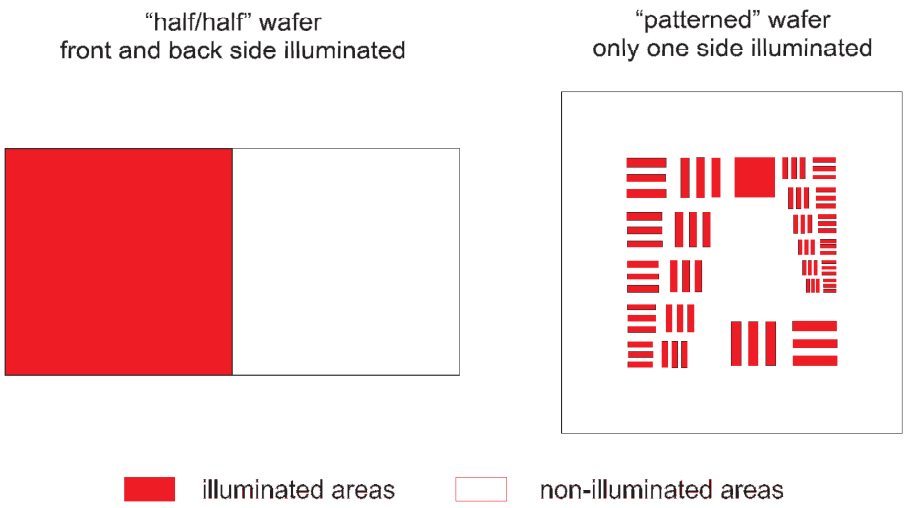

Figure 4-4: "half/half" and "patterned" wafer

For the creation of half/half wafers a fused silica window was used. One half of the glass window was covered with aluminium foil in such a way that one half of the wafer (approximately an area of 10 x 10 mm^2) was exposed to UV-irradiation, whereas the other half of the sample was kept in the dark. The lithographic box was placed above the silica window and the UV-lamp (mercury-vapor lamp) was turned on. After 2 hours, the wafer was turned around, wetted with fresh reaction solution and the back side of the UV-exposed part was irradiated for another 2 hours.

Patterned wafers were created by covering the sample with a lithographic mask (negative USAF 1951 test target, purchased from Edmund optics, substrate: fused silica, coating: vacuum deposited durable chromium).

After the hydrosilylation reaction, the wafer was taken out from the glovebox and sonicated at least three times for one minute in dichloromethane to remove physisorbed BOX-molecules from the surface.

Metalation of the BOX-ligand was carried out by immersion in a solution of palladium acetate ($Pd(OAc)_2$) in dichloromethane (0.05 mol L^{-1}) at room temperature. The sample was kept in the solution generally over night, but at least for 2 hours. The whole modification process is schematically shown in Figure 4-5. After metalation, the wafer was cleaned thoroughly by extensive sonication in dichloromethane (at least 5 times for 1 minute in fresh solvent at any one time).

If the wafer was not used for characterization or activity tests immediately after preparation, it was stored in a nitrogen-filled centrifuge tube.

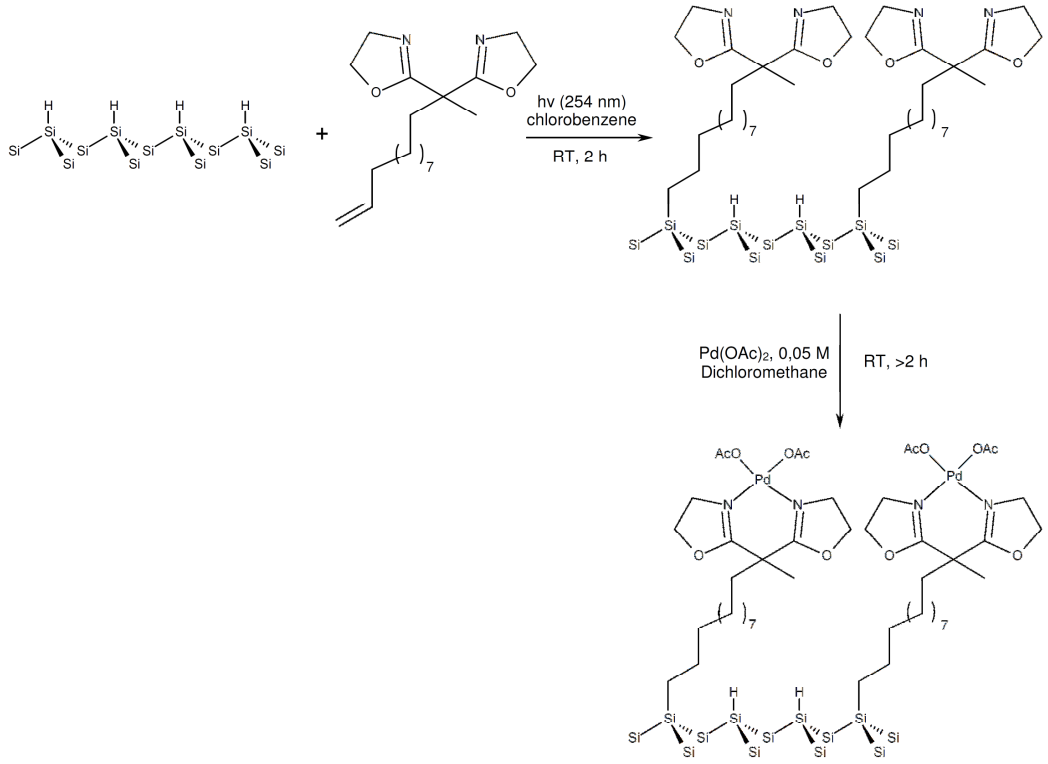

Figure 4-5: UV-induced hydrosilylation and metalation reaction

4.4 Characterization

Physical surface properties, resolution of the SAM-patterns and chemical composition of the attached monolayer were examined by goniometric contact angle measurements, optical microscopy, transmission FTIR-spectroscopy and X-ray photoelectron spectroscopy.

4.4.1 Contact Angle Measurements

The attachment of molecular monolayers or even submonolayers can significantly alter physical surface properties of the underlying substrate. A conveniently and quickly measurable surface attribute is the surface wettability. Changes in the wetting behaviour can easily be monitored by water contact angle (WCA) measurements.

A number of papers reported alterations of the water contact angle on silicon surfaces caused by the attachment of an organic monolayer. Especially the increased surface hydrophobicity after termination with long alkyl chains is well known and is considered as an indicator for the quality of the created monolayer[7, 31, 34, 71]. Thus, locally defined and stable changes of the wettability can be seen as a first evidence for

successful immobilization and patterning of the organic ligand and the catalytically active complex.

Water contact angles were determined using a KRÜSS easy drop goniometer. The measurements were performed on native oxidized silicon samples and half/half functionalized wafers using the sessile drop technique: a drop of deionized water (V = 2,5 µL) was placed on the surface and photographed by a CCD camera. The contact angle was calculated by fitting the drop contour to a circular segment function (circle fitting method).

WCAs were measured on half/half wafers after the hydrosilylation reaction (i.e. with the immobilized Box-ligand) as well as on half/half wafers with the whole catalytic complex being attached (i.e. after the metalation reaction). As mentioned in chapter 2.4.3.3, the non-irradiated part of the wafer is supposed to remain mainly H-terminated and thus distinctly hydrophobic after UV-hydrosilylation. With proceeding oxidation of the Si-H surface under ambient conditions, the hydrophobicity and, therefore, the contact angle of the non exposed areas should decrease, whereas the WCAs of the functionalized parts should remain essentially constant.

Hence, both samples were analyzed not only immediately after preparation, but also after prolonged storage in ambient air (>2 days). To get comparative data for H-terminated and natively oxidized silicon surfaces, also freshly NH_4F-etched and untreated wafers were examined. Furthermore, all samples underwent a stability test (exposure to a stirred suspension of 100 mg K_2CO_3 in 5 ml toluene for 6 hours at 110 °C) to check the stability of the organic layers under conditions similar to those required for a Suzuki-Miyaura cross-coupling reaction.

The obtained results of the static water contact angle measurements are summarized in Table 4-2. The given values represent the arithmetic mean of at least 6 WCA measurements at different positions on the analyzed surface.

As can be seen from the data below, UV-irradiation of the etched surface in a solution of the BOX-ligand leads to a significant increase of the water contact angle on the irradiated parts. Metalation of the box ligand leads to a further increase in hydrophobicity of the functionalized surface. The WCAs on both surfaces, the Si-BOX and the Si-BOX-$Pd(OAc)_2$ surface, remain almost constant at the increased level even after prolonged storage in ambient air and after stability tests. This gives clear evidence that both modifications are stable under ambient as well as under reaction conditions.

Table 4-2: Summarized results of static contact angle measurements

Wafer type	Part	Static water contact angle (θ)		
		Immediately after preparation	After storage in ambient air	After stability test*
half/half Si-BOX	irradiated	65.1 ± 2.2	67.4 ± 2.9°	64.3 ± 2.7°
half/half Si-BOX	non-irradiated	72.6 ± 2.0	43.3 ± 2.6°	36.3 ± 3.3°
half/half Si-BOX-$Pd(OAc)_2$	irradiated	69.3 ± 2.4	71.6 ± 2.6°	68.2 ± 1..0
half/half Si-BOX-$Pd(OAc)_2$	non-irradiated	56.5 ± 3.0	45.2 ± 6.3°	34.7 ± 3.2
NH_4F-etched	fully covered	86.6 ± 2.1	54.4 ± 3.6°	29.8 ± 3.1°
natively oxidized	fully covered	-	55.2 ± 3.2°	-

* exposure to a stirred suspension of 100 mg K_2CO_3 in 5 ml toluene for 6 hours at 110 °C

On the contrary, non-irradiated wafer parts are strongly hydrophobic immediately after the hydrosilylation reaction but get more and more hydrophilic when stored in ambient air. This strongly indicates that large parts of the non-irradiated surface remain H-terminated and undergo considerable oxidation during storage in air. The lower contact angle of the non-irradiated surface compared to the freshly etched wafer (72.6° vs. 86.6°) does not necessarily mean that oxidation occurs already during the hydrosilylation reaction. Since the half/half wafers were cleaned by repeated sonication in non-degassed solvents, oxidation during the cleaning process is assumed to be mainly responsible for the increased hydrophilicity. Oxidation and decrease of the WCA of the non-irradiated part occurs also during the metalation reaction. This is not surprising since no special effort was made to degas or dry the used solvent (dichloromethane).

All non-irradiated surfaces (including the NH_4F-etched wafer) showed a further drop in hydrophobicity after the stability test. The stability of the wetting properties of the irradiated surfaces on the one hand and the analogy of behavior of non-irradiated and H-terminated surfaces on the other hand indicate that a stable modification and physical functionalization occurs solely on irradiated parts whereas non-irradiated parts share significant characteristics with unmodified silicon. Hence, irradiated parts will be also referred to as “modified” and “functionalized” surfaces in the following.

The differences in wettability of functionalized and non-functionalized parts are sufficiently enough to be recognizable with the naked eye. Figure 4-6 shows water drops on different parts of a half/half wafer after the hydrosilylation and the metalation reac-

tion and after prolonged storage in ambient air (> 2 days). The appreciable effect of this physical difference will be discussed in the next chapter.

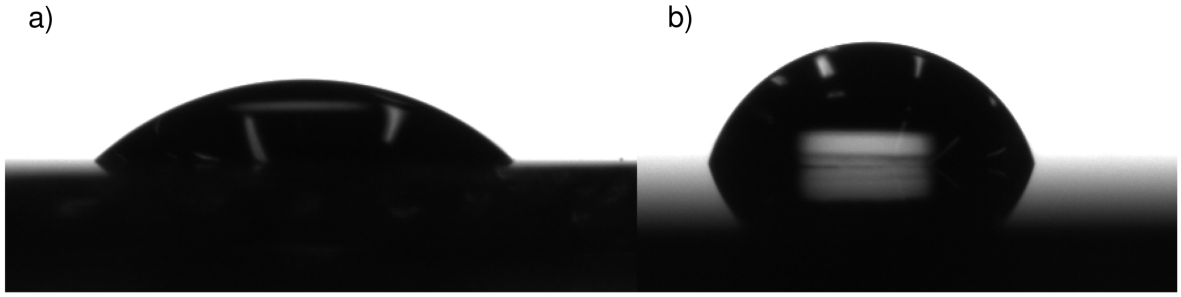

Figure 4-6: Photographs of water drops on the non-irradiated (a) and the irradiated and metalated part (b) of the same wafer

4.4.1.1 Conclusions

- WCAs on irradiated wafer parts are recognizably higher than on non-irradiated areas
- Metalation of the functionalized surface leads to a further increase in hydrophobicity
- Functionalized surfaces are stable in ambient air and under the desired reaction conditions, whereas non-functionalized areas do considerably change their physical properties during storage and handling

4.4.2 Optical microscopy

The different wettabilities of irradiated and covered parts of the wafer make a direct observation of the patterned structures possible. Condensation of air humidity or breath on cooled samples leads to the formation of drops with different sizes on functionalized and non-functionalized areas. This effect can be seen with the naked eye and can be photographed and documented with an optical microscope.

Figure 4-7 shows the boundary line between the functionalized (left side) and the non-functionalized (right side) part of a Si-BOX-Pd$(OAc)_2$ half/half wafer. Condensed water drops on the more hydrophobic, functionalized left side are recognizably smaller than the drops on the non-irradiated right side. This effect causes the functionalized side to appear slightly brighter.

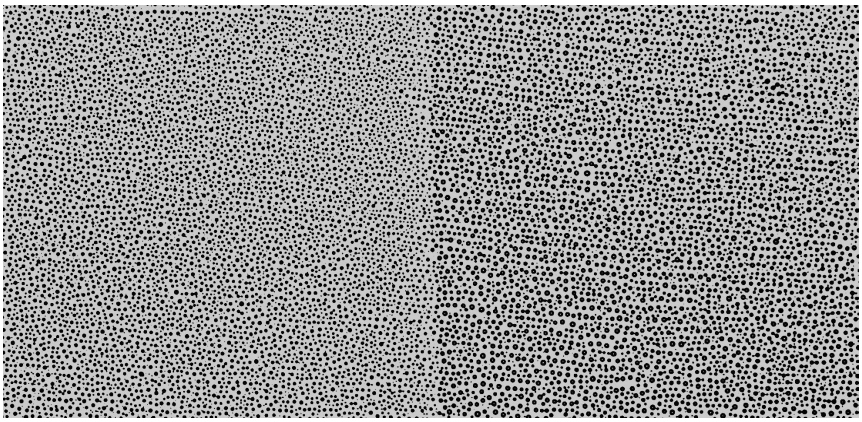

Figure 4-7: Boundary line between the functionalized (left) and the non functionalized (right) part of a half/half Si-Box-Pd(OAc)$_2$ wafer

The same observations can also be made on patterned wafers. Figure 4-8 shows breath condensation on a cooled patterned Si-BOX-Pd(OAc)$_2$-wafer and the corresponding part of the photomask.

According to manufacturer's data, the linewidth of the stripes on the photomask in the first element of group 4 is 31,25 µm. The linewidth of the same element on the patterned wafer was measured to be about 45 µm. This broadening of the patterns can be explained by the imperfectness of the lithographic unit. Nevertheless, the results show that functionalized stripes with widths below 50 µm can be easily created by very simple lithographic masking approaches.

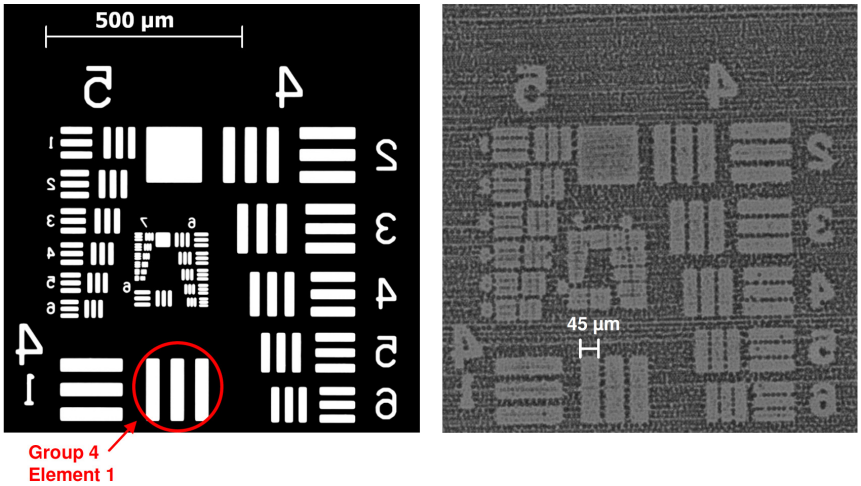

Figure 4-8: Microscopical picture of condensed water drops on a patterned Si-Box-Pd(OAc)$_2$-wafer (right) and the corresponding part of the photomask (left)

Light microscopical examinations revealed another optical effect: functionalized areas are slightly darkened after the metalation reaction. Although this staining is not visible with the naked eye, it can be observed with the digital microscope camera at

certain exposure settings. The darkening of Si-BOX-Pd(OAc)$_2$-surfaces can be observed on both, half/half and patterned wafers (Figure 4-9 and Figure 4-10, respectively).

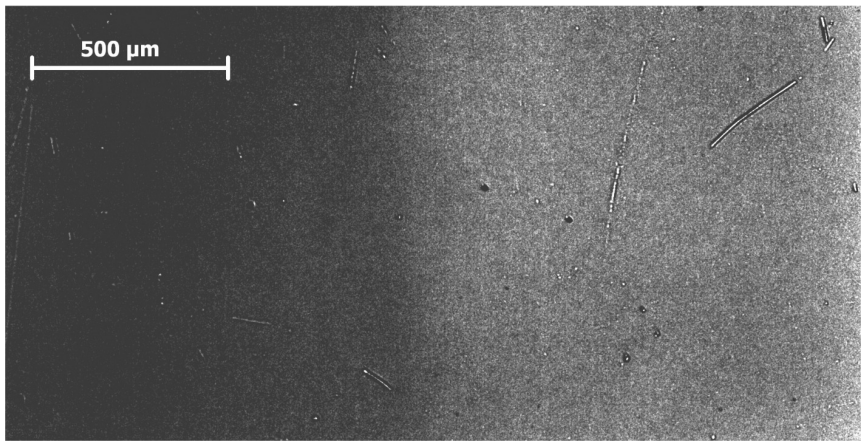

Figure 4-9: Darkening of the functionalized half (left) of a half/half Si-Box-Pd(OAc)2

Surface staining occurs exclusively on metalated wafers. Organically patterned but not metalated samples do not show any coloring at all. This indicates, together with the slightly increased water contact angle of the Si-BOX-Pd(OAc)$_2$ surface compared to the Si-Box sample, that considerable surface modification occurs not only during UV-induced hydrosilylation, but also during the metalation reaction.
Surface darkening is, just like the increased hydrophobicity, stable in ambient air and resists stability tests.

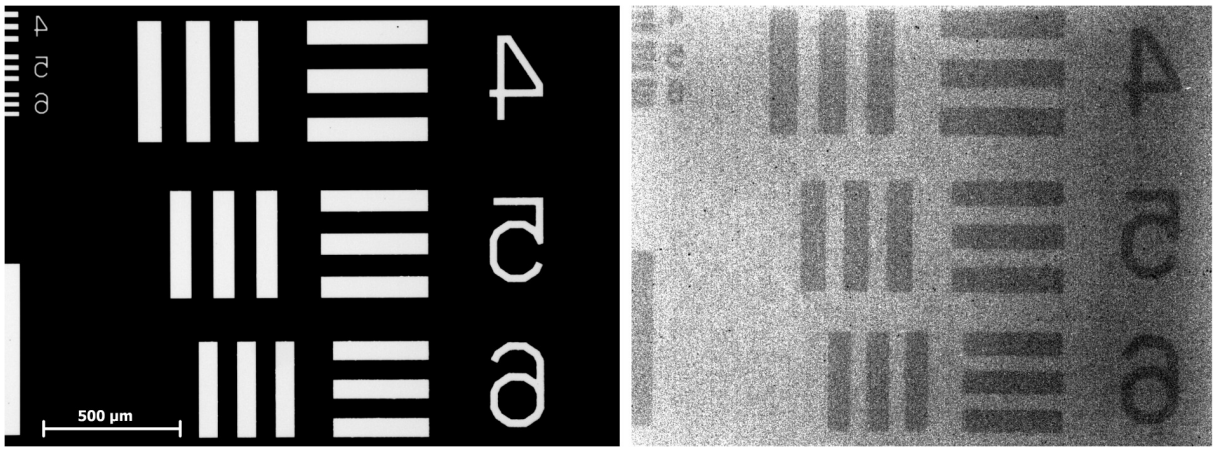

Figure 4-10: Darkening of irradiated areas on a patterened Si-Box-Pd(OAc)$_2$-wafer

4.4.2.1 Conclusions

- Differences in surface wettability make direct observation of the created structures with the naked eye or with optical microscopy possible
- Lines with thicknesses below 50 µm can be created with the used lithographic unit
- Metalation leads to a detectable darkening of the functionalized areas

4.4.3 Infrared Measurements

To get information about the chemical nature of the surface modification, functionalized surfaces were investigated by transmission FTIR-measurements. The measurements were performed using a custom made sampler shuttle[100] in an evacuated measurement chamber ($p \leq 5*10^{-4}$ bar) to avoid disturbing signals from water vapor or carbon dioxide. An oxidized silicon sample, cleaned by standard cleaning procedures SC I and SC II, was used as reference. An ATR-FTIR spectrum of the liquid bis(oxazoline)-ligand and the obtained transmission FTIR-spectra of a Si-BOX and a Si-BOX-Pd$(OAc)_2$ surface are shown in Figure 4-11. The transmission spectra are baseline-corrected, the complete and non-manipulated spectra are given in chapter 7.1.

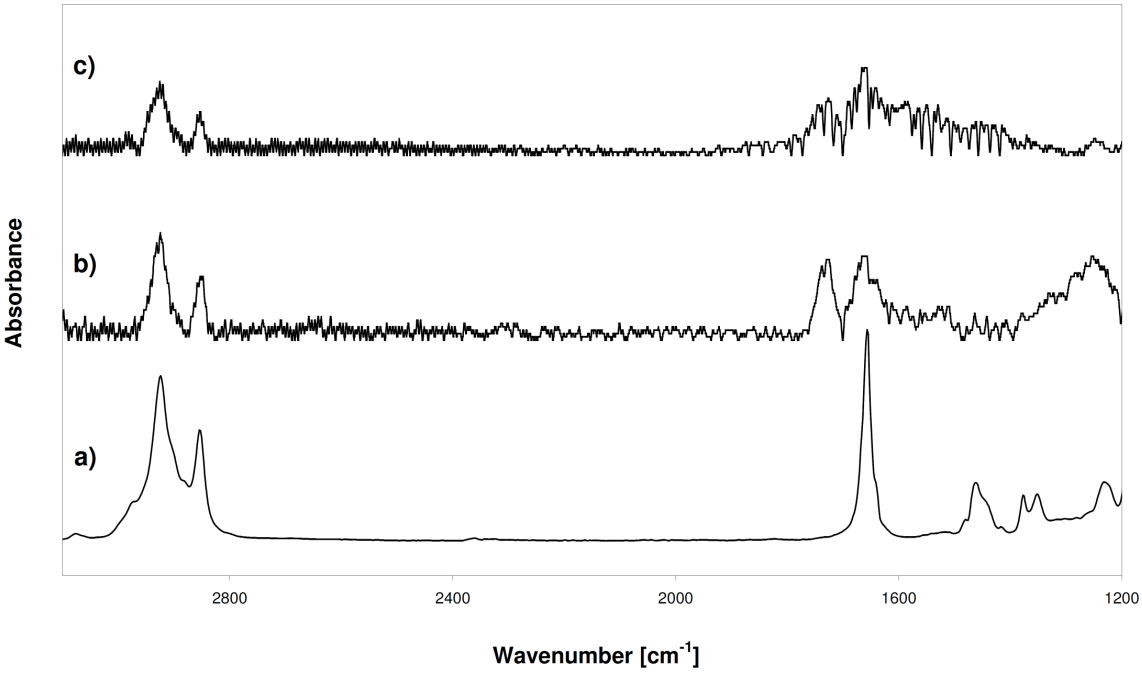

Figure 4-11: ATR-FTIR spectrum of the liquid Box-ligand (a) and transmission FTIR-spectra of the immobilized BOX-ligand (b) and the immobilized and metalated BOX-Pd complex (c)

Transmission-FTIR-spectra were recorded in the spectral range between 4000 and 600 cm^{-1}. Due to the use of oxidized silicon as reference, spectra are strongly interfered at wavenumbers lower than 1200 cm^{-1} by transverse optical (TO) and longitudinal optical (LO) phonons[101] deriving from the thin SiO_x-layer on the reference wafer. Disturbing oxide signals from the reference wafer can principally be avoided using a H-terminated silicon sample as reference. However, TO and LO SiO_x signals could also be observed employing H-terminated wafers as references. The obtained oxide signals must derive from the functionalized sample and indicate that a considerable amount of silicon oxide exists even on the modified surface. These results contradict the presence of a comprehensive, densely packed organic layer on the functionalized surfaces.

As a further consequence, the determination and interpretation of relatively weak organic IR-signals in the fingerprint region below 1200 cm^{-1} is difficult or even impossible. Furthermore, semiqualitative methods, developed by Langner et al.[2], to analyze the amount of immobilized organic molecules can not be performed with the present methods. Hence, the interpretation of the spectra concentrates on purely qualitative considerations on spectral ranges between 3200 and 1200 cm^{-1}.

Although the presence of a high-quality organic layer is disproved by the obtained results, strong indications for at least partial organic functionalization of the surface could be observed. Some characteristic signals of the bis(oxazoline)-ligand, especially asymmetric and symmetric CH_2-stretching modes at 2925 cm^{-1} and 2850 cm^{-1}, respectively, as well as a strong signal at 1660-1665 cm^{-1}, generally assigned to the C=N double bond[102, 103], can easily be identified in both, Si-BOX and Si-BOX-$Pd(OAc)_2$ spectra.

However, also an unexpected signal could be obtained: a strong band at about 1730 cm^{-1}, i.e., in the typical range of carbonyl groups, is apparent in both spectra. Since the bis(oxazoline)-ligand does not contain any carbonyl moieties, these groups must be formed during the hydrosilylation reaction or the subsequent cleaning process. The appearance of carbonyl signals in the FTIR-spectra of immobilized bis(oxazoline)-ligands has already been reported in literature[104] and is supposed to derive from hydrolysis of the BOX-ligand by traces of moisture in combination with residues of acidic species. In spite of the fact that no acidic molecules are brought into the reaction solution in our approach, we suppose that oxazoline-hydrolysis occurs already during the hydrosilylation reaction.

Since Hara et al.[4] did not report oxazoline-hydrolysis during rinsing in various solvents or even after performing catalytic reactions in water, the bis(oxazoline)-ligand seems to be very stable in different solvents in the absence of acidic species. We assume that hydrolysis of the C=N bond occurs during the UV-induced hydrosilylation is caused by the combination of UV-irradiation and water contamination. However, the strong C=N band at 1660 cm^{-1} indicates that large amounts of the bis(oxazoline)-rings are still intact on the functionalized surface.

The IR-spectrum of the metalated Si-BOX-$(PdOAc)_2$-surface looks very similar to the spectrum of the non-metalated Si-BOX-surface at first sight. Nevertheless, slight differences can be noticed on closer examination. Figure 4-12 shows the comparison of the already discussed FTIR spectra of the organically functionalized Si-BOX (black) and the metalated Si-BOX-$(PdOAc)_2$ (blue) surfaces.

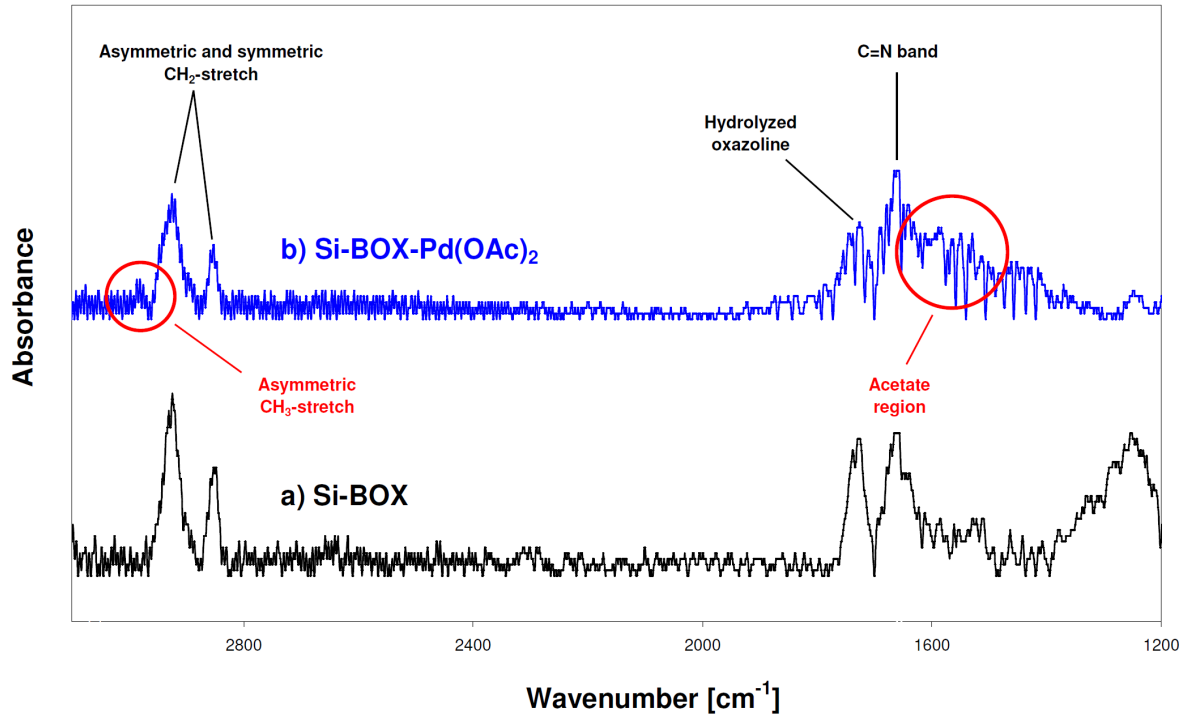

Figure 4-12: Comparison of the Si-BOX (a) and the Si-BOX-$Pd(OAc)_2$ (b) functionalized silicon surfaces

An presence of an increased signal at 2975 cm^{-1} in the Si-BOX-$Pd(OAc)_2$-spectrum is an indicator for additional CH_3-groups deriving from immobilized $Pd(OAc)_2$. Furthermore, the spectral region between 1400 and 1600, the typical range of acetate vibrations, seems to be slightly more distinctive. However, these signals are by far not as clear as the vibrational modes of the BOX-ligand.

Thus, successful metalation of the functionalized surface could not be evidenced without a doubt by FTIR-measurements but had to be confirmed by means of other analytical techniques.

4.4.3.1 Conclusions

The results of the FTIR-measurements reveal two important facts: on the one hand, UV-induced hydrosilylation was proven to be principally a suitable strategy for the immobilization of a bis(oxazoline)-ligand onto H-terminated Si(111). Well defined CH_2 stretching modes and a strong C=N band are clearly observable in both, the Si-BOX and the Si-BOX-$Pd(OAc)_2$ spectra.

On the other hand, the obtained spectra display large imperfections of the organic modification. The considerable oxidation of the silicon surface and the recognizable hydrolysis of the BOXx-ligand, both most likely caused by traces of oxygen and moisture in the reaction solution, show that extreme care has to be taken to exclude water and oxygen from all reagents and solvents which are used during the hydrosilylation reaction. The distinct sensitivity against water and oxygen contamination could be one major limitation for the practicability of this process.

The obtained results and conclusions are summarized in the following list:

- Characteristic bis(oxazoline) signals can be clearly observed on both, the Si-Box and the Si-BOX-$Pd(OAc)_2$-functionalized surfaces.
- The silicon surface is considerably oxidized after the hydrosilylation reaction. Furthermore, recognizable proportions of the oxazoline-rings are hydrolyzed after the attachment of the ligand.
- Although weak signals indicate the presence of additional acetate groups on the metalated sample, successful metalation of the ligand could not be evidenced doubtlessly by means of infrared spectroscopy.

4.4.4 XPS Measurements

X-ray photoelectron spectroscopy (XPS) is a surface analytical technique which allows the determination of the elemental composition of the top 1 to 10 nm of a substrate as well as the chemical or electronic state of each element in the surface[105, 106]. Thus, XPS-analysis is a widely used tool for the characterization of functional layers on a range of substrates including organic layers on Si(100) and Si(111) surfaces[4, 6, 73, 74].

In our approach, the main objective of the XPS analysis was to get evidence for the presence of Palladium exclusively or, at least, in a significantly higher concentration on the functionalized half of the silicon wafer. The measurements were performed by the surface science group of the Karl-Franzens-University of Graz.

The obtained spectra of the functionalized and the non functionalized part of a Si-BOX-Pd(OAc)$_2$-wafer are given in Figure 4-13 and Figure 4-14, respectively.

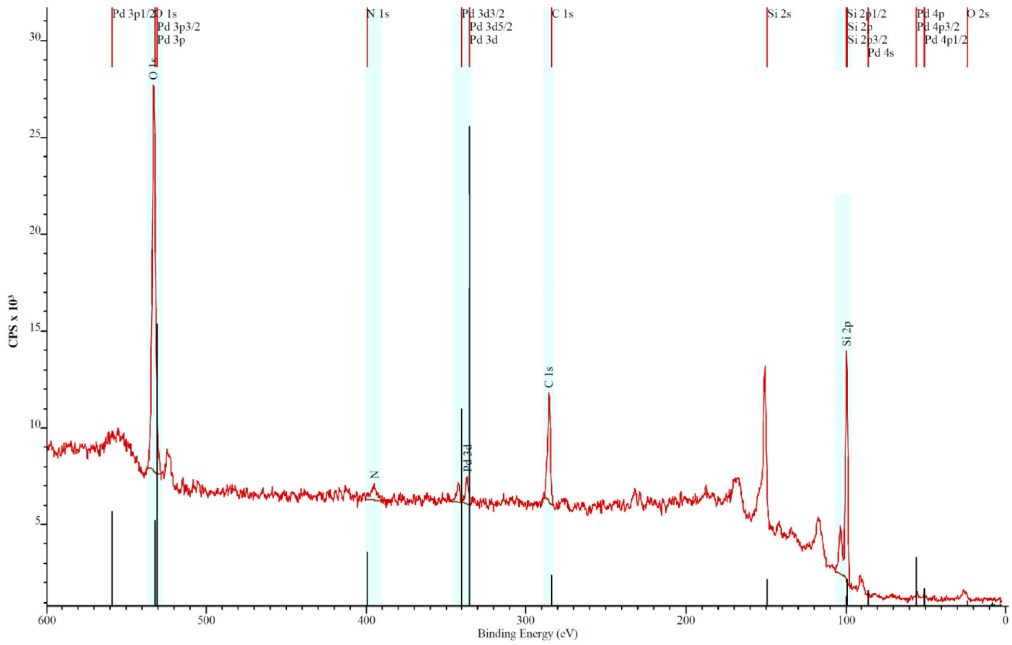

Figure 4-13: Results of the XPS-analysis of the functionalized part of a half/half Si-Box-Pd(OAc)$_2$-wafer

Figure 4-15 shows the comparison between the functionalized and non-functionalized parts in the spectral range between 235 and 410 eV (region of the N 1s, Pd 3d and C 1s signal).

Not only half/half wafers, but also two patterned wafers were analyzed by XP spectroscopy. One of those samples was examined after preparation and storage in a centrifugal tube, the other one was employed for two Suzuki-Miyaura coupling

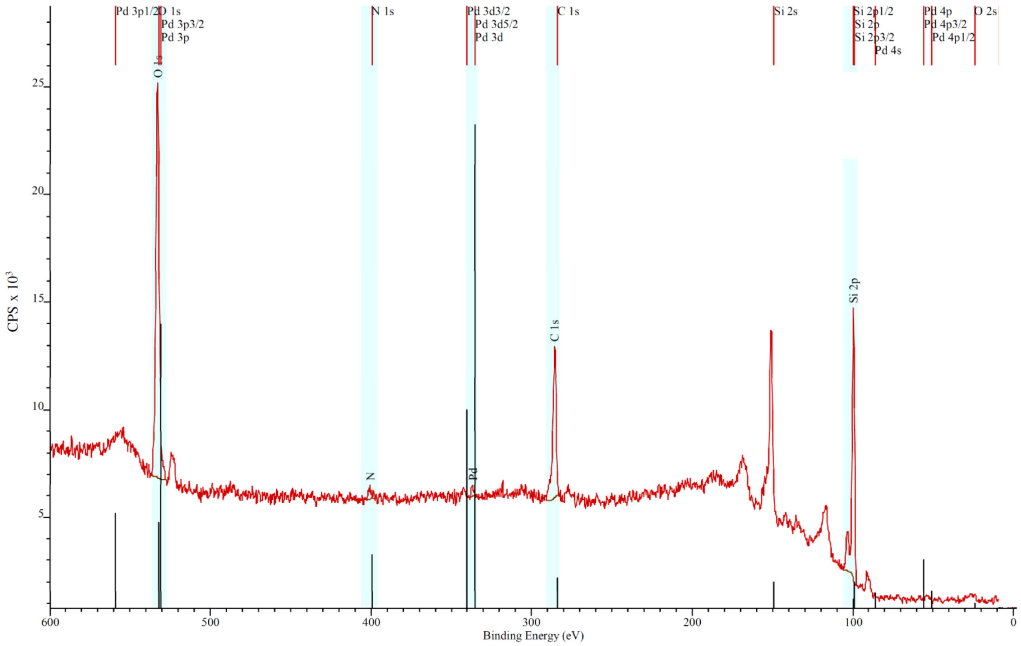

Figure 4-14: Results of the XPS-analysis of the non-functionalized part of a half/half Si-BOX-Pd(OAc)$_2$-wafer

reactions before analysis. Since XP spectroscopy does not allow spatially resolved measurements, both, functionalized and non functionalized areas were analyzed at the same time. Hence, the Pd-content of functionalized areas on these samples can not be quantitatively evaluated but some conclusions regarding the stability of the Pd-loading during the catalytic reaction can be made.

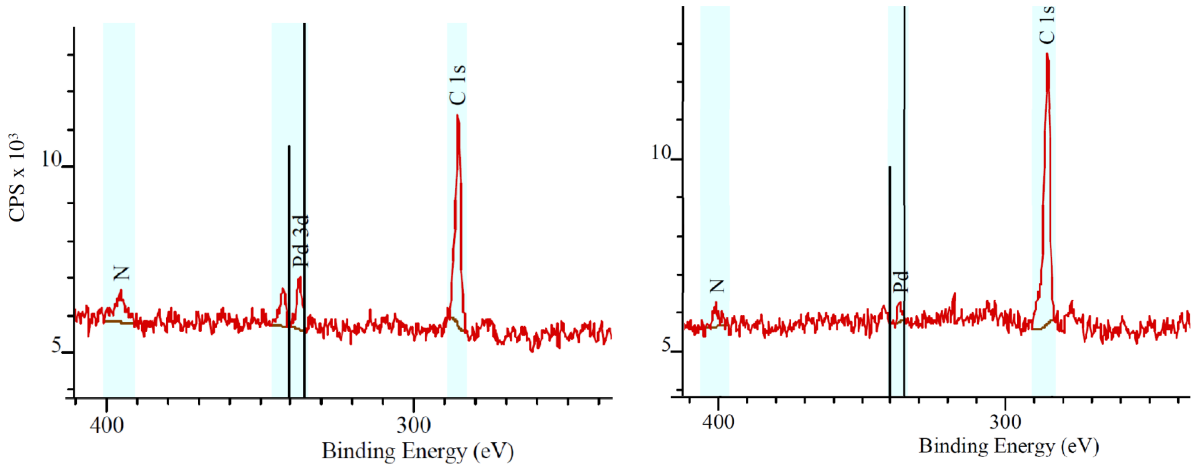

Figure 4-15: Results of the XPS-analysis of the functionalized (left) and the non-functionalized (right) half of a Si-BOX-Pd(OAc)$_2$ wafer in the region between 240 and 410 eV

Additionally, two parts of a half/half wafer created in a follow-up experiment were analyzed. One part was functionalized with the BOX-Pd(OAc)$_2$ complex, on the other

half, a catalytically active titanocene compound was supposed to be immobilized. Although titanium could not be detected on both sides, the results of these measurements provided some further information of interest for the present work. The summarized results of the XPS measurements are given in Table 4-3.

Table 4-3: Summarized data of the XPS measurements

Wafer type	Part	Atomic percent					Ratio Pd/N
		Pd	N	Si	C	O	
Reference wafer cleaned, oxidized	-	N.D.*	N.D.	44.457	31.885	23.675	N.D.
half/half BOX-$Pd(OAc)_2$	irradiated	0.600	3.774	36.629	20.339	38.657	0.159
half/half BOX-$Pd(OAc)_2$	non irradiated	0.112	1.551	35.316	29.318	33.703	0.072
BOX-$Pd(OAc)_2$ as prepared	patterned	0.449	1.626	35.893	17.559	44.472	0.276
BOX-$Pd(OAc)_2$ after 2 Suzuki reactions	patterned	0.379	N.D.	27.253	27.007	45.361	N.D.
half/half BOX-$Pd(OAc)_2$/Titanocene**	Box-$Pd(OAc)_2$	0.919	1.180	41.806	26.761	29.334	0.779
half/half BOX-$Pd(OAc)_2$/Titanocene**	Titanocene	N.D.	N.D.	40.796	19.654	39.550	N.D.

*N.D. = not detectable

**The titanium content was below the limit of detection on both samples.

Several conclusions can be drawn from the obtained data. One noticeable result is the high content of carbon on all analyzed surfaces, even on the cleaned reference wafer. Since, to our knowledge, spontaneous chemisorption of organic species on H-terminated or oxidized silicon has not been reported yet, we assume that the high carbon loading derives to a great extend from physisorption of organic contaminants at the surface. Sources of contamination are diverse: imperfect removal of the reaction solution, residues from organic solvents or contamination during storage and handling between preparation and analysis can be reasons for the high ratio of carbon on the surface. The high carbon values have another implication: evidence for the existence or absence of a chemisorbed organic layer can not be given by simple comparison of the carbon content on different surfaces.

Furthermore, it was found that all characterized samples contain large amounts of oxygen at the surface. This is not surprising for non-functionalized or patterned sam-

ples but has important consequences for the estimation of the quality of the organic layer on functionalized parts. The high degree of oxidation contradicts the existence of a comprehensive densely packed organic layer and indicates that immobilization of the organic ligand occurs rather punctual. In addition, the high values for silicon on each sample suggest that the surface layers on both, functionalized and non functionalized areas, are relatively thin and considerable amounts of the Si-signal derive from excitation of bulk silicon atoms.

Although XPS analysis gave evidence of the imperfectness of the created functional surface, one result indicates successful spatially controlled immobilization of the catalytic complex: the amount of organically bonded palladium on the functionalized part of a half/half Si-BOX-$Pd(OAc)_2$ wafer is more than 5 times higher than on the non irradiated half (0.6 At.% vs. 0.112 At.%). On the half/half BOX-$Pd(OAc)_2$/Titanocene wafer, palladium could be observed exclusively at the BOX-functionalized surfaces (0.919 At.%). Considering that both sides of the half/half wafers underwent exactly the same treatment (inclusively the metalation reaction in 0.05 mol L^{-1} $Pd(OAc)_2$-solution) and were cut apart just immediately before analysis, these findings strongly evidence the selective bonding of palladium acetate onto the Si-Box functionalized surface.

The detectable content of palladium and nitrogen on the non-irradiated part of the half/half Si-BOX-$Pd(OAc)_2$ wafer is assumed to derive from incomplete removal of physisorbed BOX and $Pd(OAc)_2$ molecules after the hydrosilylation and the metalation reaction. The total absence of both, palladium and nitrogen, on the titanocen-half of the BOX-$Pd(OAc)_2$/Titanocen wafer supports this hypothesis: significant amounts of covalently bonded BOX or $Pd(OAc)_2$ on non irradiated parts should cause measurable nitrogen and palladium signals even on the titanocen-functionalized part.

The nitrogen content on half/half wafers correlates positively with the amount of palladium. Although the obtained Pd/N ratios do not match exactly the theoretical value of 0.5, the measured quotients (0.159 – 0.779) stay within reasonable limits.

The comparison of the palladium content on the patterned wafers (0.449 At.% after preparation, 0.379 At.% after two Suzuki reactions) shows that the immobilized palladium remains to a great extend on the surface even after the catalytic reaction. These results give evidence of strong interactions between the functionalized surface and the immobilized metal and support the thesis of covalent attachment of the Pd-complex onto the silicon substrate.

4.4.4.1 Conclusions

The results of the XPS-measurements reveal, in good agreement with the obtained FTIR-data, the imperfectness of the produced surfaces:

- All analyzed surfaces are prone to organic contamination
- Both, irradiated and non irradiated parts of a wafer are strongly oxidized
- The presence of a comprehensive and densely packed organic layer could not be confirmed

Nevertheless, some results strongly evidence the successful selective immobilization of the catalytic complex on the irradiated areas:

- The palladium contents are significantly higher on irradiated wafer parts
- Palladium remains to a great extend on the surface even after repeated use in catalytic Suzuki-Miyaura reactions

4.5 Activity tests

The catalytic activities of the functionalized surfaces were investigated employing the palladium catalyzed coupling of 4-bromotoluene and phenylboronic acid with potassium carbonate as base (Suzuki-Miyaura cross-coupling reaction, see Figure 3-2). Both, half/half and patterned Si-BOX-Pd$(OAc)_2$ wafers were tested.

4.5.1 Half/half Si-BOX-Pd$(OAc)_2$-wafers

The half/half Si-BOX-Pd$(OAc)_2$-wafers were prepared as described in chapter 4.3.1. Prior to use, the partially functionalized wafers were carefully cleaned by sonication in dichloromethane for several times to remove physisorbed palladium(II)acetate to the greatest possible extent.

The functionalized and non-functionalized halves of the wafer were cut apart just immediately before the series of measurements was started. This should guarantee that both surfaces were treated in exactly the same way during the cleaning process. The samples were tested using the same equipment (flasks, stir bars, magnetic stirrer) at the same conditions (temperature, stirring rate) to ensure maximum comparability of the results. Additionally, a blank test with the same equipment but without the

use of a catalyst was performed prior to the activity test to exclude catalysis of the reaction by palladium contaminated flasks or stir bars.

The halves were tested in batch mode in an alternate order, starting with the irradiated part, in three runs. The reactions were carried out with toluene as solvent at 115 °C. Typically used concentrations of the reagents are given in Table 4-4.

Table 4-4: Typically used concentrations for the Suzuki-Miyaura cross coupling reactions

	Mass [mg]	Equivalents*
***p*-Bromotoluene**	60	1
Phenylboronic acid	100	2.2
Potassium carbonate	100	1.9

*Related to *p*-Bromotoluene as 1

The progress of the reaction was monitored by GC analysis during the first 4 hours. Dodecane was used as internal standard. Both, the relative conversion of *p*-bromotoluene and the yield of 4-phenyltoluene were quantified. Figure 4-16 shows the results of the GC analysis of Suzuki-Miyaura reactions catalyzed by the as-prepared functionalized and non-functionalized halves of the same wafer (i.e., the first run of the series of measurements).

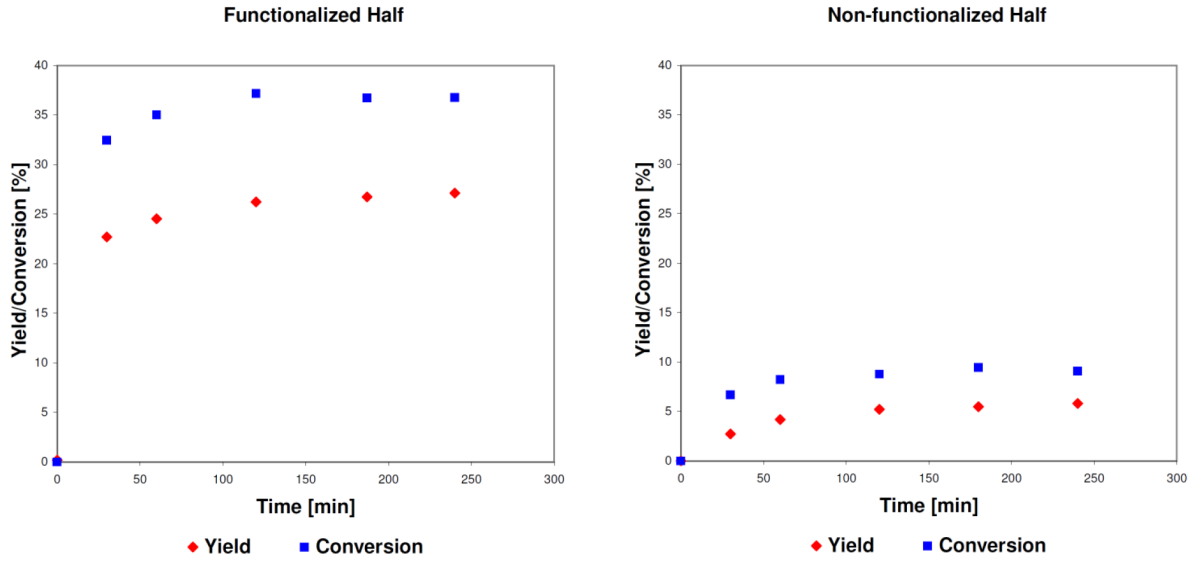

Figure 4-16: GC results of the reactivity tests using as-prepared functionalized and non-functionalized halves of the same wafer

After 4 hours, the wafers were removed from the reaction solution and cleaned by alternating sonication (one minute) in dichloromethane and ultrapure water for at least three times. Both wafer halves were used as catalyst in two more Suzuki reactions. The results of these tests are summarized in Figure 4-17 and Table 4-5.

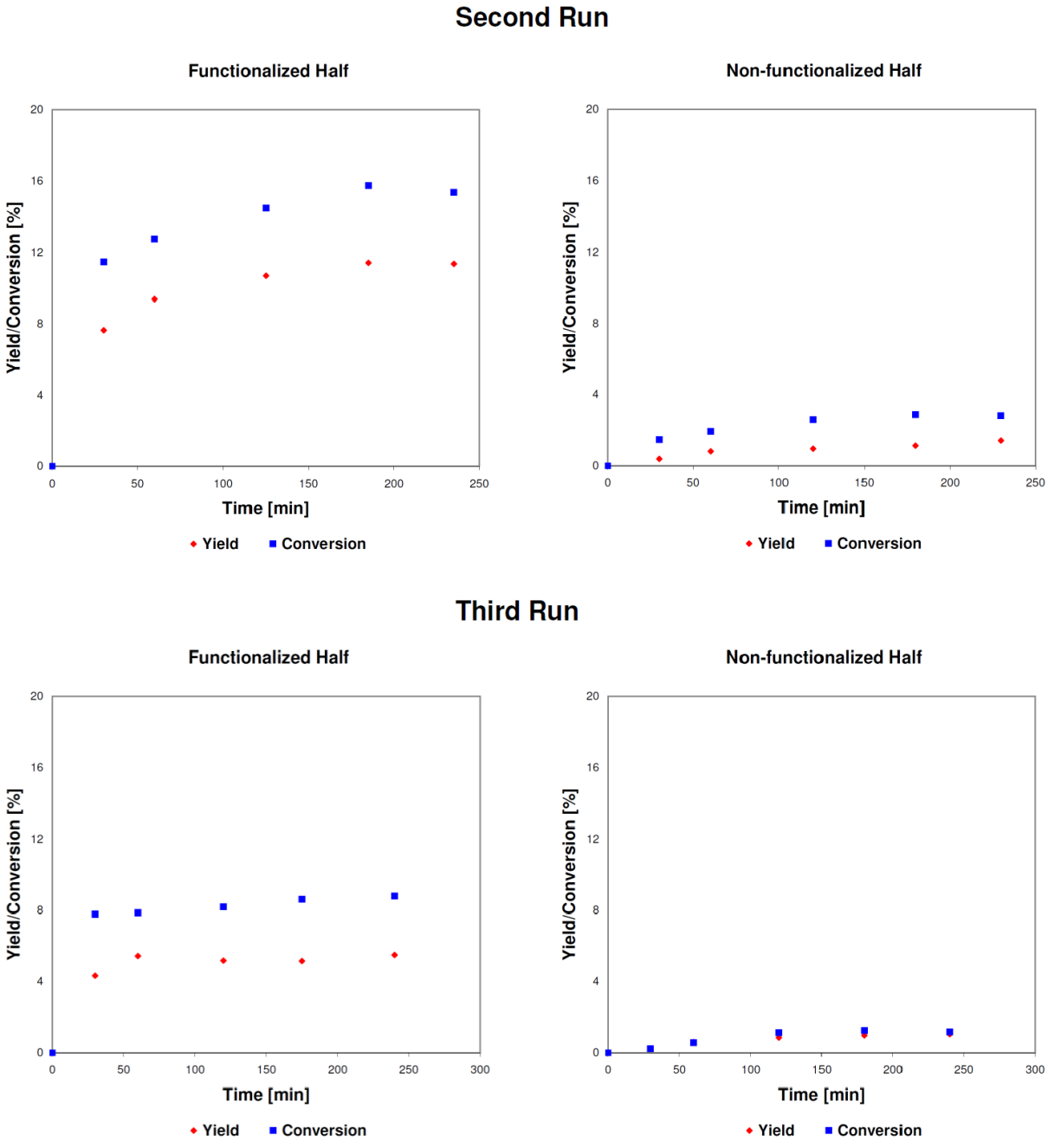

Figure 4-17: GC results of the second and third reactivity tests using functionalized and non-functionalized halves of the same wafer

Table 4-5: Relative yields and conversions after a reaction time of 4 hours

	Functionalized Half		Non-functionalized Half		Ratio of Yields Funct./Non-funct.
	Yield [%]	Conversion [%]	Yield [%]	Conversion[%]	
First Run	27.1	36.8	5.8	9.1	4.7
Second Run	11.4	15.4	1.4	2.9	8.1
Third Run	5.5	8.8	1.1	1.2	5.0
Blind Test	no catalyst was used		0.2	0.7	-

The obtained results provide clear evidence that the produced wafer is significantly catalytically active and that the catalytic activity is concentrated to the greatest extend on the functionalized half of the sample. The employment of the functionalized half as catalyst yielded in each run at least 4.7 times more 4-methylbiphenyl than the use of the non-functionalized part. However, also the non-functionalized half showed some catalytic activity in the first coupling reaction. In accordance to the results of the XPS analysis (see Figure 4-15 and Table 4-3) we suppose that small amounts of physisorbed palladium(II)acetate, which remain on the surface even after careful cleaning, induce recognizable reactivity. The decrease of the yield of 4-methylbiphenyl almost down to the level of the blind test in the second and third run supports the assumption that the activity of the non-functionalized half derives from non-covalently bonded $Pd(OAc)_2$-contamination.

On the contrary, the clearly observable activity of the functionalized part even in the third coupling reaction suggests that a considerable amount of a catalytically active species is bonded onto the irradiated surface via rather strong interactions. However, a significant loss of catalytic activity can be observed during the reaction as well as after each run.

A possible explanation for the decreasing activity during the reaction could be the succesive cumulation of solid potassium carbonate on the wafer surface. Since the solubility of K_2CO_3 in toluene is limited, the reaction mixture is rather a suspension than a clear solution. When the wafer halves were removed from the reaction mixture, the presence of a thin layer of a white solid could be noticed visually. It is likely that the formation of such a layer reduces significantly the mass transfer to the surface and, thus, causes deactivation of the catalyst.

The decrease of catalytic activity after each run is probably more difficult to interpret. Physisorbed palladium acetate, dissolving into the reaction mixture and acting as

homogeneous catalyst, can increase the yield of product in the first run. Given that palladium contamination is not available in the second and third reaction (which is indicated by the results for the non-functionalized part), a significantly lower catalytic activity in the second run can be explained. However, a considerable drop of both, yield and conversion, can also be observed comparing the second and third reaction. Explanations for the continuous loss of catalytic activity can range from mechanical damage of the surface (the wafer was in close contact to the stir bar) to proceeding leaching of the immobilized palladium right up to more fundamental considerations, whether supported Pd-catalysts do catalyze coupling reactions principally in a homogeneous or heterogeneous manner[107, 108]. Although detailed studies of the mechanisms and principals of the used reaction system seem to go beyond the scope of this thesis, such investigations certainly have great relevance in further work.

Nevertheless, the results clearly confirm that modified surfaces show recognizable catalytic activity for at least three times and that the activity is spatially concentrated on the irradiated wafer part.

4.5.2 Patterned Si-BOX-Pd(OAc)$_2$-Wafers

Patterned wafers were tested in the same way as the half/half functionalized wafers. The purpose of these tests was not only to provide evidence for catalytic activity of the wafers but also to examine the effects of repeated use in Suzuki-reactions on the functionalized patterns. The results of the activity tests are summarized in Figure 4-18 and Table 4-6.

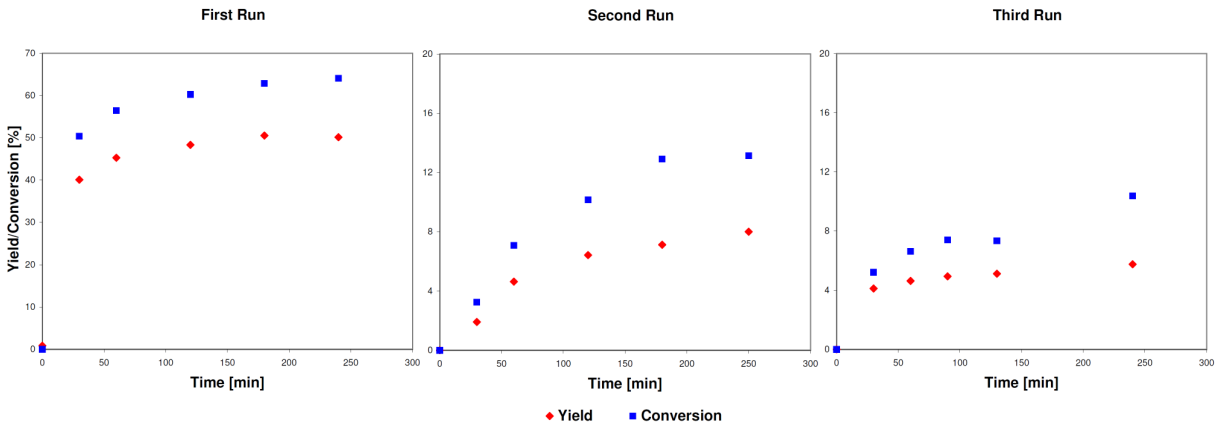

Figure 4-18: GC results of the reactivity tests using a patterned Si-Box-Pd(OAc)$_2$-wafer

Table 4-6: Relative yields and conversions after a reaction time of 4 hours

	Yield [%]	Conversion [%]
First Run	50.2	64.1
Second Run	8.0	13.1
Third Run	5.8	10.4
Blind Test	0.6	1.8

The patterned wafer shows, just like the functionalized part of the half/half wafer, significant catalytic activity even in the third coupling reaction. Another common feature of both functionalized surfaces is the massive drop of yield and conversion after the first run. Hence, we suppose that the results of the first reaction depend much more on the success of wafer cleaning after metalation than on the quality of the functionalized surface. However, the repeated activity of the wafer strongly indicates that a catalytically active species was successfully immobilized on the silicon wafer.
The used wafer was investigated by optical microscopy after three runs. The obtained photographs are shown in Figure 4-19.

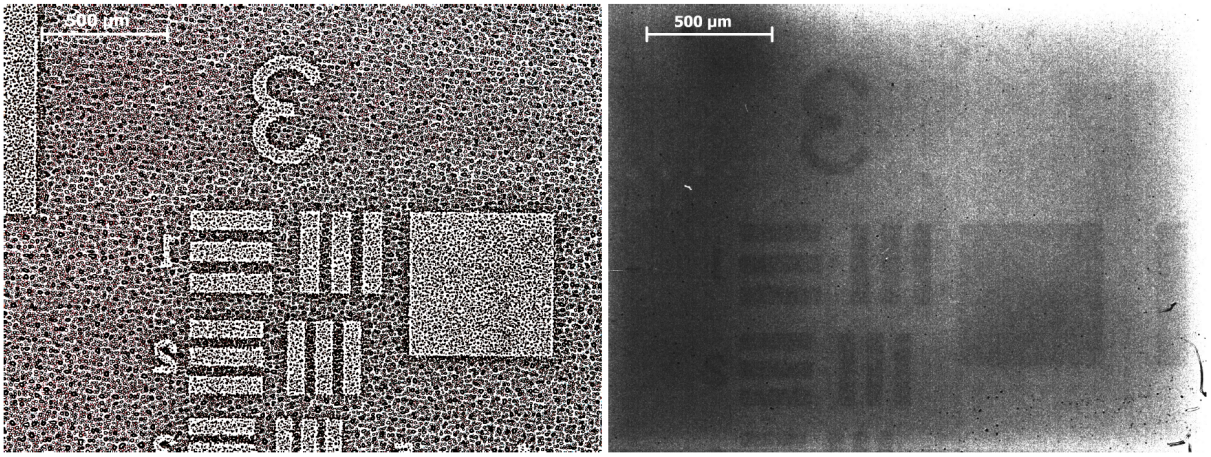

Figure 4-19: Different surface wettabilities and surface darkening on a patterned wafer after three Suzuki-Miyaura coupling reactions

Both increased surface hydrophobicity as well as darkening of the modified surface parts are clearly and directly observable with optical microscopy even after three Suzuki-Miyaura cross coupling reactions. Together with the repeated usability as catalyst and the results of the XPS-analysis, these pictures prove the excellent stability and spatial integrity of the functionalized patterns.

4.5.3 Conclusions

- The presented functionalized surfaces are catalytically active in Suzuki-Miyaura cross-coupling reactions for at least three times.
- The catalytic activity is concentrated to the greatest extend on the irradiated part of the silicon wafer.
- Both increased hydrophobicity and surface darkening of the functionalized patterns are observable even after three Suzuki-Miyaura reactions.

5 SUMMARY

5.1 Achievements

The overall aim of this work was the spatially controlled immobilization of a catalytically active bis(oxazoline)-palladium complex on Si(111) employing the UV-induced hydrosilylation reaction of terminal carbon-carbon double bonds with hydrogen terminated silicon surfaces. A two step strategy, consisting of the laterally defined attachment of a terminally unsaturated bis(oxazoline)-ligand and the subsequent metalation of the immobilized organic precursor with palladium(II)acetate, was pursued to achieve this goal.

A simple lithographic unit was designed to make spatial controlled functionalization of the silicon surfaces by masking procedures possible. The created surfaces were investigated and characterized by means of water contact angle measurements, optical microscopy, FTIR spectroscopy and X-ray photoelectron spectroscopy. The catalytic activity of the functionalized silicon surfaces was tested employing a Suzuki-Miyaura cross-coupling reaction.

The obtained results from surface analysis and activity tests strongly indicate that successful and spatially controlled immobilization of the Box-palladium complex could actually be achieved. Findings which support this point of view are summarized in the following:

- Functionalization leads to a significant change in the wetting behaviour of the silicon surface. Water contact angles on modified surface parts remain stable at a comparatively high, hydrophobic level even after prolonged storage in air and after stability tests, whereas non-functionalized areas undergo considerable increase in hydrophilicity during these treatments.
- The change the of wetting properties of non-irradiated surface parts evidences the lack of a stable functionalization on these areas. Moreover, clear analogies regarding the increase in hydrophilicity between non-functionalized and H-terminated surfaces can be drawn. This strongly indicates that non-functionalized surface parts remain at least partially hydrogen terminated after the hydrosilylation reaction.
- Due to the different wettabilities, condensation of air humidity or breath on cooled samples leads to the formation of drops with different sizes on functionalized and

non-functionalized areas. This effect makes direct observation of the functionalized patterns via optical microscopy possible. The obtained pictures show that functionalized lines with thicknesses below 50 µm can be created with the used lithographic unit.

- Optical microscopy also revealed slight darkening of the functionalized areas after the metalation reaction. This effect could not be observed after the hydrosilylation reaction and is, thus, an indicator for successful metalation of the BOX-ligand.
- Characteristic infrared absorption bands of the bis(oxazoline)-ligand could be identified in the transmission FTIR-spectra of both Si-BOX and Si-BOX-$Pd(OAc)_2$-functionalized samples. Although successful metalation of the BOX-ligand could not be confirmed definitively by means of FTIR-analysis, indications for the presence of acetate moieties on the Si-BOX-$Pd(OAc)_2$ surfaces could be found.
- XPS measurements showed that the amount of palladium on functionalized surfaces is at least 5 times higher compared to non-functionalized surface parts. Furthermore, analysis of patterned surfaces gave clear evidence that large amounts of the attached palladium remain on the surface even after usage of the samples as catalyst in two Suzuki-Miyaura cross-coupling reactions.
- The created functionalized surfaces are catalytically active in Suzuki-Miyaura cross-coupling reactions for at least three times. The activity tests showed that the catalytic activity is concentrated to the greatest extend on the functionalized part of the silicon wafers. Furthermore, characteristic surface properties of the functionalized areas (increased hydrophobicity and darkening of the surface) are clearly observable even after three Suzuki-Miyaura reactions.

Nevertheless, FTIR and XP-spectroscopy also displayed the imperfectness of the functionalized surfaces. Considerable surface oxidation was determined by both spectroscopic techniques in good agreement. These results strongly suggest the absence of a densely packed, high quality organic layer and indicate that the surface is only partially functionalized. Furthermore, due to the results of the FTIR analysis, we assume that partial hydrolysis of the oxazoline-groups occurs during the hydrosilylation reaction. Since surface oxidation and oxazoline hydrolysis are commonly associated with traces of oxygen and moisture in the reaction solution[1, 104], these results reveal the extreme sensitivity of the applied immobilization process towards air and water contamination.

Although catalytic activity of the functionalized surfaces could be obtained in at least three Suzuki-Miyaura cross-coupling reactions, the examined samples showed a significant decrease in activity after each run. Since activity tests were primarily performed to confirm repeated usability of functionalized surfaces as heterogeneous catalysts and not to determine the effectivity and stability of the BOX-$Pd(OAc)_2$ system in principle, the reasons for the loss of activity were not extensively studied. However, detailed investigations of the mechanisms, which lead to catalyst deactivation, will be a crucial task in further work.

5.2 Final Conclusion

The obtained results strongly indicate that the spatially defined immobilization of the catalytically active bis(oxazoline)-palladium complex via UV-induced hydrosilylation could be achieved with the developed lithographic method. The use of the custom made lithographic unit allowed the creation of functionalized patterns with line widths below 50 µm. Functionalized surfaces were proven to catalyze Suzuki-Miyaura cross-coupling reactions repeatedly.

However, since spectroscopic results revealed imperfectness of the organic modification, significant improvement of the quality of functionalized surfaces seem to be available by further optimization of the reaction conditions during the hydrosilylation reaction.

5.3 Outlook

As already mentioned at the beginning of this thesis, the spatially controlled functionalization of H-terminated silicon is only the first step in the development of multicatalytic surfaces. The next step is the immobilization of other catalytically active molecules or their organic precursors onto the non-functionalized surface parts.

A promising strategy involves covalent attachment of tethered ethylenebis(indenyl) (=EBI) metalocenes onto the non-modified surface parts via hydrosilylation reactions. Successful immobilization of tethered EBI zirconocenes and titanocenes on H-terminated silicon employing UV-mediated alkene hydrosilylation was already achieved by our group[5, 109].

The determination of the optimal hydrosilylation method (thermally, radical initiator or UV-induced hydrosilylation) and the development of suitable one-step (attachment of

the entire organometallic complex) or two step (attachment of the organic ligand and subsequent metalation) strategies for the immobilization of the second catalyst while considering the implications of the used procedures on the already immobilized complexes seem to be challenging but crucial tasks in further research.

Future work may also focus on the improvement of the catalytic performance of the functionalized surfaces. An increase in catalytic activity of supported heterogeneous catalysts can generally be achieved either by increasing the amount of the catalytically active species on the surface or by enlargement of the available surface area.
In our approach, the amount of immobilized metal is directly determined by the quality of the functional organic layer. The optimization of the reaction conditions during hydrosilylation, especially the even more rigid removal of oxygen and moisture from the reaction solution, could avoid surface oxidation and, thus, lead to significantly improved layer qualities. Methods for the extreme careful exclusion of oxygen and water contamination from hydrosilylation reaction solutions, e.g. the use of Schlenk line techniques[110] and the drying of solvents and reagents over Na/K alloy[1], have already been reported.
The use of hydrogen terminated porous silicon surfaces instead of flat H-Si(111) wafers could yield a massive gain in active surface area. H-terminated porous silicon surfaces can be created from monocrystalline silicon wafers by anodic etching in hydrofluoric acid[85]. Organic functionalization[36] and even photopatterning[76] of porous silicon surfaces have already been reported. The enlarged area of the surface also facilitates spectroscopical investigations of the chemical and physical nature of modifications. Moreover, since photochemical hydrosilylation on porous silicon can be induced by light with wavelengths above 400 nm[32], also UV-sensitive molecules can be immobilized directly.

6 EXPERIMENTAL DETAILS

6.1 General Remarks

Silicon samples were irradiated with a GPH303T5L low pressure **mercury vapor lamp**, radiated power: 4,3 W at 254 nm.

Static **water contact angles** were measured on a KRÜPP EasyDrop DSA20 goniometer equipped with a monochrome interline CCD camera.

Optical microscopy was performed on a Leica DM4000 M equipped with a Leica DFC290 CMOS camera. Digital image processing was done using the software Leica Application Suite, Version 2.7.1.

Transmission-FTIR spectra for the characterization of the **H-terminated** silicon wafers were recorded on a Bruker VERTEX 70 using a custom-made sample shuttle, spectral resolution: 4 cm^{-1}, polarization of the IR-beam: non-polarized, angle of incidence: 50°, aperture: 2 mm, detector: D316 – MCT cooled with liquid nitrogen, 1000 scans, 4000-600 cm^{-1}. The sample chamber was purged with nitrogen during the measurements.

ATR-FTIR spectra for the characterization of the Bis(oxazoline)-Ligand and its synthetic precursors were recorded on the same instrument using a DLaTGS detector and an ATR unit: MVP Pro Star, Diamond crystal, resolution: 4 cm^{-1}, 16 scans, 4000-600 cm^{-1}.

Transmission-FTIR spectra for the characterization of the **organically functionalized** silicon wafers were recorded on a Bruker VERTEX 66 using a custom-made sample shuttle, spectral resolution: 4 cm^{-1}, polarization of the IR-beam: s-polarized, angle of incidence: 30,59°, aperture: 7 mm, detector: MCT cooled with liquid nitrogen, 15000 scans, 4000-600 cm^{-1}. The sample chamber was evacuated down to $5*10^{-4}$ bar during the measurements.

XPS analysis was performed by the surface science group of the Institute for Experimental Physics, Karl-Franzens-University of Graz,.

GC analysis was carried out on a Perkin Elmer Clarus 500 using an Optima-5 MS capillary column (Machery-Nagel, 30.0 m × 320 µm × 0.25 µm nominal) with a flame ionization detector and nitrogen as carrier gas.

^{1}H and ^{13}C NMR spectra were recorded on a Varian Inova 500 MHz spectrometer at 499.82 MHz and 125.69 MHz, respectively. Chemical shifts are listed in delta (δ/ppm) employing the residual protio solvent resonance as internal standard (δ = 7.24 ppm in ^{1}H spectra and 77.0 ppm in ^{13}C spectra for $CHCl_3$).

6.2 Wafer Specification

The used silicon samples were cut from silicon wafers which were purchased from Topsil Semiconductor Materials A/S, Frederikssund, Denmark. The circular wafers had the following specifications:

Diameter (mm):	99,8 – 100,2
Finish:	Polished
Method/Dopant/type:	FZ/Ph/N
Orientation:	1-1-1
Thickness (µm):	515 – 535
Resistivity (Ω·cm):	≥ 10000
Topsil Item no:	235-1100-0525-003
(S)Customer Spec:	HiRes <111> N DSP
(1T)Ingot no:	213680-6
(Q)Total Qty:	23
(D)Date	10/18/2006
(1T)WWX Lot:	4P6A0011
6 WWX PIN:	Top294D

Silicon shards of the desired size were cut from the (as received) wafers by scoring with a hard metal scriber and subsequent mechanical breaking.

6.3 Degassing of Liquids

Reaction solutions for the UV-induced hydrosilylation were degassed using the freeze pump thaw method. This technique takes advantage of the low gas solubility at reduced pressure. The separate steps of the degasification procedure are described in detail in the following list:

1. The reaction solution (0.05 mol L^{-1} of the BOX-ligand in anhydrous chlorobenzene) was placed in an argon filled Schlenk flask. Not more than 50% of the volume of the flask were filled to prevent shattering during the process.
2. The stopcock was closed and the liquid was frozen in a bath of liquid nitrogen.
3. When the liquid was frozen, the stopcock was opened to vacuum and the atmosphere was pumped off from the flask for 10 minutes.
4. The flask was sealed.
5. The solvent was thawn using a tepid water bath. When the solution melted, the formation of gas bubbles could be observed. Considerable care was taken to not disturb the liquid during thawing.
6. The water bath was replaced by the cooling bath to refreeze the solvent.
7. Steps 3 to 6 were repeated until no more gas bubble evolution could be observed but at least 3 times.

After completed degasification, the Schlenk flask was transferred immediately into a nitrogen filled glove box.

6.4 Preparation of the BOX-Ligand

The used bis(oxazoline)-ligand (2,2'-(1-methyl-11-dodecenylidene)bis(4,5-dihydrooxazole)) was prepared following a three step synthetic route published by Hara et al.[4] in 2007. The identity of the intermediates and the final product was analyzed after each synthetic step by ATR-FTIR as well as by ^{13}C- and ^{1}H-NMR spectroscopy.

6.4.1 Step one: Methyl(10-undecenyl) Malonic Acid

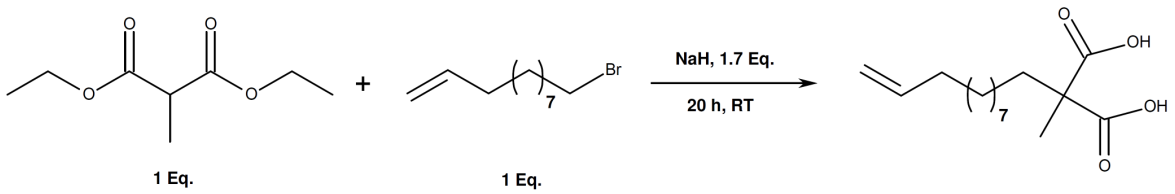

Figure 6-1: Synthesis of methyl(10-undecenyl) malonic acid

Diethyl methylmalonate (1 eq.) was added dropwise under stirring to a solution of NaH (60% dispersion in mineral oil, 1.7 eq) in dry DMF. The cloudy colorless suspension was stirred for 30 minutes at room temperature and 11-bromo-1-undecene (1 eq.) was added. The solution cleared up and turned yellow. After stirring for 20 hours a white precipitate could be observed. The reaction was quenched with H_2O and was acidified with HCl (37%) to pH 2.

The mixture was extracted with diethyl ether and the extract was washed with saturated aqueous NaCl solution, dried over Na_2SO_4 and concentrated under reduced pressure to yield a yellow oil.

A solution of the crude alkylated product in ca. 15% ethanolic NaOH was heated to reflux for 1 hour. The ethanol was removed under reduced pressure, the residue was dissolved in H_2O and acidified with HCl (1 N) to pH 1 while cooling the mixture at 0 °C. The mixture was extracted with CH_2Cl_2, the extract was dried over Na_2SO_4 and concentrated under reduced pressure. The received precipitate was recrystallized from cyclohexane/CH_2Cl_2 to afford white crystals.

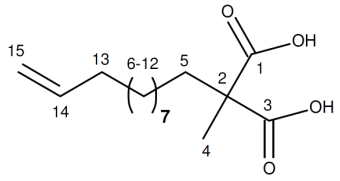

Figure 6-2: Intermediate one: 1-methyl-(10-undecenyl) malonic acid

NMR data: ^{13}C: 178.2 (C1, 3); 139.2 (C14); 114.1 (C15); 53.8 (C2); 35.6 (C13); 33.8 (C5); 29.8 – 28.9 (C7–12); 24.3 (C6); 19.8 (C4)

^{1}H: 5.84-5.78 (14); 5.01-4.91 (15); 2.06-2.01 (13); 1.89 (5, 10); 1.48 (4); 1.38-1.34 (2); 1.30 (10); 1.27 (6-12)

ATR-FTIR data: ν_{max}/cm^{-1}: 3080w, 2968w, 2920s, 2851m, 2648br, 1718s, 1703s, 1643w, 1470m, 1453m, 1302m, 1285m, 1276m, 1258m, 1233m, 991m, 922s, 905s, 764w, 693w

6.4.2 Step two: N,N'-Bis(2-hydroxyethyl)-2-methyl(10-undecenyl)-1,3-propanediamide

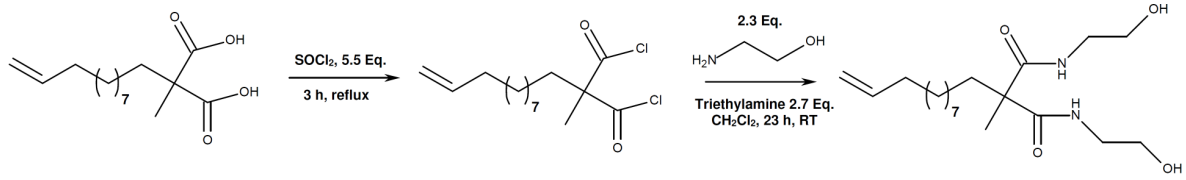

Figure 6-3: Synthesis of *N,N'*-bis(2-hydroxyethyl)-2-methyl(10-undecenyl)-1,3-propanediamide

A mixture of the malonic acid (1 eq.) and $SOCl_2$ (5,5 eq.) was heated to reflux for 3 hours. The excess $SOCl_2$ was abscised under reduced pressure to yield the crude dichloride quantitatively as a yellow oil. A solution of the crude dichloride in CH_2Cl_2 was added drop wise to an ice-cold solution of ethanolamine (2.3 eq.) in CH_2Cl_2 over 30 minutes. A white precipitate formed immediately. After complete addition, triethylamine (2.7 eq.) was added quickly.

After stirring for 23 hours at room temperature, the mixture was poured into a saturated aqueous NaCl solution and acidified with 0.1 N HCl to facilitate phase separation. The organic layer was separated and the aqueous phase was extracted with CH_2Cl_2. The combined organic extracts were washed with HCl (0,1 N), dried over Na_2SO_4 and concentrated under reduced pressure. Purifying of the crude diamide was done by silica gel chromatography (CH_2Cl_2:MeOH = 9:1) to afford a yellow oil.

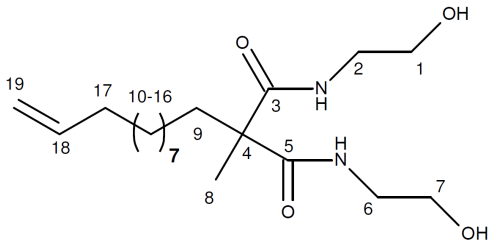

Figure 6-4: Intermediate two: N,N'-Bis(2-hydroxyethyl)-2-methyl(10-undecenyl)-1,3-propanediamide

NMR data: ^{13}C: 174.1 (C3, 5); 138.9 (C18); 113.8 (C19); 61.5 (C1, 7); 53.4 (C4); 42.2 (C2, 6); 38.1 (C17); 33.5 (C9); 29.6-28.6 (C11, 12, 13, 14, 15, 16); 24.4 (C10); 18.5 (C8)

^{1}H: 7.034-7.012 (2xNH2); 5.828-5.773 (C18); 5.0-4.911 (C19); 3.687-3.668 (C1, 7); 3.418-3.388 (C2, 6); 2.045-2.003 (C9); 1.853-1.821 (C17); 1.417 (C4-16); 1.368-1.341 (C8)

ATR-FTIR data: ν_{max}/cm^{-1}: 3334br, 3076w, 2976w, 2925s, 2854s, 1640brs, 1524brs, 1466m, 1437m, 1262br, 1060s, 992w, 908s and 720w

6.4.3 Step three: 2,2'-(1-Methyl-11-Dodecenylidene)Bis(4,5-Dihydro-oxazole)

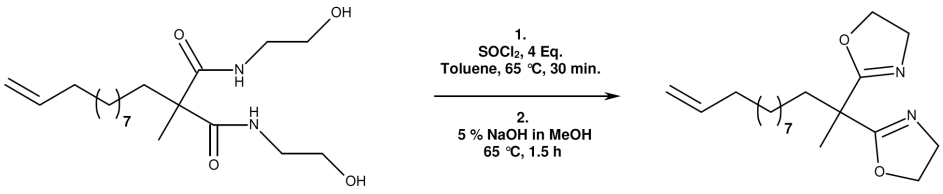

Figure 6-5: Syntesis of 2,2'-(1-methyl-11-dodecenylidene)bis(4,5-dihydrooxazole)

$SOCl_2$ (4 eq.) was quickly added to a suspension of the diamide in Toluene at 65 °C. The resulting mixture was stirred for 30 minutes. After that, the mixture was cooled to 0 °C, quenched with a saturated aqueous $NaHCO_3$ solution and extracted with CH_2Cl_2. The organic layers were combined, dried over Na_2SO_4 and concentrated under reduced pressure. The crude amide was heated to reflux for 1.5 hours in a 5 % methanolic NaOH solution. Then, the mixture was allowed to cool down to room temperature and concentrated under reduced pressure.

The residue was partitioned between CH_2Cl_2 and H_2O, the aqueous phase was extracted with CH_2Cl_2 and the combined organic layers were dried over Na_2SO_4 and concentrated under reduced pressure to afford the Box-ligand as yellow oil.

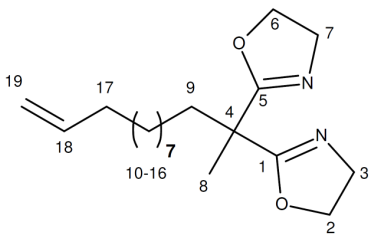

Figure 6-6: Final product: 2,2'-(1-methyl-11-dodecenylidene)bis(4,5-dihydrooxazole)

NMR data: ^{13}C: 169.5 (C1, 5); 139.4 (C18); 114.2 (C19); 67.9 (C2, 6); 54.4 (C3; 7); 42.0 (C4); 36.6 (C17); 33.9 (C9); 29.9 – 29.0 (C11-16); 24.3 (C10); 21.5 (C8)

^{1}H: 5.80 (1H, m, H18); 4.96 (2H, 2 dd, J=1.63, 17.29 Hz, H19), 4.28 (4H, t, J=9.28 Hz, H2, H6); 3.87 (4H, t, J=9.52 Hz, H3, H7); 2.01 (2H, m, H9); 1.90 (2H, m, H17); 1.48 (3H, s, H8), 2.24 (14H, m, H10-H16)

ATR-FTIR data: ν_{max}/cm^{-1}: 3076w, 2924s, 2854s, 1656s, 1480w, 1461m, 1376m, 1352m, 1231br, 1194m, 1138br, 1108m, 1087m, 982s, 954s, 912s, 723w

The detailed ATR-FTIR spectrum of the bis(oxazoline) ligand is shown in Figure 2-1.

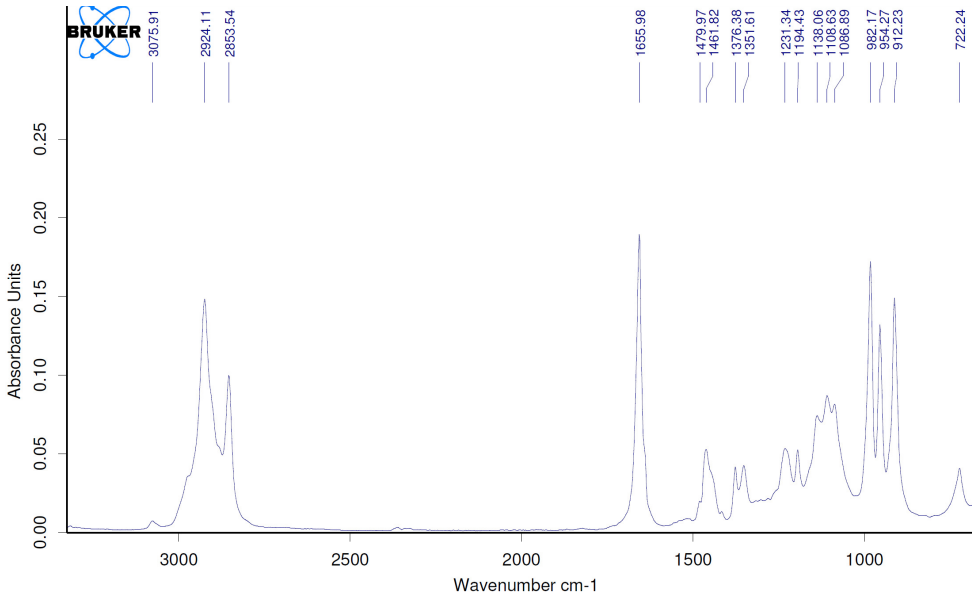

Figure 6-7: ATR-FTIR spectrum of the bis(oxazoline ligand

6.5 Used chemicals and solvents

Deionized water for wafer cleaning and etching was ultrapure water, produced by a TKA Pacific ultra pure water system, σ = 0,065 µS cm^{-1} at 26 °C.

Deionized water for water contact angle measurements was ultrapure water, produced by a TKA MicroPure ultra pure water system, σ = 0,075 µS cm^{-1} at 25,5 °C.

All other used chemicals and solvents are listed in Table 6-1.

Table 6-1: List of chemicals and solvents

Compound	Abbr.	Notes	Product No.	Company
11-bromo-1-undecene		95%	467642	Aldrich
Acetone			442010	Brenntag
Ammonium fluoride	NH_4F	40%	40292	Sigma-Aldrich
Ammonium hydroxide	NH_4OH	33%	5002	Sigma-Aldrich
Ammonium sulfite monohydrate	$(NH_4)_2SO_3 \cdot H_2O$	92%	35,898-3	Sigma-Aldrich
Chlorobenzene, anhydrous	C_6H_5Cl	99.80%	28,451-3	Aldrich
Cyclohexane	Cy	≥99.5%	6570.4	Roth
Dichloromethane	CH_2Cl_2	≥99,5%	6053.1	Roth
Diethymethylmalonate		99%	123136	Aldrich
Dodecane		>98%	44020	Fluka
Ethanolamine		≥99%	2400	Fluka
Hydrochloric acid	HCl	≥37%	30721	Sigma-Aldrich
Hydrofluoric acid	HF	50%	S151100	Riedel
Hydrogen peroxide	H_2O_2	30%	8070.1	Roth
Methanol	MeOH	≥99%	8388.5	Roth
N,N-Dimethylformamid	DMF	≥99.8%	T921.2	Roth
Palladium(II)-acetate	$Pd(OAc)_2$	98%	20,586-9	Aldrich
p-Bromotoluene		98%	18510	Fluka
Phenylboronic acid		≥97%	78181	Fluka
Potassium carbonate	K_2CO_3	≥99%	X894.1	Roth
Sodium chloride	NaCl	>99.8%	9265.2	Roth
Sodium hydride	NaH	60% dispersion in mineral oil	45.291-2	Aldrich
Sodium hydrogen carbonate	$NaHCO_3$	≥99%	0.965.3	Roth
Sodium hydroxide	NaOH	≥99%	6771.1	Roth
Sodium sulfate	Na_2SO_4	≥99%	8631.2	Roth
Thionyl chloride	$SOCl_2$	≥99%	88950	Fluka
Toluene		≥99,5%	7115.1	Roth
Triethylamine	Et_3N	≥99.5%	47.128-3	Sigma-Aldrich

7 APPENDIX

7.1 Additional transmission-FTIR-Spectra

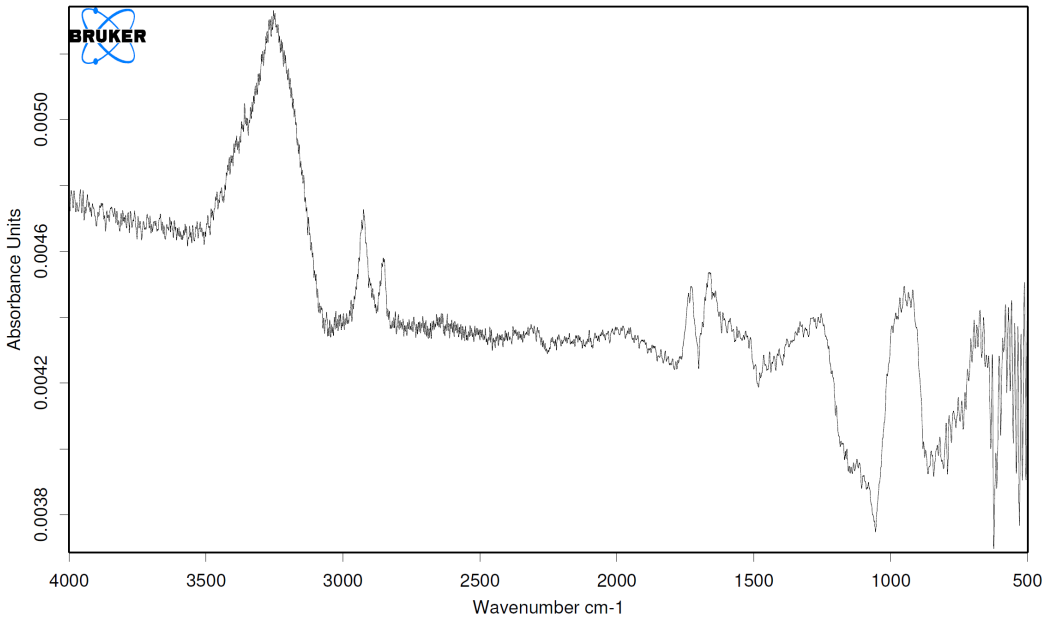

Figure 7-1: Unmodified transmission-FTIR-spectrum of the Si-BOX functionalized surface

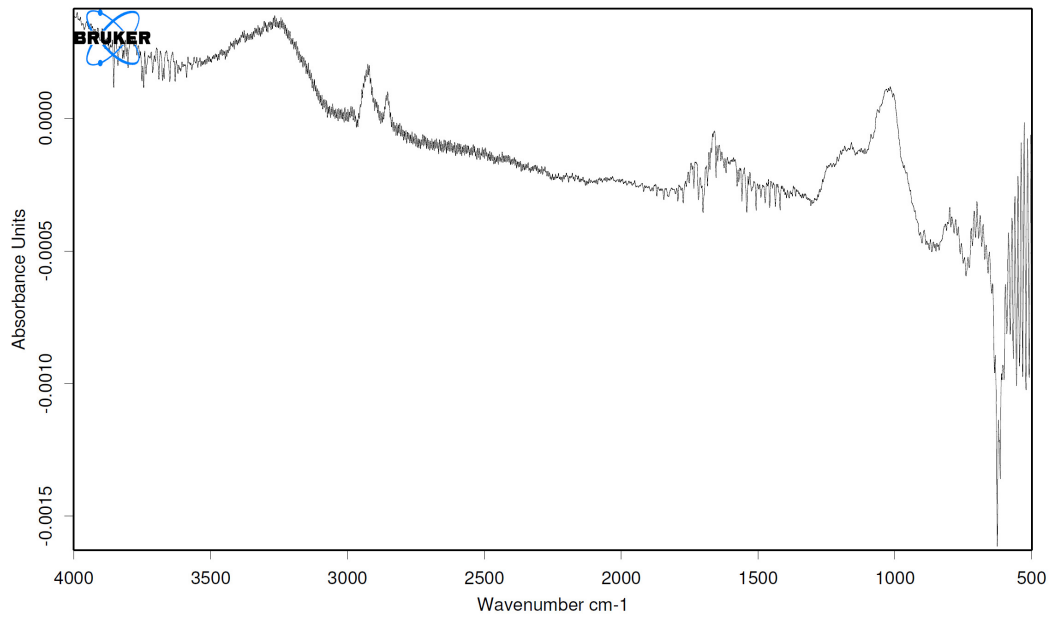

Figure 7-2: Unmodified transmission-FTIR-spectrum of the Si-BOX-Pd(OAc)$_2$ functionalized surface

7.2 Additional XP Spectra

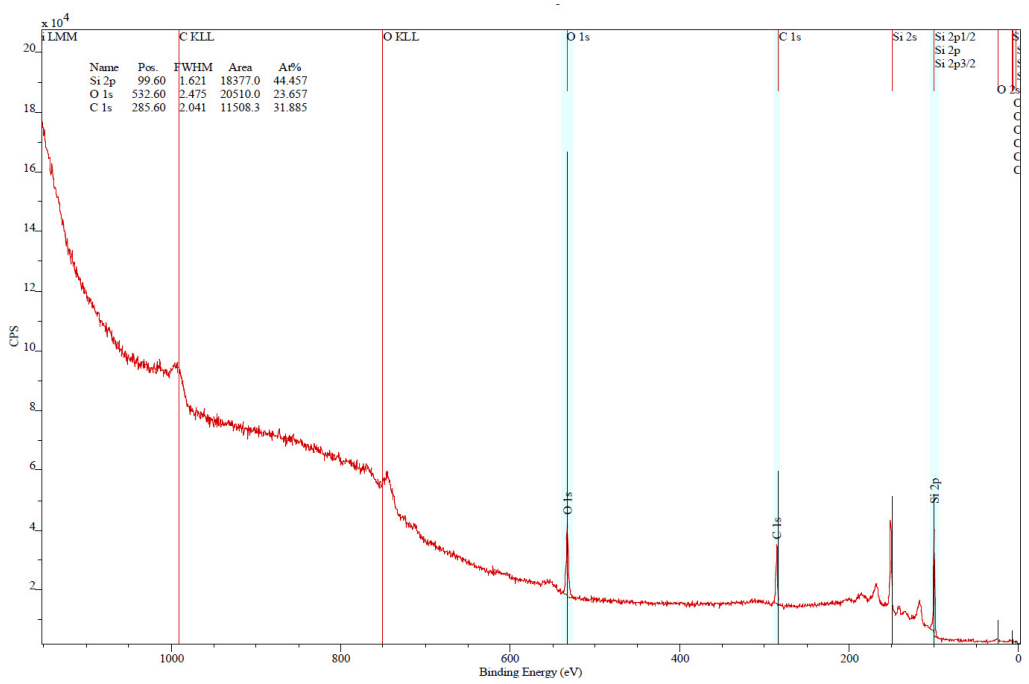

Figure 7-3: XP spectrum of a cleaned, oxidized silicon wafer (reference spectrum)

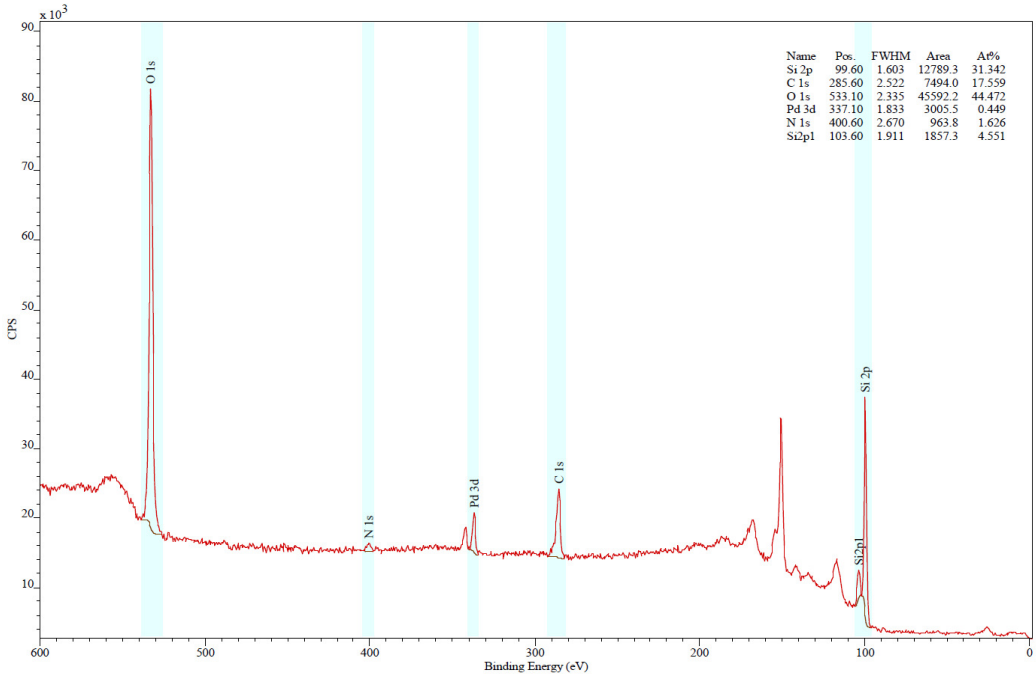

Figure 7-4: XP spectrum of a patterend Si-BOX-Pd(OAc)$_2$ wafer after preparation

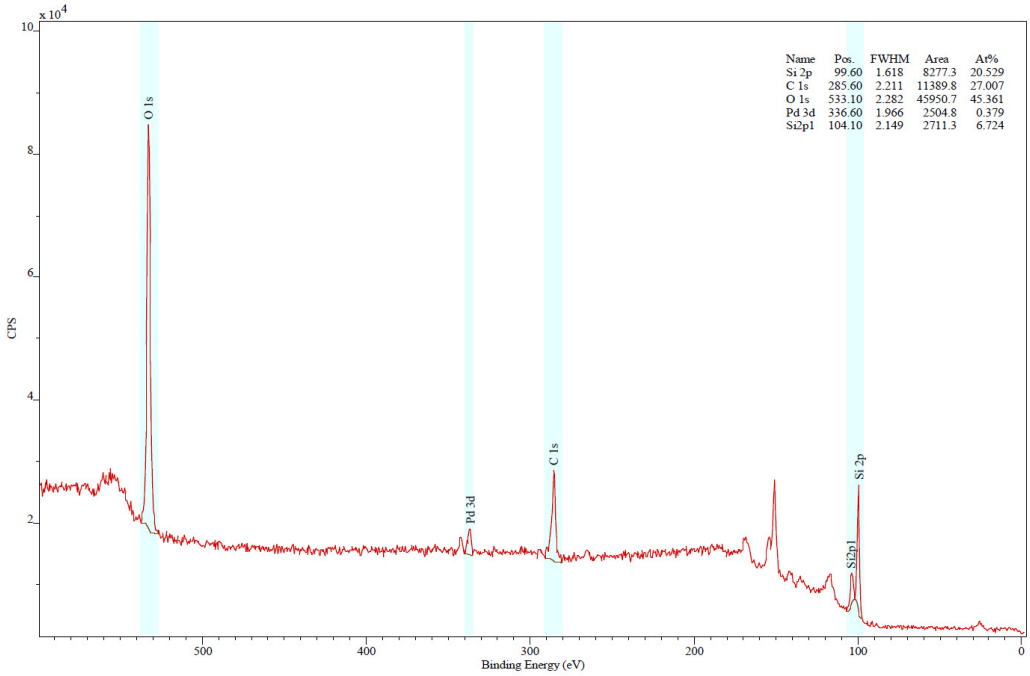

Figure 7-5: XP spectrum of a patterned Si-BOX-Pd(OAc)$_2$ wafer after two Suzuki reactions

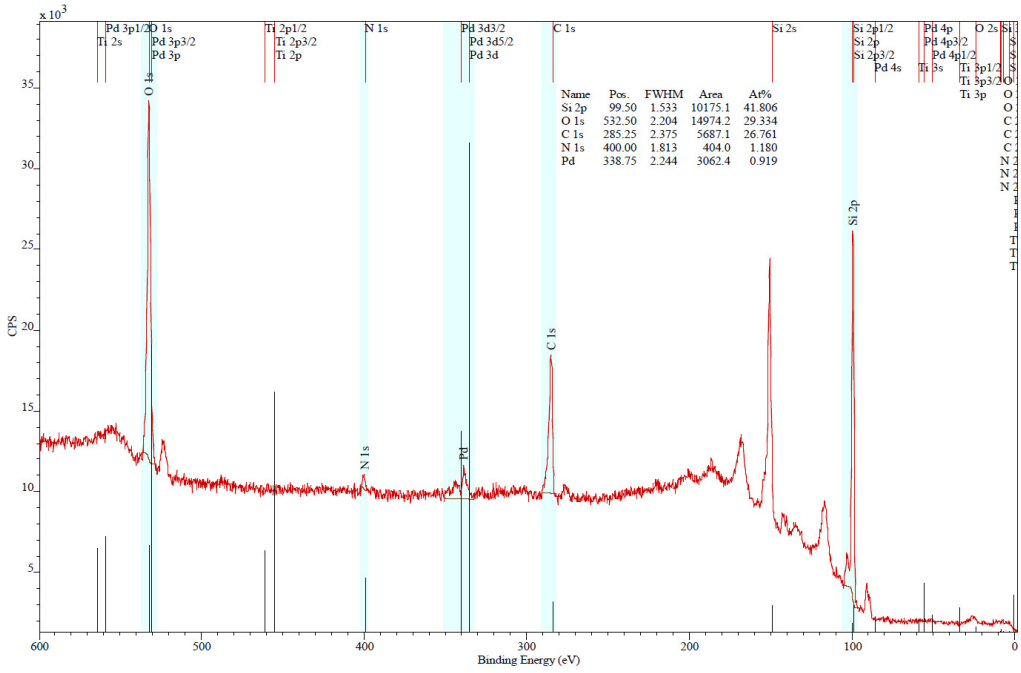

Figure 7-6: XP spectrum of the Si-BOX-Pd(OAc)$_2$-functionalized half of a half/half BOX-Pd(OAc)$_2$/Titanocene wafer

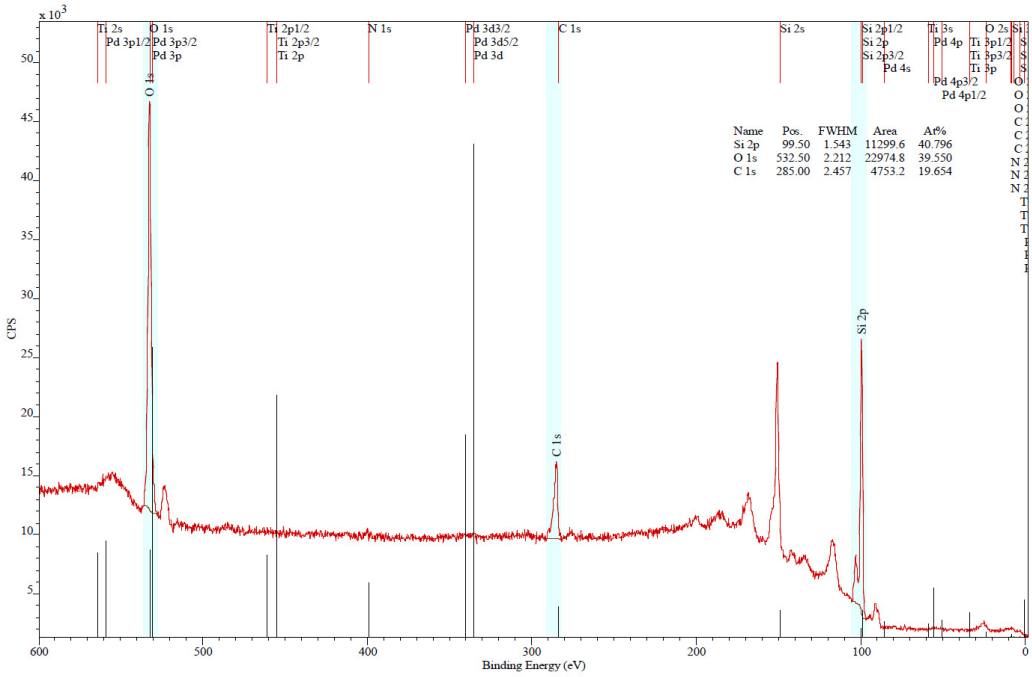

Figure 7-7: XP spectrum of the titanocene-functionalized half of a half/half BOX-$Pd(OAc)_2$/Titanocene wafer

8 REFERENCES

1. Cicero, R. L.; Linford, M. R.; Chidsey, C. E. D. Langmuir 2000, 16, 5688.

2. Langner, A.; Panarello, A.; Rivillon, S.; Vassylyev, O.; Khinast, J. G.; Chabal, Y. J. J Am Chem Soc 2005, 127, 12798.

3. Lagrost, C.; Alcaraz, G.; Bergamini, J.; Fabre, B.; Serbanescu, I. Chem Commun 2007, 1050.

4. Hara, K.; Tayama, S.; Kano, H.; Masuda, T.; Takakusagi, S.; Kondo, T.; Uosaki, K.; Sawamura, M. Chem Commun 2007, 4280.

5. Gruber-Woelfler, H.; Amy, S. R.; Chabal, Y. J.; Schitter, G.; Polo, E.; Ringwald, M.; Khinast, J. G. Chem Commun 2008, 1329.

6. Jeanquartier, C.; Schider, G.; Feichtenhofer, S.; Schwab, H.; Schennach, R.; Stettner, J.; Winkler, A.; Gruber-Woelfler, H.; Schitter, G.; Eder, R. J. P.; Khinast, J. G. Langmuir 2008, 24, 13957.

7. Effenberger, F.; Götz, G.; Bidlingmaier, B.; Wezstein, M. Angewandte Chemie International Edition 1998, 37, 2462.

8. Augustine, R. L. Heterogeneous Catalysis for the Synthetic Chemist; Marcel Dekker, Inc.: New York, 1996.

9. Schüth, F. Chemie in unserer Zeit 2006, 40, 92.

10. Thomas, J. M.; Thomas, W. J. Principles and Practice of Heterogeneous Catalysis; VCH Verlagsgesellschaft mbH: Weinheim, 1997.

11. Hagen, J. Industrial Catalysis; WILEY-VCH Verlag: Weinheim, 2006.

12. Wang, Z.; Ding, K.; Uozumi, Y. In Handbook of Asymmetric Heterogeneous Catalysis, King, K.; Uozumi, Y.Eds.; WILEY-VCH Verlag: Weinheim, 2008, 1-24.

13. Heitbaum, M.; Glorius, F.; Escher, I. Angewandte Chemie International Edition 2006, 45, 4732.

14. Song, C. E.; Lee, S. Chem Rev 2002, 102, 3495.

15. http://nobelprize.org/nobel_prizes/chemistry/laureates/2010/#, 05.05.2011, 08:00.

16. Yin; Liebscher, J. Chem Rev 2007, 107, 133.

17. Miyaura, N.; Yamada, K.; Suzuki, A. Tetrahedron Lett 1979, 20, 3437.

18. Milstein, D.; Stille, J. K. J Am Chem Soc 1978, 100, 3636.

19. Negishi, E.; King, A. O.; Okukado, N. J Org Chem 1977, 42, 1821.

20. Heck, R. F.; Nolley, J. P. J Org Chem 1972, 37, 2320.

21. Sonogashira, K.; Tohda, Y.; Hagihara, N. Tetrahedron Lett 1975, 16, 4467.

22. Guram, A. S.; Rennels, R. A.; Buchwald, S. L. Angew Chem Int Ed Engl 1995, 34, 1348.

23. Nyström, J. E.; Rein, T.; Bäckvall, J. E. Org Synth 1993, 8, 9.

24. Radaschitz, P. Diplomarbeit 2009.

25. Miyaura, N.; Suzuki, A. Chem Rev 1995, 95, 2457.

26. Casado, A. L.; Espinet, P. Organometallics 1998, 17, 954.

27. Braga, A. A. C.; Ujaque, G.; Maseras, F. Organometallics 2006, 25, 3647.

28. Sumimoto, M.; Iwane, N.; Takahama, T.; Sakaki, S. J Am Chem Soc 2004, 126, 10457.

29. Braga, A. A. C.; Morgon, N. H.; Ujaque, G.; Maseras, F. J Am Chem Soc 2005, 127, 9298.

30. Goossen, L. J.; Koley, D.; Hermann, H. L.; Thiel, W. Organometallics 2006, 25, 54.

31. Linford, M. R.; Chidsey, C. E. D. J Am Chem Soc 1993, 115, 12631.

32. Buriak, J. M. Chem Rev 2002, 102, 1271.

33. Henrion, W.; Rebien, M.; Angermann, H.; Röseler, A. Appl Surf Sci 2002, 202, 199.

34. Linford, M. R.; Fenter, P.; Eisenberger, P. M.; Chidsey, C. E. D. J Am Chem Soc 1995, 117, 3145.

35. Cleland, G.; Horrocks, B. R.; Houlton, A. J Chem Soc , Faraday Trans 1995, 91, 4001.

36. Bateman, J. E.; Eagling, R. D.; Worrall, D. R.; Horrocks, B. R.; Houlton, A. Angewandte Chemie International Edition 1998, 37, 2683.

37. Wayner, D. D. M.; Wolkow, R. A. J Chem Soc , Perkin Trans 2 2002, 23.

38. Ciampi, S.; Harper, J. B.; Gooding, J. J. Chem Soc Rev 2010, 39, 2158.

39. Murray Bullis, W. In Handbook of Semiconductor Silicon Technology, O'Mara, W. C.; Herring, R. B.; Hunt, L. P.Eds.; Noyes Publications: Park Ridge, New Jersey, 1990, 347-450.

40. Hamers, R. J.; Wang, Y. Chem Rev 1996, 96, 1261.

41. Higashi, G. S.; Chabal, Y. J.; Trucks, G. W.; Raghavachari, K. Appl Phys Lett 1990, 56, 656.

42. Dumas, P.; Chabal, Y. J.; Jakob, P. Surf Sci 1992, 269-270, 867.

43. Allongue, P.; Henry de Villeneuve, C.; Morin, S.; Boukherroub, R.; Wayner, D. D. M. Electrochim Acta 2000, 45, 4591.

44. Kato, H.; Taoka, T.; Suto, S.; Nishikata, S.; Sazaki, G.; Nakajima, K.; Yamada, T.; Czajka, R.; Wawro, A.; Kasuya, A. e-Journal of Surface Science and Nanotechnology 2009, 7, 557.

45. Sakaue, H.; Fujiwara, S.; Shingubara, S.; Takahagi, T. Appl Phys Lett 2001, 78, 309.

46. Higashi, G. S.; Becker, R. S.; Chabal, Y. J.; Becker, A. J. Appl Phys Lett 1991, 58, 1656.

47. Jakob, P.; Chabal, Y. J. J Chem Phys 1991, 95, 2897.

48. Pietsch, G. J.; Kohler, U.; Henzler, M. J Appl Phys 1993, 73, 4797.

49. Roche, J. R.; Ramonda, M.; Thibaudau, F.; Dumas, P.; Mathiez, P.; Salvan, F.; Allongue, P. Microsc.Microanal.Microstruct. 1994, 5, 291.

50. Ramonda, M.; Dumas, P.; Salvan, F. Surf Sci 1998, 411, L839.

51. Wade, C. P.; Chidsey, C. E. D. Appl Phys Lett 1997, 71, 1679.

52. Garcia, S. P.; Bao, H.; Hines, M. A. Surf Sci 2003, 541, 252.

53. Kern, W. In Handbook of Silicon Wafer Cleaning Technology, Reinhardt, K. A.; Kern, W.Eds.; William Andrew Inc.: Norwich, 2008, 3-92.

54. Bearda, T.; Mertens, P. W.; Beaudoin, S. P. In Handbook of Silicon Wafer Cleaning Technology, Reinhardt, K. A.; Kern, W.Eds.; William Andrew Inc.: Norwich, 2008, 93-164.

55. Allongue, P.; Kieling, V.; Gerischer, H. Electrochim Acta 1995, 40, 1353.

56. Hines, M. A. Annu Rev Phys Chem 2003, 54, 29.

57. Chabal, Y. J.; Higashi, G. S.; Small, R. J. In Handbook of Silicon Wafer Cleaning Technology, Reinhardt, K. A.; Kern, W.Eds.; William Andrew Inc.: Norwich, 2008, 523-618.

58. Fukidome, H.; Matsumura, M. Appl Surf Sci 1998, 130-132, 146.

59. Saito, N.; Youda, S.; Hayashi, K.; Sugimura, H.; Takai, O. Surf Sci 2003, 532-535, 970.

60. Sano, H.; Maeda, H.; Ichii, T.; Murase, K.; Noda, K.; Matsushige, K.; Sugimura, H. Langmuir 2009, 25, 5516.

61. Nyffenegger, R. M.; Penner, R. M. Chem Rev 1997, 97, 1195.

62. Hurley, P. T.; Ribbe, A. E.; Buriak, J. M. J Am Chem Soc 2003, 125, 11334.

63. Wacaser, B. A.; Maughan, M. J.; Mowat, I. A.; Niederhauser, T. L.; Linford, M. R.; Davis, R. C. Appl Phys Lett 2003, 82, 808.

64. Hamers, R. J.; Coulter, S. K.; Ellison, M. D.; Hovis, J. S.; Padowitz, D. F.; Schwartz, M. P.; Greenlief, C. M.; Russell, J. N. Acc Chem Res 2000, 33, 617.

65. Strother, T.; Cai, W.; Zhao, X.; Hamers, R. J.; Smith, L. M. J Am Chem Soc 2000, 122, 1205.

66. de Smet, Louis C. P. M.; Stork, G. A.; Hurenkamp, G. H. F.; Sun, Q.; Topal, H.; Vronen, P. J. E.; Sieval, A. B.; Wright, A.; Visser, G. M.; Zuilhof, H.; Sudhölter, E. J. R. J Am Chem Soc 2003, 125, 13916.

67. Chatgilialoglu, C. Acc Chem Res 1992, 25, 188.

68. Cicero, R. L.; Chidsey, C. E. D.; Lopinski, G. P.; Wayner, D. D. M.; Wolkow, R. A. Langmuir 2002, 18, 305.

69. Eves, B. J.; Sun, Q.; Lopinski, G. P.; Zuilhof, H. J Am Chem Soc 2004, 126, 14318.

70. Lopinski, G. P.; Wayner, D. D. M.; Wolkow, R. A. Nature 2000, 406, 48.

71. Sieval, A. B.; Vleeming, V.; Zuilhof, H.; Sudhölter, E. J. R. Langmuir 1999, 15, 8288.

72. Terry, J.; Mo, R.; Wigren, C.; Cao, R.; Mount, G.; Pianetta, P.; Linford, M. R.; Chidsey, C. E. D. Nuclear Instruments and Methods in Physics Research Section B: Beam Interactions with Materials and Atoms 1997, 133, 94.

73. Terry, J.; Linford, M. R.; Wigren, C.; Cao, R.; Pianetta, P.; Chidsey, C. E. D. Appl Phys Lett 1997, 71, 1056.

74. Buriak, J.,M. Chem Commun 1999, 1051.

75. Voicu, R.; Boukherroub, R.; Bartzoka, V.; Ward, T.; Wojtyk, J. T. C.; Wayner, D. D. M. Langmuir 2004, 20, 11713.

76. Stewart, M. P.; Buriak, J. M. Angewandte Chemie International Edition 1998, 37, 3257.

77. Stewart, M. P.; Buriak, J. M. J Am Chem Soc 2001, 123, 7821.

78. Sun, Q.; de Smet, Louis C. P. M.; van Lagen, B.; Wright, A.; Zuilhof, H.; SudhÃ¶lter, E. J. R. Angewandte Chemie International Edition 2004, 43, 1352.

79. Sun, Q.; de Smet, Louis C. P. M.; van Lagen, B.; Giesbers, M.; Thune, P. C.; van Engelenburg, J.; de Wolf, F. A.; Zuilhof, H.; Sudholter, E. J. R. J Am Chem Soc 2005, 127, 2514.

80. Kanabus-Kaminska, J.; Hawari, J. A.; Griller, D.; Chatgilialoglu, C. J Am Chem Soc 1987, 109, 5267.

81. Laarhoven, L. J. J.; Mulder, P.; Wayner, D. D. M. Acc Chem Res 1999, 32, 342.

82. Wang, X.; Ruther, R. E.; Streifer, J. A.; Hamers, R. J. J Am Chem Soc 2010, 132, 4048.

83. Miura, T.; Niwano, M.; Shoji, D.; Miyamoto, N. Appl Surf Sci 1996, 100-101, 454.

84. Wojtyk, J. T. C.; Tomietto, M.; Boukherroub, R.; Wayner, D. D. M. J Am Chem Soc 2001, 123, 1535.

85. Holland, J. M.; Stewart, M. P.; Allen, M. J.; Buriak, J. M. Journal of Solid State Chemistry 1999, 147, 251.

86. Buriak, J. M.; Allen, M. J. J Am Chem Soc 1998, 120, 1339.

87. Boukherroub, R.; Morin, S.; Bensebaa, F.; Wayner, D. D. M. Langmuir 1999, 15, 3831.

88. Royea, W. J.; Juang, A.; Lewis, N. S. Appl Phys Lett 2000, 77, 1988.

89. He, J.; Patitsas, S. N.; Preston, K. F.; Wolkow, R. A.; Wayner, D. D. M. Chemical Physics Letters 1998, 286, 508.

90. Bansal, A.; Li, X.; Lauermann, I.; Lewis, N. S.; Yi, S. I.; Weinberg, W. H. J Am Chem Soc 1996, 118, 7225.

91. de Villeneuve, C. H.; Pinson, J.; Bernard, M. C.; Allongue, P. The Journal of Physical Chemistry B 1997, 101, 2415.

92. Allongue, P.; de Villeneuve, C. H.; Pinson, J.; Ozanam, F.; Chazalviel, J. N.; Wallart, X. Electrochim Acta 1998, 43, 2791.

93. Balaur, E.; Zhang, Y.; Djenizian, T.; Boukherroub, R.; Schmuki, P. Journal of Electroceramics 2006, 16, 71.

94. Fabre, B.; Wayner, D. D. M. Comptes Rendus Chimie 2005, 8, 1249.

95. Harnett, C. K.; Satyalakshmi, K. M.; Craighead, H. G. Langmuir 2001, 17, 178.

96. Headrick, J. E.; Armstrong, M.; Cratty, J.; Hammond, S.; Sheriff, B. A.; Berrie, C. L. Langmuir 2005, 21, 4117.

97. Yan, Y. D.; Sun, T.; Pan, B.; Zhao, J. W.; Dong, S. J Vac Sci Technol B 2009, 27, 1247.

98. Gruber-Wölfler, H.; Eder, R.; Radaschitz, P.; Feenstra, P.; Radaschitz, P.; Cappello, V.; Khinast, J. G. Chemie Ingenieur Technik 2009, 81, 1169.

99. Watanabe, S.; Nakayama, N.; Ito, T. Appl Phys Lett 1991, 59, 1458.

100. Kutschi, K. Diplomarbeit 2008.

101. Shaganov, I. I.; Perova, T. S.; Moore, R. A.; Berwick, K. J Mater Sci : Mater Electron 2001, 12, 351.

102. Burguete, M. I.; Fraile, J. M.; GarcÃa, J. I.; GarcÃa-Verdugo, E.; HerrerÃas, C. I.; Luis, S. V.; Mayoral, J. A. J Org Chem 2001, 66, 8893.

103. Fraile, J. M.; García, J. I.; Harmer, M. A.; Herrerías, C. I.; Mayoral, J. A. Journal of Molecular Catalysis A: Chemical 2001, 165, 211.

104. Fraile, J. M.; García, J. I.; Herrerías, C. I.; Mayoral, J. A.; Harmer, M. A. Journal of Catalysis 2004, 221, 532.

105. Hollander, J. M.; Jolly, W. L. Acc Chem Res 1970, 3, 193.

106. http://en.wikipedia.org/wiki/X-ray_photoelectron_spectroscopy. 05.07.2011, 14:01.

107. Richardson, J. M.; Jones, C. W. Journal of Catalysis 2007, 251, 80.

108. Webb, J. D.; MacQuarrie, S.; McEleney, K.; Crudden, C. M. Journal of Catalysis 2007, 252, 97.

109. Gruber-Woelfler, H. Dissertation 2007.

110. Faucheux, A.; Gouget-Laemmel, A.; Henry, d. V.; Boukherroub, R.; Ozanam, F.; Allongue, P.; Chazalviel, J. Langmuir 2006, 22, 153.